AD-A195 127 QUANTUM CHEMICAL INVESTIGATIONS OF THE MECHANISM OF 1/2
CATIONIC POLYMERIZATI (U) JOHNS HOPKINS UNIV BALTIMORE
MD J J KAUFMAN 15 NOV 87 TR-8 N00014-88-C-0003
UNCLASSIFIED F/G 7/3 NL

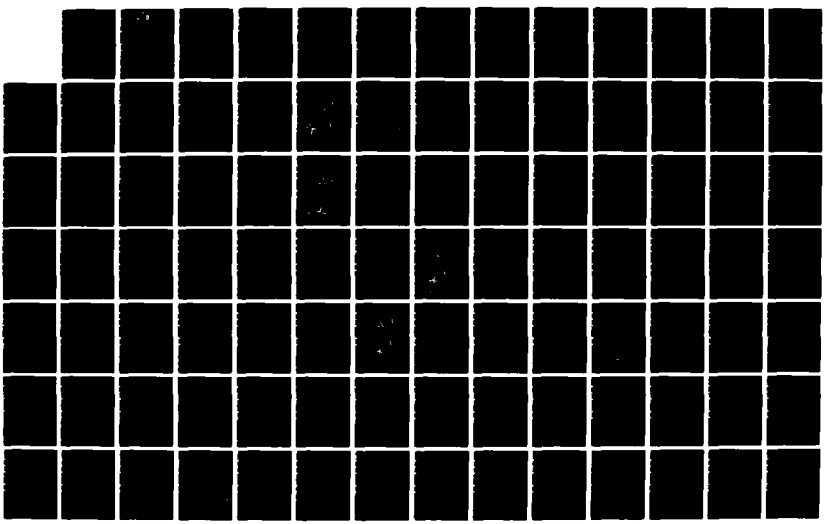

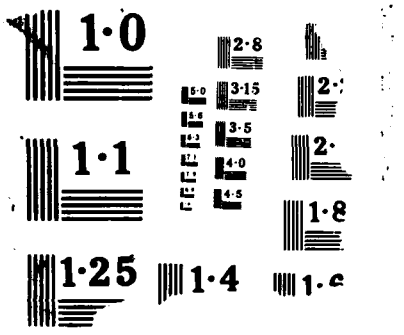
1·0
1·1
1·25
1·4
2·8
3·15
3·5
4·0
4·5
1·8

AD-A195 127

DTIC ELECTE MAY 23 1988 S D H

REPORT DOCUMENTATION PAGE

1b. RESTRICTIVE MARKINGS	
2a. SECURITY CLASSIFICATION AUTHORITY	3. DISTRIBUTION/AVAILABILITY OF REPORT: Unlimited distributions
2b. DECLASSIFICATION/DOWNGRADING SCHEDULE	
4. PERFORMING ORGANIZATION REPORT NUMBER(S): ONR-NR093964-TR8	5. MONITORING ORGANIZATION REPORT NUMBER(S): Office of Naval Research
6a. NAME OF PERFORMING ORGANIZATION: The Johns Hopkins University	6b. OFFICE SYMBOL (If applicable):
6c. ADDRESS (City, State, and ZIP Code): Charles and 34th Streets, Baltimore, Maryland 21218	7a. NAME OF MONITORING ORGANIZATION: Office of Naval Research
8a. NAME OF FUNDING/SPONSORING ORGANIZATION: Office of Naval Research	8b. OFFICE SYMBOL (If applicable): Code 473P
8c. ADDRESS (City, State, and ZIP Code): 800 N. Quincy Street, Arlington, Virginia 22217	7b. ADDRESS (City, State, and ZIP Code): 800 N. Quincy Street, Arlington, Virginia 22217
	9. PROCUREMENT INSTRUMENT IDENTIFICATION NUMBER: Contract N00014-80-C-0003
	10. SOURCE OF FUNDING NUMBERS: PROGRAM ELEMENT NO. / PROJECT NO. / TASK NO. / WORK UNIT ACCESSION NO: 4326-064

11. TITLE (Include Security Classification): Quantum Chemical Investigations of the Mechanism of Cationic Polymerization and Theoretical Prediction of Crystal Densities and Decomposition Pathways of Energetic Molecules

12. PERSONAL AUTHOR(S): Kaufman, Joyce J.

13a. TYPE OF REPORT	13b. TIME COVERED	14. DATE OF REPORT (Year, Month, Day)	15. PAGE COUNT
Annual	FROM 86/10/1 TO 87/9/30	87/11/15	164

16. SUPPLEMENTARY NOTATION

17. COSATI CODES: FIELD	GROUP	SUB-GROUP

18. SUBJECT TERMS (Continue on reverse if necessary and identify by block number): Cationic Polymerization/Energetic Polymers/Oxetanes/Quantum Chemical Calculations/Configuration Interaction (CI)/Multi-Reference Double Excitation - Configuration Interaction (cont

19. ABSTRACT (Continue on reverse if necessary and identify by block number)

I. Program Enhancements and New Program Developments on the CRAY Supercomputer
II. MRD-CI Calculations for Cationic Polymerization of Energetic Oxetanes
III. Ab-Initio MRD-CI Calculations for Breaking a Chemical Bond in a Molecule in a Crystal or Other Solid Environment
IV. POLY-CRYST

I. This past year we have made a significant breakthrough. We developed and implemented and used successfully the strategy for ab-initio MRD-CI (multireference double excitation - configuration interaction) calculations for breaking a chemical bond in a molecule in a crystal or other solid environment. (Keywords)

II. A. Ab-Initio MRD-CI Calculations for the Propagation Step

Our major emphasis this past year has been to carry out in-depth detailed ab-initio MRD-CI

20. DISTRIBUTION/AVAILABILITY OF ABSTRACT	21. ABSTRACT SECURITY CLASSIFICATION
☒ UNCLASSIFIED/UNLIMITED ☐ SAME AS RPT ☐ DTIC USERS	Unclassified
22a. NAME OF RESPONSIBLE INDIVIDUAL: Richard S. Miller	22b. TELEPHONE (Include Area Code): (202) 696-4403 / 22c. OFFICE SYMBOL: Code 473P

DD FORM 1473, 84 MAR — 83 APR edition may be used until exhausted. All other editions are obsolete. SECURITY CLASSIFICATION OF THIS PAGE

DISTRIBUTION STATEMENT A
Approved for public release;
Distribution Unlimited

18. (MRD-CI)/Energetic Compounds/MRD-CI for breaking Chemical Bond in Crystal/Crystal and Polymer Orbitals

19. (multireference double excitation - configuration interaction) calculations on the propagation step of cationic polymerization of oxetane (or an energetic substituted oxetane) reacting with protonated oxetane (or a protonated energetic substituted oxetane).

MRD-CI calculations (based on localized orbitals) along the potential energy surfaces have been carried out for a very large number of geometry variations for the angles between the rings, the inter-ring distance (O_{1B}-C_{4A}) (where the A ring is the protonated ring and the B ring is the non-protonated ring), the angle of opening the C_{4A}-O_{1A} ring and the orientation of the H atoms on C_{4A}.

These MRD-CI calculations have enabled us to map out the reaction coordinates of the propagation step reaction of oxetane (or an energetic substituted oxetane) reacting with protonated oxetane (or with a protonated energetic substituted oxetane), to identify the transition state of the propagation step and to identify when the C_{4A}-O_{1A} bond in the protonated ring will start to open as a function of inter-ring distance and angle for each different pair of substituted reactants.

This year we first carried out MRD-CI calculations for the prototype systems OXET + $OXETH^+$, OXET + $FNOXH^+$, FNOX + $OXETH^+$, FNOX + $FNOXH^+$, to gain the understanding of the basic mechanism of the propagation step. We then carried out MRD-CI calculations for the systems AMMO + $OXETH^+$, OXET + $AMMOH^+$ and AMMO + $AMMOH^+$.

B. Ab-Initio MRD-CI Calculations of the Protonation of Oxetane

Oxetane + H^+ is not the lowest energy state of separated fragments of protonated oxetane at the dissociation asymptote. The lowest energy state is oxetane$^+$ + H since the IP of oxetane is lower than that of H. Thus, no single determinant SCF calculation for protonation/deprotonation can describe the system properly. Our MRD-CI results indicated that the lowest ground $^1A_1$ state at equilibrium dissociated to oxetane$^+$ ($^2A_1$) + H. The potential surface arising from oxetane ($\tilde{X}\,^1A_1$) + H^+ was repulsive. There were also a wealth of other states arising at the dissociation asymptote from higher states.

III. This past year we derived and implemented an extension of our MRD-CI technique based on localized orbitals to ab-initio MRD-CI calculations for breaking a chemical bond in a molecule in a crystal or other solid environment. In this procedure the SCF is solved explicitly for the molecules in a unit cell (or larger piece of crystal) in the multipole field of yet further out surrounding molecules. The SCF wave function is localized and the localized orbitals (occupied and virtual) in the region of the bond being broken are included explicitly in the MRD-CI calculations. This method is completely general and applicable to any molecule in any kind of a crystal or other solid environment. This development has led to an important breakthrough which will lead to crucial understanding of the initiation of detonation and the subsequent processes leading to detonation. Results will presented on the CH_3 - NO_2 decomposition of nitromethane in nitromethane crystal. This system is the prototype of ^5C-NO_2 dissociation.

IV. We devoted only minimal but still scientifically significant effort to further development and testing of the POLY-CRYST program. We derived and incorporated into the POLY-CRYST including the multipole effects of farther out molecules to include long range effects also. We then meshed this multipole procedure back into the MRD-CI programs to enable us to include multipole effects when breaking a chemical bond in a crystal. We also derived and implemented a procedure for calculating the charge imbalance caused by various integral thresholds to give a precise measure of the effect on the crystal orbital calculation of dropping integrals of various sizes. The POLY-CRYST program has promise for yielding important fundamental results on crystalline energetic materials.

We carried out ab-initio crystal orbital calculations on several unit cells of nitromethane to verify that our SCF method in the field of multipoles described above in Part III did correctly describe a crystal of nitromethane.

Report Number ONR-NR093964-TR8

SUMMARY

ANNUAL REPORT

QUANTUM CHEMICAL INVESTIGATIONS OF THE MECHANISM OF CATIONIC POLYMERIZATION

and

THEORETICAL PREDICTION OF CRYSTAL DENSITIES

and

DECOMPOSITION PATHWAYS OF ENERGETIC MOLECULES

Joyce J. Kaufman, Principal Investigator
The Johns Hopkins University
Baltimore, Maryland 21218

Contract N00014-80-C-0003
Office of Naval Research

Dr. Richard Miller, ONR Contract Monitor

Period Covered October 1, 1986 - September 30, 1987

November 15, 1987

Quantum Chemical Investigations of the Mechanism of Cationic Polymerization and Theoretical Prediction of Crystal Densities and Decomposition Pathways of Energetic Molecules

Joyce J. Kaufman, Principal Investigator

TABLE OF CONTENTS

Concise Summary 1

I. Program Enhancements and New Program Developments on the CRAY Supercomputer. 6

II. MRD-CI Calculations for Cationic Polymerization of Energetic Oxetanes. 7

A. Ab-Initio MRD/CI Calculations for the Propagation Step. 7

B. Ab-Initio MRD-CI Calculations of the Protonation of Oxetane. 125

III. Ab-Initio MRD-CI Calculations for Breaking a Chemical Bond in a Molecule in a Crystal or Other Solid Environment 127

A. Methodology. 127

B. Calculations Carried out on Nitromethanes. 128

C. Detailed Results of Calculations Carried Out For Nitromethane: Various Choices of Size and Description of System 135

IV. POLY-CRYST. 149

V. Lectures Presented and Publications on This ONR Research. . 150

VI. Project Personnel 154

Distribution List 155

QUANTUM CHEMICAL INVESTIGATIONS OF THE MECHANISM OF CATIONIC POLYMERIZATION

and

THEORETICAL PREDICTION OF CRYSTAL DENSITIES

and

DECOMPOSITION PATHWAYS OF ENERGETIC MOLECULES

Joyce J. Kaufman, Principal Investigator
Department of Chemistry
The Johns Hopkins University

CONCISE SUMMARY

I. Program Enhancements and New Program Developments on the CRAY Supercomputer

This past year we have made a significant breakthrough. We developed and implemented and used successfully the strategy for ab-initio MRD-CI (multireference double excitation - configuration interaction) calculations for breaking a chemical bond in a molecule in a crystal or other solid environment. In this procedure the SCF is solved explicitly for the molecules in a unit cell (or larger piece of crystal) in the multipole field of yet further out surrounding molecules. The SCF wave function is localized and the localized orbitals (occupied and virtual) in the region of the bond being broken are included explicitly in the MRD-CI calculations. This method will be detailed in section III. This method is completely general and the results lead to an understanding of fractoemission and of the initiation of detonation and the subsequent processes leading to detonation.

We continue to serve on the NSF San Diego Supercomputer Center (SDSC) computer time allocation committee on their CRAY XMP 4/8. We also receive computer time grants from SDSC which we use for the bulk of our quantum chemical calculations on this ONR research.

II. MRD-CI Calculations for Cationic Polymerization of Energetic Oxetanes

Our major emphasis this past year has been to carry out in-depth detailed ab-initio MRD-CI (multireference double excitation - configuration interaction) calculations on the propagation step of cationic polymerization of prototype substituted energetic oxetanes.

Cationic polymerization consists essentially of two major steps: initiation and then propagation. There is considerable Navy interest in energetic polymers made by cationic polymerization of oxetanes substituted

or disubstituted by exotic energetic substituents such as azido, azidomethyl, nitrato, nitraminomethyl, etc. as well as fluoro and nitro groups. The initiation step (which is crucial for cationic polymerization to take place) is governed by the propensity of the substituted oxetane to undergo protonation. Our previous ab-intio quantum chemical SCF calculations on the energetic oxetane monomers and electrostatic molecular potential contour (EMPC) maps we generated from these electronic wave functions, which predict the order of protonation and hence initiation, were able to predict correctly the propensity of the energetic substituted oxetane monomers to undergo polymerization <u>even</u> prior to the synthesis of the monomers.

A. Ab-Initio MRD/CI Calculations for the Propagation Step

1. Discussion

As was suggested to us by several different experimentalists in cationic polymerization (primarily Gerry Manser) the mechanism seems to be attack of protonated oxetanes on oxetanes (or vice versa) with concomitant ring opening of the protonated oxetane according to the following general scheme

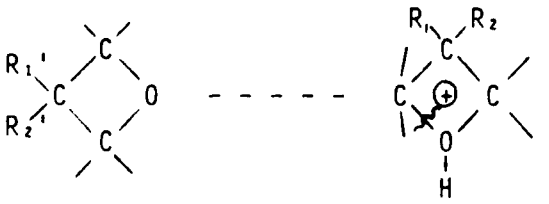

"B" ring "A" ring

We have carried out this past year and are continuing to carry out ab-initio MRD-CI calculations on the subsequent propagation step of oxetane (or an energetic substituted oxetane) reacting with protonated oxetane (or a protonated energetic substituted oxetane).

MRD-CI calculations along the potential energy surfaces have been carried out for a very large number of geometry variations for the angles between the planes of the substituted oxetane and protonated substituted oxetane rings (which can be different in each direction in the case of substituted rings), the inter-ring distance (O_{1B}-C_{4A}) (where the A ring is the protonated ring and the B ring is the non-protonated ring), the angle of opening the C_{4A}-O_{1A} ring and the orientation of the H atoms on C_{4A}.

The preferred direction of attack appears to be the reaction of the oxygen of the unprotonated oxetane ring (which we call O_{1B}) with the α

carbon (which we call C_{4A}) of the protonated substituted oxetane ring along the C_{4A}-O_{1A} bond direction with concommitant pulling back (inversion of the H atoms on C_{4A}) and opening of the C_{4A}-O_{1A} bond in the protonated oxetane ring and formation of an O_{1B}-C_{4A} bond.

The ab-initio MRD-CI calculations on the propagation step of the protonated oxetane ring opening in the course of interaction with oxetane were carried out based on localized orbitals on the pertinent regions involved in the reaction.

These MRD-CI calculations have enabled us to map out the reaction coordinates of the propagation step reaction of oxetane (or an energetic substituted oxetane) reacting with protonated oxetane (or with a protonated energetic substituted oxetane), to identify the transition state of the propagation step and to identify when the C_{4A}-O_{1A} bond in the protonated ring will start to open as a function of inter-ring distance and angle for each different pair of substituted reactants.

2. Detailed Results

This year we first carried out such detailed MRD-CI calculations for the prototype systems OXET + $OXETH^+$, OXET + $FNOXH^+$, FNOX + $OXETH^+$, FNOX + $FNOXH^+$, to gain the understanding of the basic mechanism of the propagation step involving energetic substituted oxetanes without the additional complication of floppyside chain groups. We then carried out such detailed MRD-CI calculations for the systems AMMO + $OXETH^+$, OXET + $AMMOH^+$ and AMMO + $AMMOH^+$. We are currently carrying out similar calculations involving BAMO and $BAMOH^+$ and will carry such calculations out for other energetic substituted oxetanes. These results will enable us to understand and to predict copolymerization propensities.

B. Ab-Initio MRD-CI Calculations of the Protonation of Oxetane

Oxetane + H^+ is not the lowest energy state of separated fragments of protonated oxetane at the dissociation asymptote. The lowest energy state is oxetane$^+$ + H since the IP of oxetane is lower than that of H. Thus, no single determinant SCF calculation for protonation/deprotonation can describe the system properly. Our MRD-CI results indicated that the lowest ground $^1A_1$ state at equilibrium dissociated to oxetane$^+$ ($^2A_1$) + H. The $^1A_1$ potential surface arising from oxetane ($\bar{X}\ ^1A_1$) + H^+ was repulsive. There were also a wealth of other states arising at the dissociation asymptote from higher states.

III. Ab-Initio MRD-CI Calculations for Breaking a Chemical Bond in a Molecule in a Crystal or Other Solid Environment

The challenge arose to extend our MRD-CI (multireference double excitation - configuration interaction) technique based on localized/local orbitals to the breaking of a chemical bond in a molecule in a crystal (or other solid environment). This past year we have derived, implemented, and used successfully a procedure for doing this. We made the first presentation of results using this method, spring 1987, at the ONR Workshop on Dynamic Deformation, Fracture and Transient Combustion of Energetic Compounds.

This development has led to an important breakthrough which will lead to crucial understanding of fractoemission and of the initiation of detonation and the subsequent processes leading to detonation. Our method is completely general and applicable to any molecule in any kind of a crystal or other solid environment. The crystal can have defects, deformations, dislocations, impurities, dopants, edges and surface boundaries, etc.

Results will presented on the CH_3 - NO_2 decomposition of nitromethane in nitromethane crystal. This system is the prototype of >C-NO_2 dissociation.

IV. POLY-CRYST

POLY-CRYST is the program we previously derived and wrote for ab-initio calculations on crystals and polymers using the translational symmetry in a crystal and the translational-rotational symmetry in a polymer. Commensurate with the ONR priorities expressed to us by our ONR Contract Monitor, we devoted only minimal but still scientifically significant effort to further development and testing of the POLY-CRYST program. As options we had already included in POLY-CRYST our own ab-initio MODPOT (ab-initio effective core model potentials) and VRDDO (charge conserving integral prescreening evaluation) options. It is these features, particularly VRDDO, which will enable POLY-CRYST to handle molecular crystals of large molecules and with large numbers of large molecules per unit cell. This year we derived and incorporated into the POLY-CRYST including the multipole effects of farther out molecules to include long range effects also. We then meshed this multipole procedure back into the MRD-CI programs to enable us to include multipole effects when breaking a chemical bond in a crystal. We also ran some tests on POLY-CRYST on integral thresholds and numbers of unit cells necessary for convergence. These preliminary tests identified necessary criteria.

Toward this convergence criteria goal, we also derived and implemented a procedure for calculating the charge imbalance caused by various integral thresholds to give a precise measure of the effect on the crystal orbital calculation of dropping integrals of various sizes. The POLY-CRYST program

has promise for yielding important fundamental results on crystalline energetic materials.

We carried out ab-initio crystal orbital calculations on several unit cells of nitromethane to verify that our SCF method in the field of multipoles described above in Part III did correctly describe a crystal of nitromethane.

QUANTUM CHEMICAL INVESTIGATIONS OF THE MECHANISM OF CATIONIC POLYMERIZATION

and

THEORETICAL PREDICTION OF CRYSTAL DENSITIES

and

DECOMPOSITION PATHWAYS OF ENERGETIC MOLECULES

Joyce J. Kaufman, Principal Investigator
Department of Chemistry
The Johns Hopkins University

I. Program Enhancements and New Program Developments on the CRAY Supercomputer.

This past year we have made a significant breakthrough. We developed and implemented and used successfully the strategy for ab-initio MRD-CI (multireference double excitation - configuration interaction) calculations for breaking a chemical bond in a molecule in a crystal or other solid environment. In this procedure the SCF is solved explicitly for the molecules in a unit cell (or larger piece of crystal) in the multipole field of yet further out surrounding molecules. The SCF wave function is localized and the localized orbitals (occupied and virtual) in the region of the bond being broken are included explicitly in the MRD-CI.

This method will be detailed in Section III.

This method is completely general and the results lead to an understanding of fractoemission and the initiation of detonation and the subsequent processes leading to detonation.

We continue to serve on the NSF San Diego Supercomputer Center (SDSC) computer time allocation committee on their CRAY XMP 4/8.

Dr. Kaufman served at the December 1986 Allocation committee meetings, Dr. Hariharan served at the March and June 1987 meetings and Dr. Koski at the September 1987 meeting.

We also receive computer time grants from SDSC which we use for the bulk of our quantum chemical calculations on this ONR research.

II. MRD-CI Calculations for Cationic Polymerization of Energetic Oxetanes

Our major emphasis this past year has been to carry out in-depth detailed ab-initio MRD-CI (multi-reference double excitation-configuration interaction) calculations on the propagation step of cationic polymerization of prototype substitued energetic oxetanes. Cationic polymerization consists essentially of two major steps: initiation and then propagation. There is considerable Navy interest in energetic polymers made by cationic polymerization of oxetanes substituted or disubstituted by exotic energetic substituents such as azido, azidomethyl, nitrato, nitraminomethyl, etc. as well as fluoro and nitro groups. The initiation step (which is crucial for cationic polymerization to take place) is governed by the propensity of the substituted oxetane to undergo protonation. Our previous ab-intio quantum chemical SCF calculations on the energetic oxetane monomers and electrostatic molecular potential contour (EMPC) maps we generated from these electronic wave functions which predict the order of protonation and hence initiation, were able to predict correctly the propensity of the energetic substituted oxetane monomers to undergo polymerization even prior to the synthesis of the monomers.

A. Ab-Initio MRD/CI Calculations for the Propagation Step

1. Discussion of Calculation Procedure and Pathways of Attack

As was suggested to us by several different experimentalists in cationic polymerization (primarily Gerry Manser) the mechanism seems to be attack of protonated oxetanes on oxetanes (or vice versa) with concomitant ring opening of the protonated oxetane according to the following general scheme

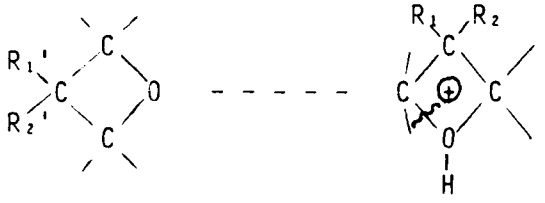

We have carried out this past year and are continuing to carry out ab-initio MRD-CI calculations on the subsequent propagation step of oxetane (or an energetic substituted oxetane) reacting with protonated oxetane (or a protonated energetic substituted oxetane).

In order to understand and to be able to predict copolymerization propensities of various energetic substituted oxetanes it is necessary to trace the reaction pathways of the propagation step in cationic polymerization.

Although geometries of reactants and products may generally be obtained experimentally using a wide varietyof spectroscopic methods these same techniques provide little information about reaction pathways. Thus, the only way that the pathways of reactions and geometries of reaction transition structures may be obtained is from the quantum chemical

calculations theory. Such quantum chemical theory can be used to examine any arrangement of nuclei.

These energetic oxetanes are large molecules for MRD-CI calculations and the systems of energetic oxetanes and protonated oxetanes are even larger and thus beyond the size in which MRD-CI calculations can be carried out in the cpu memory and disc storage of current CRAY XMP supercomputers. Thus we had derived, implemented and tested a new computational strategy for MRD-CI calculations for intermolecular reactions and for molecular decompositions based on localized orbitals. (The strategy is described in more detail later in this section).

MRD-CI calculations along the potential energy surfaces have been carried out for a very large number (at least 25 separate MRD-CI calculated points at different geometries are necessary for each set of reacting partners) of α angles between the planes of the substituted oxetane and protonated substituted oxetane rings (which can be different in each direction in the case of substituted rings), the inter-ring distances (O_{1B}-C_{4A}) (where the A ring is the protonated ring and the B ring is the non-protonated ring), angles δ of opening the C_{4A}-O_{1A} bond in ring A and the orientation of the H atoms on C_{4A} as a function of the inter-ring distance.

For the MRD-CI calculations on oxetanes and protonated oxetanes

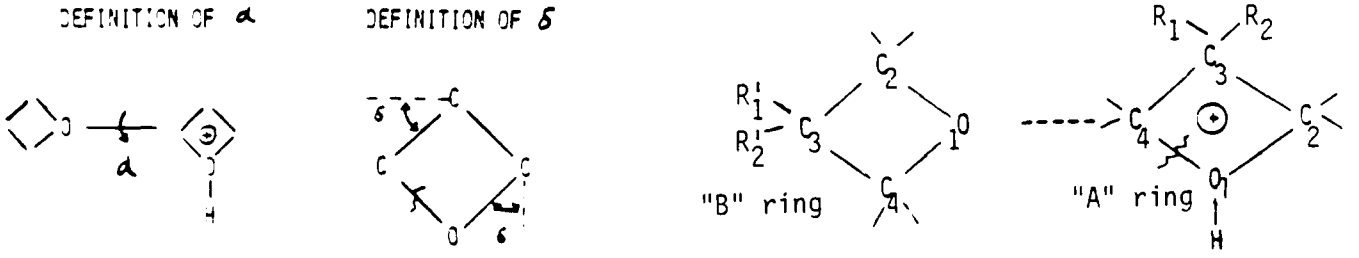

we considered the localized bonds in the C_{4A}-O_{1A} bond, the C_{3A}-C_{4A} bond, the C_{2A}-C_{4A} bond, the O_{1A}-H^+ bond, the lone pairs on O_{1A} and the bonds connecting hydrogens to C_{2A} and C_{4A}, the O_{1B}-C_{4B} bond, the O_{1B}-C_{2B} bond, the bonds connecting hydrogens to C_{2B} and C_{4B} and the inter-ring O_{1B}-C_{4A} bond. This choice of localized orbitals has the great advantage since energetic oxetanes are substituted in the 3 position that it preserves the similarity in the MRD-CI among all the energetic substituted oxetanes and protonated oxetanes and provides a sound basis for comparison.

The preferred direction of attack appears to be the reaction of the oxygen (which we call O_{1B}) of the unprotonated oxetane ring on the α carbon

(which we call C_{4A}) of the protonated substituted oxetane ring along the C_{4A}-O_{1A} bond direction with concomitant pulling back (inversion of the H atoms on C_{4A}) and opening of the C_{4A}-O_{1A} bond in the protonated oxetane ring, similar to an S_N2 reaction mechanism.

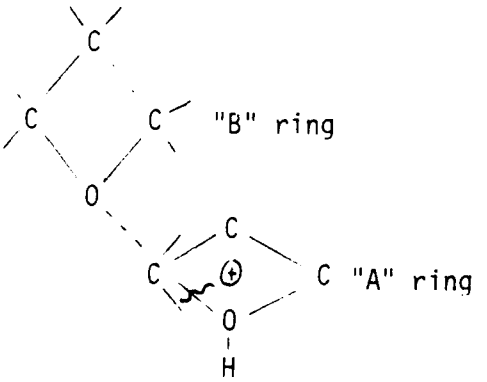

The angle α between the two rings is determined for $R(O_{1B}\text{-}C_{4A})$ = 2.6 - 2.9 - 3.4 bohrs and is used for all other geometries.

Two bonds are essential. C_{4A}-O_{1A} and O_{1B}-C_{4A} are essential to describe the reaction pathway. The bond inside the protonated oxetane ring (C_{4A}-O_{1A}) varies from R = 2.8 to R = 4.9 bohrs which correspond to the fully closed and fully open ring of the protonated oxetane. This bond is described by the parameter δ which varies from 0° (fully closed ring) to 19° (fully open ring) and corresponds to the degree of openness of the ring.

The O_{1B}-C_{4A} bond is changed from $R(O_{1B}\text{-}C_{4A})$ from R = 2.1 bohrs to R = 10.0 bohrs.

Positions of the proton H^+ and hydrogens connected to C_{4A} atom are the most affected by opening the ring and their positions were determined for the prototype system OXET + $FNOXH^+$. These proton and hydrogen positions were then used for subsequent studies of propagations reactions involving other protonated energetic oxetanes.

We had previously shown that ab-initio MODPOT/VRDDO MRD-CI calculations for oxetanes and protonated oxetanes gave energy differences and MRD-CI coefficients very close to those from much larger basis set all-electron MRD-CI calculations.

Ab-initio MODPOT/VRDDO MRD-CI calculations have been carried out for each point of the potential surface of oxetanes reacting with protonated

oxetanes in the propagation step of cationic polymerization. Because of the size of the intermolecular complex molecular orbitals selected from localized space are used in the MRD-CI calculations. The geometries studied include the most sensitive part of the complex in the the MRD-CI procedure. Ten of the most important main reference configurations have been used in MRD-CI treatment, and the same set of main reference configurations have been kept through whole potential surface. All single and double excitations were allowed relative to these main configurations. The energies of each of the thousands of contributing configurations is estimated by a perturbation procedure; a threshold is set for which contributions wil be included explicitly in the MRD-CI, in the following tables, this MRD-CI energy is designated CI. Then the energies of all of the other configurations generated but not included explicitly in the MRD-CI are extrapolated and added back in, this energy is designated EX. Finally a Davidson type correction (which has been shown to be a good correction) for size extensivity is added in.

$$E(\text{full CI estimate}) = E(EX) + \left(1 - \sum_{p}^{ref} C_p^2\right) [E(EX) - E(Ref)]$$

and the summation is over all reference species. The use of multiconfigurational scheme is to assure avoiding of possible artifacts.

Our MRD-CI results support the suggestions of Gerry Manser as to the mechanism of the propagation step in cationic polymerization of oxetanes. We discussed this with Gerry and he was quite gratified that our theoretical results were in accord with his hypothesis.

These MRD-CI calculations have enabled us to map out the reaction coordinates of the propagation step reaction of oxetane (or an energetic substituted oxetane) reacting with protonated oxetane (or with a protonated energetic substituted oxetane), to identify the transition state of the propagation step and to identify when the C_{4A}-O_{1A} bond in the protonated oxetane will start to open as a function of inter-ring distance and angle for each different pair of substituted reactants.

By comparing these results for different pairs of reacting substituted oxetanes and protonated substituted oxetanes we shall be able to gain insight into preferred copolymer candidates and relative reactivity ratios.

As we mentioned above, the substituted oxetanes are large molecular systems and their interactions with protonated substituted oxetanes lead to even larger systems. These are larger molecular systems than have ever been calculated with MRD-CI methods and also exceed the amount of data that can be handled even in the current CRAY-XMP series with the available core and disc space.

We had previously developed and validated a new MRD-CI approach based on localized orbitals in the reaction/interaction region with the remainder of the non-participating localized occupied molecular orbitals being folded into an effective CI Hamiltonian. We had shown by test examples that the

MRD-CI based on localized orbitals give a potential energy surface for molecular decomposition essentially parallel to that using the entire valence space MRD-CI. These MRD-CI calculations for the reaction of substituted protonated oxetanes with substituted oxetanes are a computationally and labor intensive project. For each different inter- and intra-molecular geometry point, first the SCF calculation must be run, then the resulting SCF canonical delocalized molecular orbitals must be localized. In addition to determining the centroids of the localized bonds compared to the bonds and atoms involved in the interaction/reaction, this past year we supplemented this with additional procedures to ensure that all pertinent bonds, lone pairs, vacant orbitals etc. would be included in the localized orbital MRD-CI. After localization a small single reference CI must be carried out to determine the major reference configurations to include in the subsequent MRD-CI. A great advantage in our carrying out the ab-initio MRD-CI calculations based on the important localized orbitals in the interaction/reaction region is the reasonable similarity of types of major reference configurations for the variously energetic substituted oxetanes and energetic substituted protonated oxetanes.

By first carrying out detailed MRD-CI calculations on the partners (oxetanes and protonated oxetanes) of oxetane itself, with the prototype energetic oxetane, FNOX (3-fluoro-3-nitrooxetane) we have been able to identify the most pertinent portions of the interaction surface and their electronic characteristics. This behavior was verified by our similar calculations involving protonated with non-protonated partners of oxetane and AMMO (3-azidomethyl-3-methyloxetane) We can now focus on these regions for our calculations involving other even larger energetic substituted oxetanes and protonated substituted oxetanes to identify copolymerizaton propensities and optimal copolymer candidates.

2. Detailed Results for Prototype Examples are presented in the following pages.

(1). OXET + $OXETH^+$, OXET + $FNOXH^+$, FNOX + $OXETH^+$, FNOX + $FNOXH^+$

(a). Energies

1'. Oxetane (OXET) + protonated oxetane ($OXETH^+$)

a'. Determination of The Pathway

The addition of oxetane (OXET) to protonated oxetane ($OXET^+$) has the features of an S_N2 reaction as we reported preliminarily last year. The approach presented utilizes these features to the greatest extent. Geometry of the reacting system: The reaction of OXET with $OXETH^+$ is assumed to be an S_N2 reaction with molecule B (OXET) attacking molecule A ($OXETH^+$) along the O_{1B}-C_{4A}-O_{1A} line. It is found that head on geometry for approaching oxetane is energetically preferred, thus the C_{3B} is also kept on the O_{1B}-C_{4A}-O_{1A} line.

The geometry for the oxetane-protonated oxetane complex is presented in Figure II-1, "The Geometry for Oxetane - Protonated Oxetane Complex"

The optimal angle α between the rings has been found to be 90°, but differences between different angles are not significant.

The opening (C_{4A}-O_{1A}) of the protonated oxetane ring starts at $R(O_{1B}\text{-}C_{4A})$ = 4.6 bohrs. Next both: O_{1B}-C_{4A} and C_{4A}-O_{1A} change simultaneously until the complex reaches the stabilization point at $R(O_{1B}\text{-}C_{4A})$ at 2.9 bohrs and δ = 19° (fully open). The stabilization energy at R = 2.9 bohrs and δ = 19° is -.04378 a.u. = -27.97 kcal/mol. The estimated activation energy is 6.27 kcal/mol.

b'. Method of calculation

The ab-initio MODPOT/VRDDO calculations have been carried out for each point of the surface. Because of the size of the intermolecular complex of the two reacting species molecular orbitals selected from the localized space were used in the MRD-CI calculations. The geometries studied include the most sensitive part of the complex (Figure II-8) in the CI procedure. Ten of the most important main reference configurations have been used in MRD-CI treatment, and the same set of main reference configurations has been kept through whole

potential surface. The use of multiconfigurational scheme is to assure avoiding of the possible artifacts.

The potential energy surfaces and reaction potential map of OXET - $OXETH^+$ complex are presented in Figures II-2 to II-5.

Figure II-2: MRD-CI Extrapolated Energy for Oxetane-Protonated Complex for Fixed Angle δ and Different Intermolecular Distances R(O1B-C4A)

Figure II-3: MRD-CI Extrapolated Energy for Oxetane-Protonated Oxetane Complex for Fixed Intermolecular Distances R(O1B-C4A) and Different δ Angle Values

Figure II-4: OXET-$OXETH^+$, Extrapolated CI Energy Along the Reaction Coordinate for Oxetane plus Protonated Oxetane Addition Reaction.

Figure II-5: The Potential Energy Surface for OXET Approaching Protonated OXET

The detailed tables of results follow.

Table II-1: "OXET + $OXETH^+$ [R(O1B-C4A) = 3.4 bohrs] (different α values)

Table II-2: OXET + $OXETH^+$ δ = 0° (fully closed), Energies (a.u.) as a function of R(O1B-C4A)

Table II-3: OXET + $OXETH^+$ δ = 5° , Energies (a.u.) as a function of R(O1B-C4A)

Table II-4: OXET + $OXETH^+$ δ = 10° , Energies (a.u.) as a function of R(O1B-C4A)

Table II-5: OXET + $OXETH^+$ δ = 15° , Energies (a.u.) as a function of R(O1B-C4A)

Table II-6: OXET + $OXETH^+$ δ = 19° , Energies (a.u.) as a function of R(O1B-C4A)

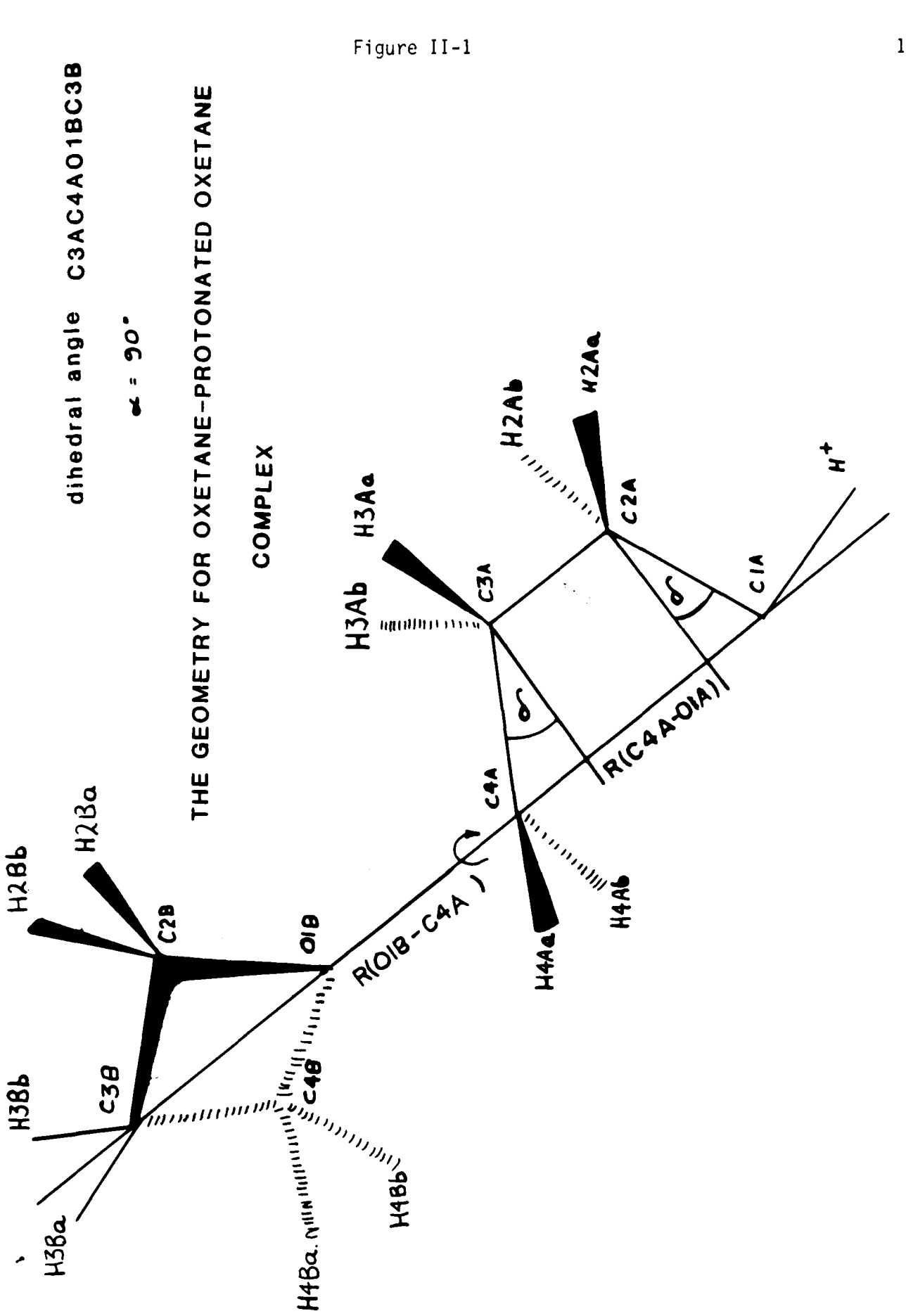
THE GEOMETRY FOR OXETANE-PROTONATED OXETANE COMPLEX
dihedral angle C3AC4AO1BC3B
α = 90°
H2Bb
H2Ba
C2B
O1B
R(O1B-C4A)
C4A
H4Ab
H4Aa
H2Ab
H2Aa
C2A
H3Aa
H3Ab
C3A
C1A
R(C4A-O1A)
H+
H3Bb
C3B
C4B
H4Bb
H4Ba
H3Ba

MRD-CI EXTRAPOLATED ENERGY FOR OXETANE-PROTONATED COMPLEX FOR FIXED ANGLE δ

E (A=0°, B=5°, C=10°, D=15°, E=19°) AND DIFFERENT INTERMOLECULAR DISTANCES R

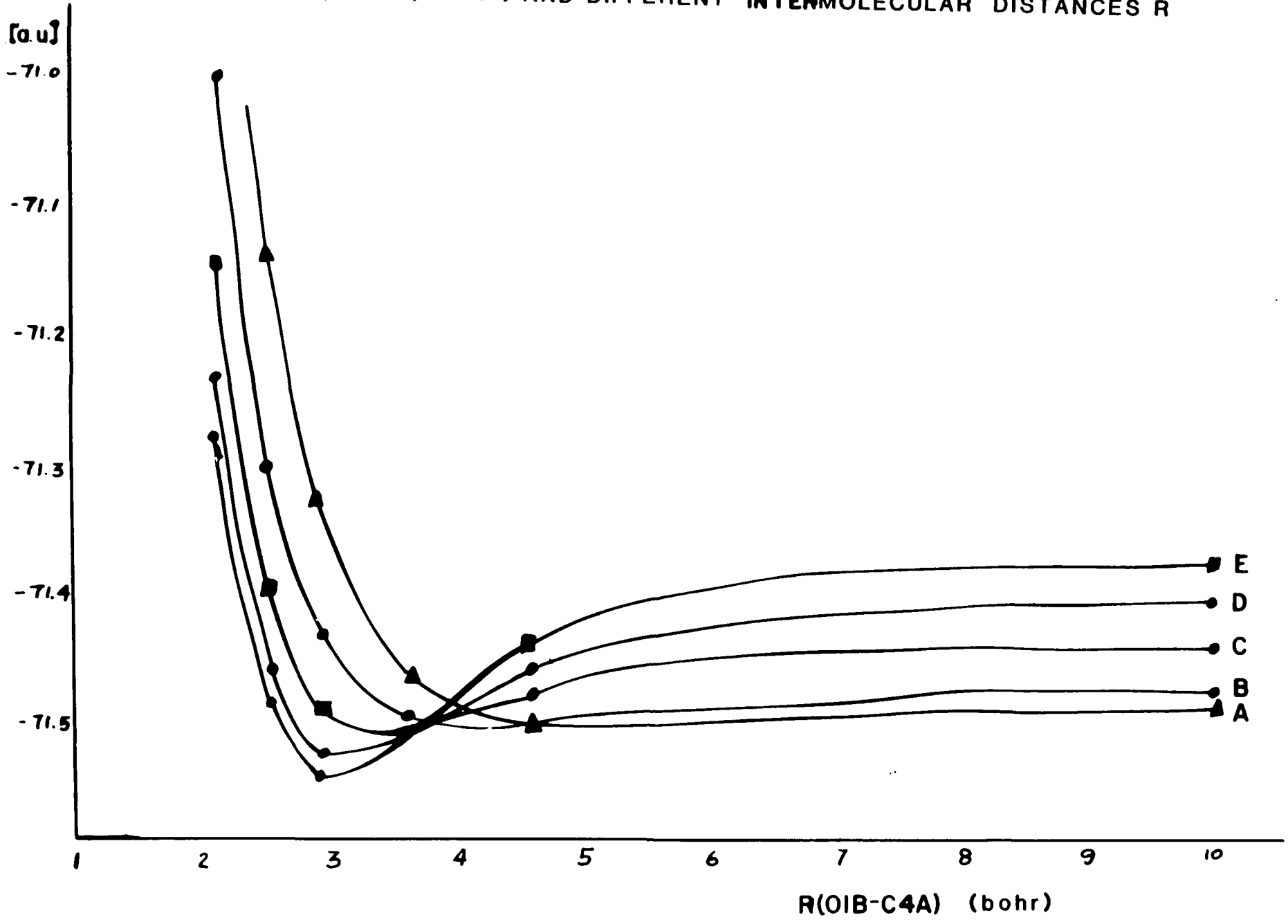

Fiaure II-2

MRD-CI EXTRAPOLATED ENERGY FOR OXETANE-PROTONATED OXETANE COMPLEX FOR FIXED INTERMOLECULAR DISTANCES R(O1B-C4A) AND DIFFERENT δ ANGLE VALUES

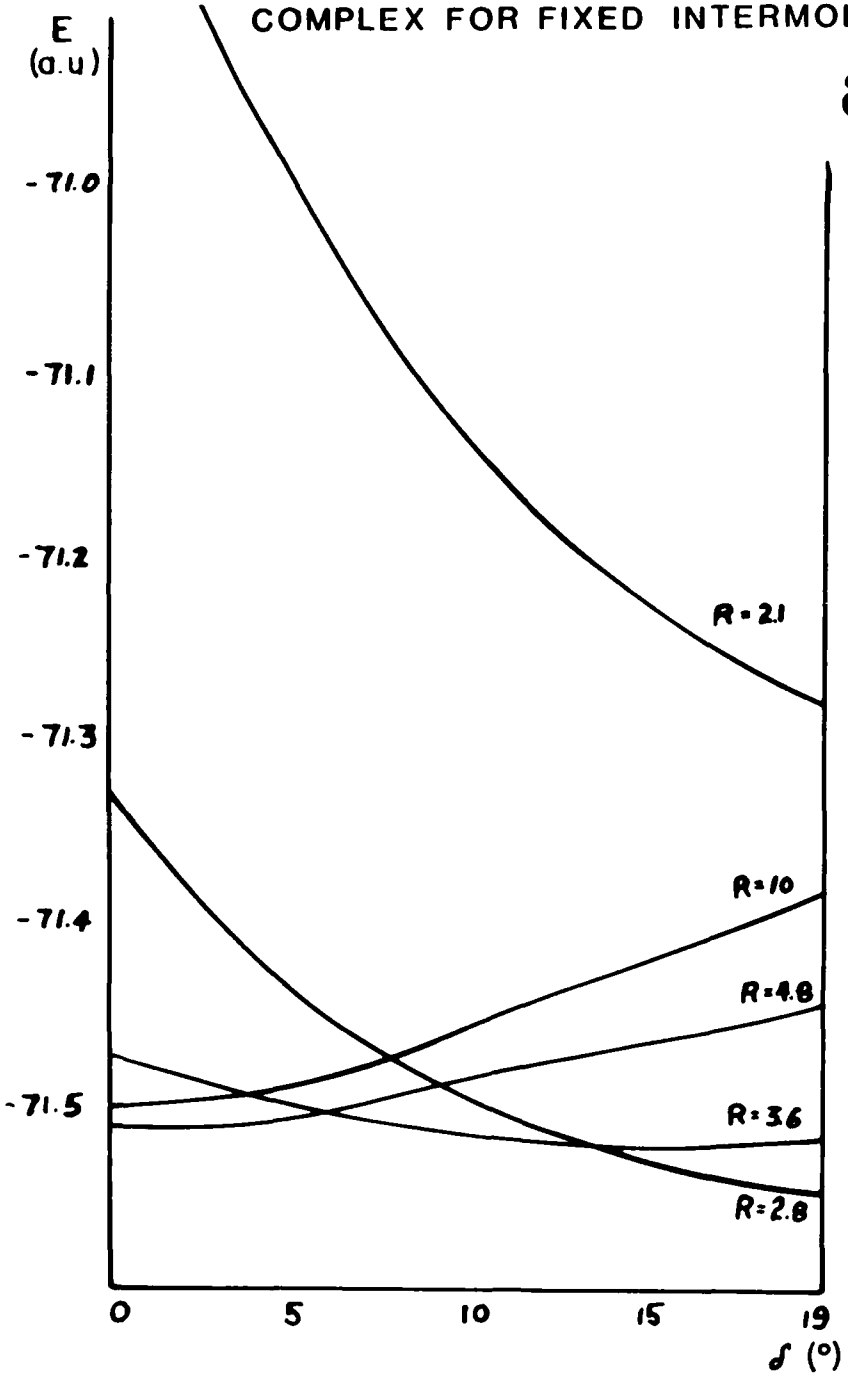

Figure II-3

Figure II-4

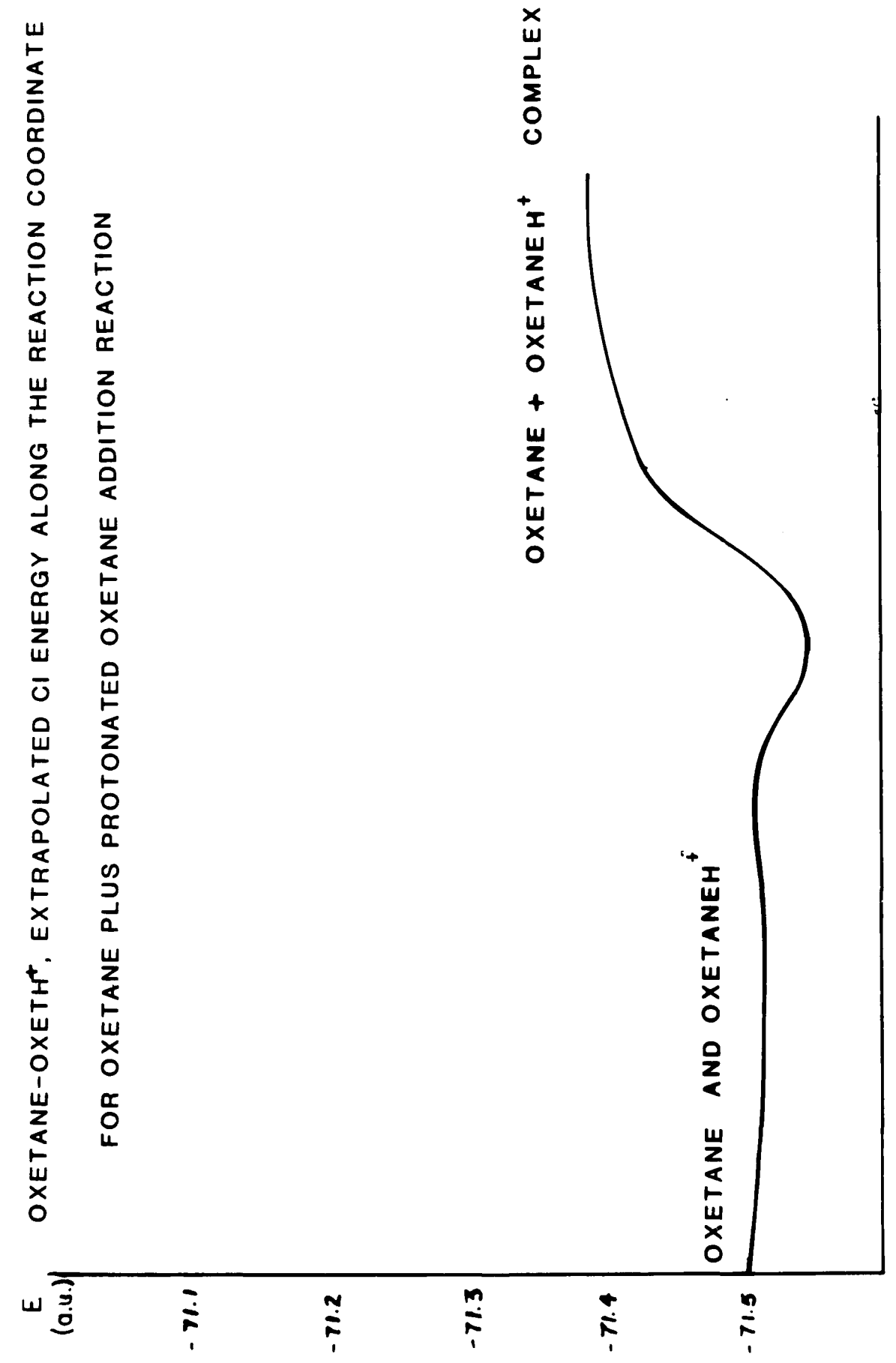
OXETANE-OXETH+, EXTRAPOLATED CI ENERGY ALONG THE REACTION COORDINATE
FOR OXETANE PLUS PROTONATED OXETANE ADDITION REACTION
E (a.u.)
-71.1
-71.2
-71.3
-71.4
-71.5
OXETANE + OXETANEH+ COMPLEX
OXETANE AND OXETANEH+
REACTION COORDINATE

THE POTENTIAL ENERGY SURFACE FOR OXET APPROACHING PROTONATED OXET. THE DASHED LINE IS THE REACTION COORDINATE. THE VALUES ON THE GRAPH CORRESPOND TO EXTRAPOLATED MRD-CI ENERGY BY EQUATION E -71.5+a (a.u.)

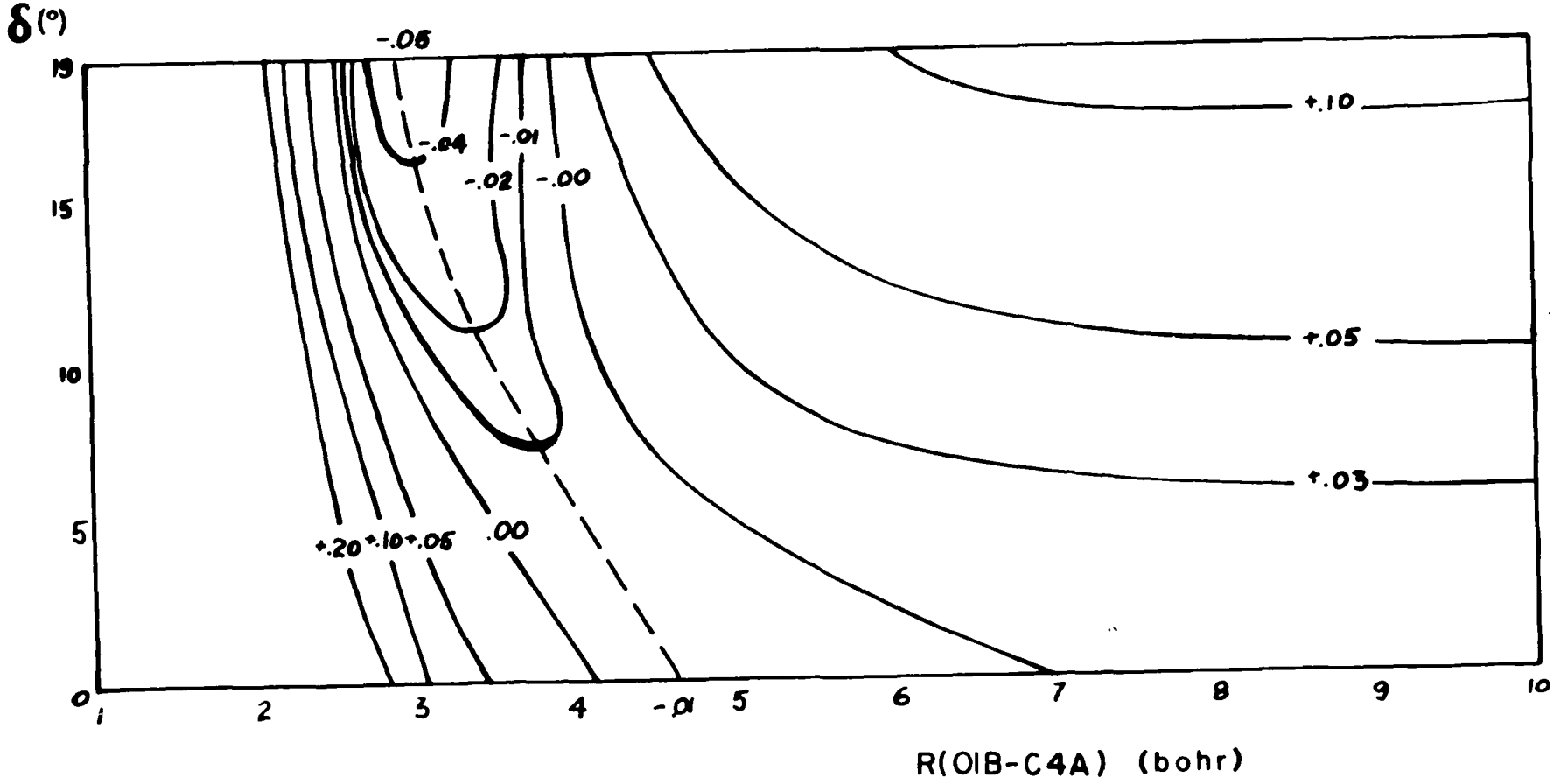

Figure II-5

TABLE II - 1

OXET + $OXETH^+$ [R(O1B-C4A) = 3.4 bohrs]
(DIFFERENT α VALUES)

ENERGIES (a.u.)

	δ = 0° (FULLY CLOSED)		δ = 19° (FULLY OPEN)	
α (°)	SCF	CI,EX	SCF	CI,EX
90	-71.165534	-71.359265	-71.120867	-71.306027
135	-71.163113	-71.355541	-71.120512	-71.304423
180	-71.160545	-71.352441	-71.119567	-71.301750

minimum for α = 90°

α = angle between planes of rings

δ = angle of opening of protonated ring

TABLE II - 2

A

OXET + $OXETH^+$

$\delta = 0^o$ (FULLY CLOSED)

ENERGIES (a.u.)

R(O1B-C4A) (bohrs)	2.1	2.5	2.9
SCF	-70.560381	-70.935433	-71.133963
CI	-70.755971	-71.130522	-71.325511
EX	-70.764130	-71.138320	-71.332365
DAV	-70.767576	-71.141576	-71.335368
c^2	.963	.964	.964
gs	.904	.905	.905

R(O1B-C4A) (bohrs)	3.6	4.1	4.6
SCF	-71.282489	-71.3153506	-71.3248406
CI	-71.467731	-71.498166	-71.506188
EX	-71.474386	-71.503304	-71.511483
DAV	-71.476889	-71.505569	-71.513815
c^2	.967	.968	.989
gs	.905	.905	.905

R(O1B-C4A) (bohrs)	10.0
SCF	-71.315625
CI	-71.497548
EX	-71.501413
DAV	-71.503505
c^2	.969
gs	.903

c^2 is the contribution of all of the reference configurations

gs is the contribution of the ground state SCF wave functions

TABLE II - 3

B

OXET + $OXETH^+$

($\delta = 5^o$)

ENERGIES (a.u.)

R(O1B-C4A) (bohrs)	2.1	2.5	2.9
SCF	-70.804448	-71.109877	-71.241954
CI	-70.991765	-71.298261	-71.429245
EX	-70.998971	-71.305820	-71.437324
DAV	-71.001469	-71.308416	-71.440114
c^2	.968	.967	.965
gs	.905	.905	.904

R(O1B-C4A) (bohrs)	3.6	4.1	4.6
SCF	-71.315482	-71.324034	-71.322182
CI	-71.498182	-71.505390	-71.502834
EX	-71.503904	-71.510932	-71.507776
DAV	-71.506605	-71.513540	-71.510269
c^2	.964	.964	.965
gs	.904	.902	.901

R(O1B-C4A) (bohrs)	10.0
SCF	-71.303100
CI	-71.485062
EX	-71.488757
DAV	-71.491173
c^2	.965
gs	.898

TABLE II - 4

C

$OXET + OXETH^{+}$

($\delta = 10^{o}$)

ENERGIES (a.u.)

R(O1B-C4A) (bohrs)	2.1	2.5	2.9
SCF	-70.958600	-71.217923	-71.308731
CI	-71.138404	-71.399798	-71.491715
EX	-71.144042	-71.405662	-71.497156
DAV	-71.146096	-71.407782	-71.499457
c^2	.971	.970	.968
gs	.908	.907	.905

R(O1B-C4A) (bohrs)	3.6	4.1	4.6
SCF	-71.330412	-71.318510	-71.305275
CI	-71.509340	-71.494130	-71.478736
EX	-71.514915	-71.499211	-71.483719
DAV	-71.517429	-71.501685	-71.486078
c^2	.965	.964	.965
gs	.903	.904	.903

R(O1B-C4A) (bohrs)	10.0
SCF	-71.273589
CI	-71.446907
EX	-71.450690
DAV	-71.452995
c^2	.964
gs	.901

TABLE II - 5

D

OXET + $OXETH^+$

($\delta = 15^o$)

ENERGIES (a.u.)

R(O1B-C4A) (bohrs)	2.1	2.5	2.9
SCF	-71.052683	-71.281971	-71.347995
CI	-71.227256	-71.459679	-71.527670
EX	-71.232863	-71.464859	-71.532460
DAV	-71.234740	-71.466807	-71.535503
c^2	.973	.971	.962
gs	.912	.909	.906

R(O1B-C4A) (bohrs)	3.6	4.1	4.6
SCF	-71.338394	-71.312645	-71.290592
CI	-71.516580	-71.486829	-71.460933
EX	-71.521608	-71.491883	-71.465153
DAV	-71.523932	-71.494220	-71.467242
c^2	.966	.965	.967
gs	.902	.902	.904

R(O1B-C4A) (bohrs)	10.0
SCF	-71.246902
CI	-71.414410
EX	-71.417747
DAV	-71.419465
c^2	.970
gs	.903

TABLE II - 6

E

$OXET + OXETH^+$

$\delta = 19^o$ (FULLY OPEN)

ENERGIES (a.u.)

R(O1B-C4A) (bohrs)	2.1	2.5	2.9
SCF	-71.101569	-71.310287	-71.360621
CI	-71.274272	-71.486679	-71.540063
EX	-71.279263	-71.491058	-71.545193
DAV	-71.281108	-71.492874	-71.547200
c^2	.973	.972	.970
gs	.913	.910	.906

R(O1B-C4A) (bohrs)	3.6	4.1	4.6
SCF	-71.332170	-71.297912	-71.269955
CI	-71.512029	-71.474238	-71.441685
EX	-71.516097	-71.478066	-71.445050
DAV	-71.518387	-71.480429	-71.447196
c^2	.966	.964	.966
gs	.901	.900	.902

R(O1B-C4A) (bohrs)	10.0
SCF	-71.217258
CI	-71.383225
EX	-71.385572
DAV	-71.387004
c^2	.973
gs	.905

2'. Oxetane (OXET) + Protonated 3-fluoro-3-nitrooxetane ($FNOXH^+$)

a'. Determination of the pathway for oxetane (OXET) and protonated 3-fluoro-3-nitrooxetane ($FNOXH^+$) addition reaction.

The addition of oxetane (OXET) to protonated 3-fluoro-3-nitrooxetane ($FNOXH^+$) has the features of the S_N2 reaction, and the approach presented utilizes these to the greatest extent.

The geometry of reacting system.

The reaction of oxetane with protonated FNOX is assumed to be the S_N2 type reaction, with molecule B attacking molecule A (Figure II - 6) along the O_{1B}-C_{4A}-O_{1A} line. Figure II-6: "The Geometry For Oxetane - Protonated FNOX Complex" Since it was found for oxetane reacting with protonated oxetane that head on geometry for approaching oxetane is energetically preferred the C_{3B} atom is also kept on O_{1B}-C_{4A}-O_{1A} line. Because essential structural changes are expected to appear relative to the plane of FNOX ring the angle alpha between the two rings was determined for $R(O_{1B}$-$C_{4A}) = 2.6$ bohrs and was used for all other geometries. The optimal alpha angle has been found to be 55 degrees. Figure II-7, Table II-7 "OXET + $FNOXH^+$, SCF And CI Energy For Different Values of Angle Between Two Rings (Alpha) (Fully Closed Geometry)"

Two bonds: C4A-O1A and O1B-C4A are essential to describe the reaction pathway. The bond inside the FNOX ring (C4A-O1A) changes only from R = 2.8 bohrs to R = 4.9 bohrs, which corresponds to the fully closed and fully open ring of $FNOXH^+$. This bond is later described by the more natural parameter δ which varies from 0° (fully closed) to 19° (fully open), and corresponds to degree of openess of the ring. The O1B-C4A bond is changed from R = 2.1 bohrs to R = 10.0 bohrs.

Positions of proton H^+ and hydrogens connected to C_{4A} atom are the most affected by opening the ring and these positions have been determined optimally for each different $FNOXH^+$-ring geometry.

b'. Method of Calculation

The ab-initio MODPOT/VRDDO calculations have been carried out for each point of the surface. Because

of the size of the intermolecular complex of the two reacting species molecular orbitals selected from the localized space were used in the MRD-CI calculations. The geometries studied include the most sensitive part of the complex (Figure II - 8: "The Geometrical State of Oxetane-$FNOXH^+$ Selected for MRD-CI Calculations") in the CI procedure. Ten of the most important main reference configurations have been used in MRD-CI treatment, and the same set of main reference configurations has been kept through whole potential surface. The use of multiconfigurational scheme is to assure avoiding of possible artifacts.

c'. Results for oxetane and $FNOXH^+$.

The ring opening starts when oxetane approaches $FNOXH^+$ for $R(O_{1B}-C_{4A})$ = 4.6 bohrs. Next, both: $O_{1B}-C_{4A}$ and $C_{4A}-O_{1A}$ change simultaneously until the complex reaches the stabilization point at $R(O_{1B}-C_{4A})$ = 2.9 bohrs. and δ = 19° (fully open). The stabilization energy for the complex is -0.0603 a.u. = -39.7 kcal/mol. The reaction goes through transition state with activation energy approximately .005 a.u. = 3.13 kcal/mol.

The potential energy surfaces and reaction potential map for oxetane-$FNOXH^+$ complex are presented in Figures II-9 to II-11.

Figure II-9: "MRD-CI Extrapolated Energy for Oxetane Approaching Protonated FNOX for Fixed Angle δ and Different Intermolecular Distances R(01B-C4A)

Figure II-10: "MRD-CI Extrapolated Energy for Oxetane-Protonated FNOX Complex For Fixed Intermolecular Distances R(01B-C4A) and Different δ Angle Values

Figure II-11: "OXET + $FNOXH^+$, Extrapolated CI Energy Along The Reaction Coordinate For Oxetane-Protonated FNOX Addition Reaction

Figure II-12: "The Potential Energy for Oxetane Approaching FNOX"

The detailed tables of results follow.

Table II-8: "OXET + $FNOXH^+$ δ = 0° (fully closed), Energies (a.u.) as a function of R(01B-C4A)"

Table II-9: "OXET + $FNOXH^+$ δ = 5°, Energies (a.u.) as a function of R(01B-C4A)"

Table II-10: "OXET + $FNOXH^+$ δ = 10°, Energies (a.u.) as a function of R(01B-C4A)"

Table II-11: "OXET + $FNOXH^+$ δ = 15°, Energies (a.u.) as a function of R(01B-C4A)"

Table II-12: "OXET + $FNOXH^+$ δ = 19° (fully open), Energies (a.u.) as a function of R(O1B-C4A)"

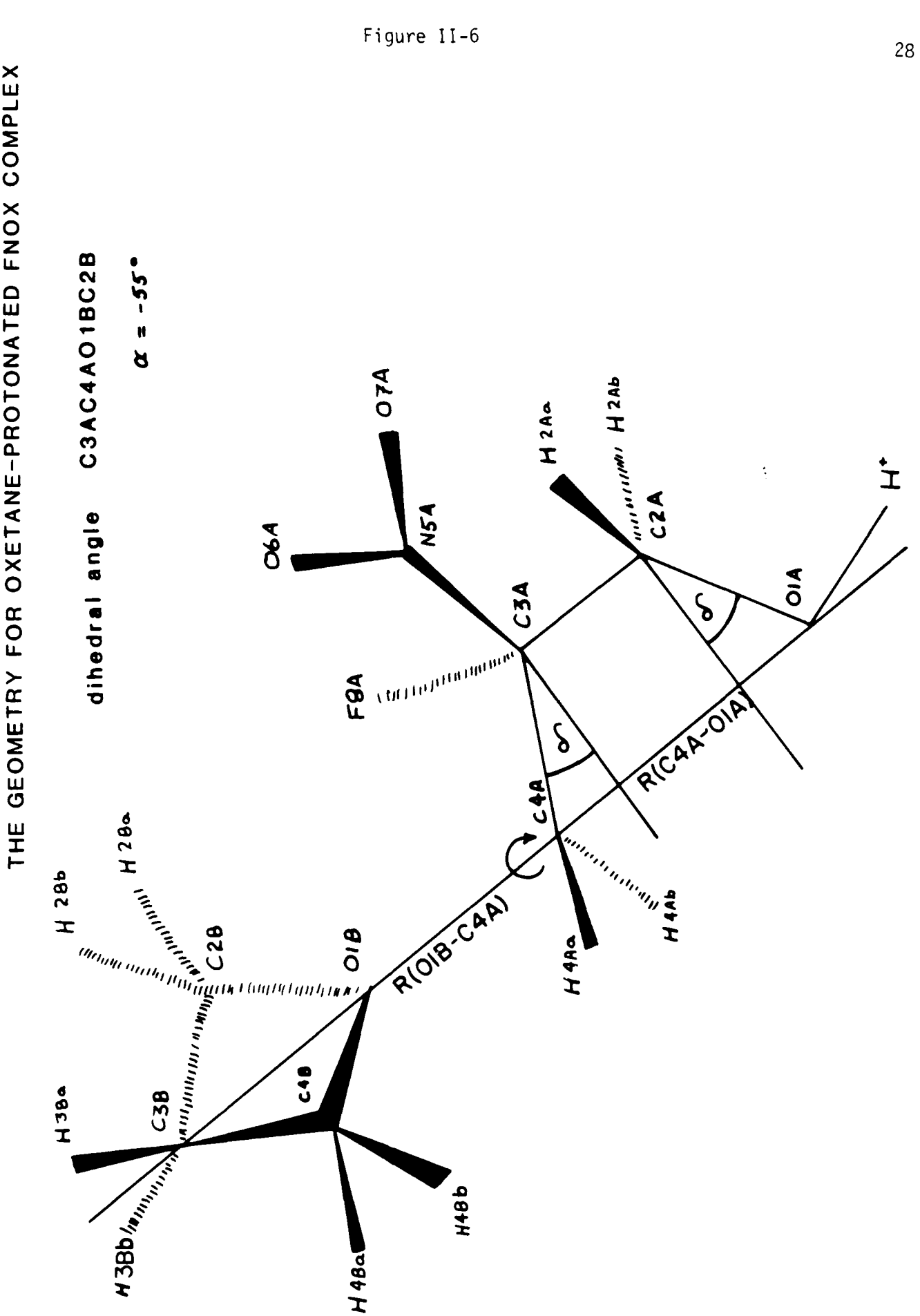
THE GEOMETRY FOR OXETANE-PROTONATED FNOX COMPLEX
dihedral angle C3AC4AO1BC2B
α = -55°
O7A
O6A
N5A
C3A
F8A
H 2Aa
H 2Ab
C2A
O1A
H+
R(C4A-O1A)
C4A
R(O1B-C4A)
H 4Aa
H 4Ab
H 28b
H 28a
C2B
O1B
H 38a
C3B
C4B
H 38b
H 48a
H 48b

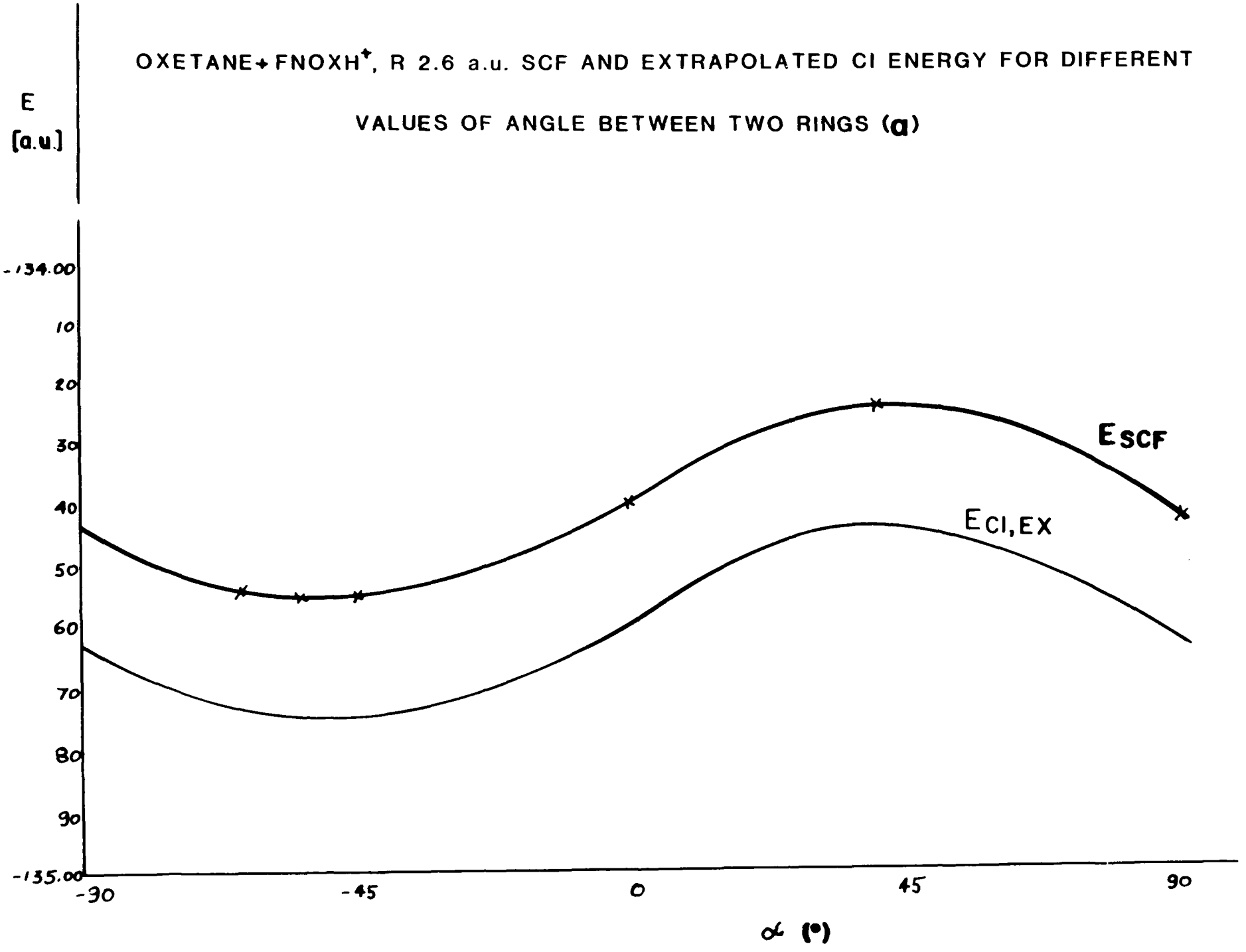
OXETANE + FNOXH+, R 2.6 a.u. SCF AND EXTRAPOLATED CI ENERGY FOR DIFFERENT VALUES OF ANGLE BETWEEN TWO RINGS (α)
E [a.u.]
-134.00
10
20
30
40
50
60
70
80
90
-135.00
-90
-45
0
45
90
α (°)
ESCF
ECI,EX

Figure II-7

THE GEOMETRICAL STATE OF OXETANE-FNOXH$^+$ SELECTED FOR MRD-CI CALCULATIONS

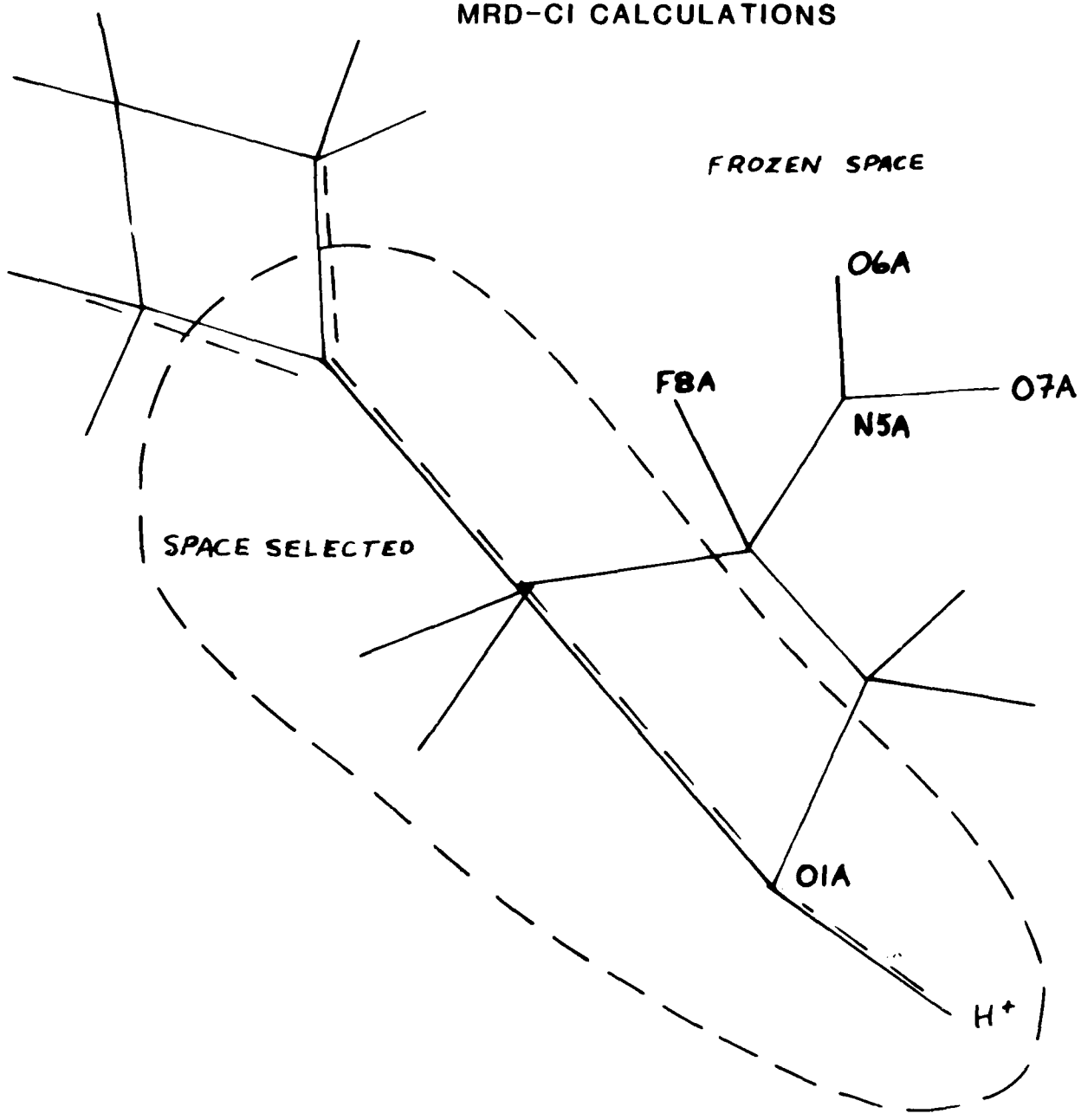

Figure II-3

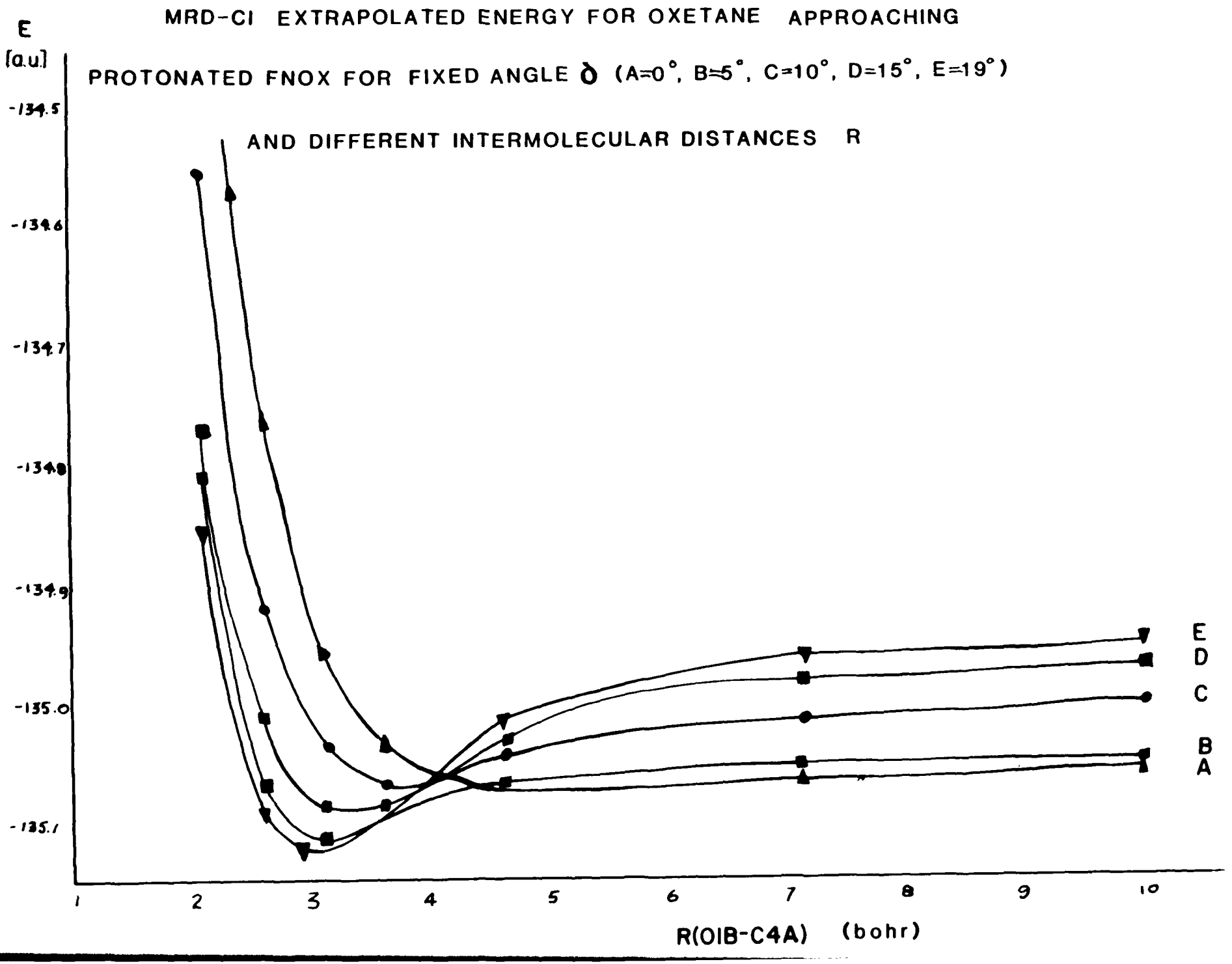
MRD-CI EXTRAPOLATED ENERGY FOR OXETANE APPROACHING
PROTONATED FNOX FOR FIXED ANGLE δ (A=0°, B=5°, C=10°, D=15°, E=19°)
AND DIFFERENT INTERMOLECULAR DISTANCES R
E
[a.u]
-134.5
-134.6
-134.7
-134.8
-134.9
-135.0
-135.1
1
2
3
4
5
6
7
8
9
10
R(O1B-C4A) (bohr)
E
D
C
B
A

Figure II-9

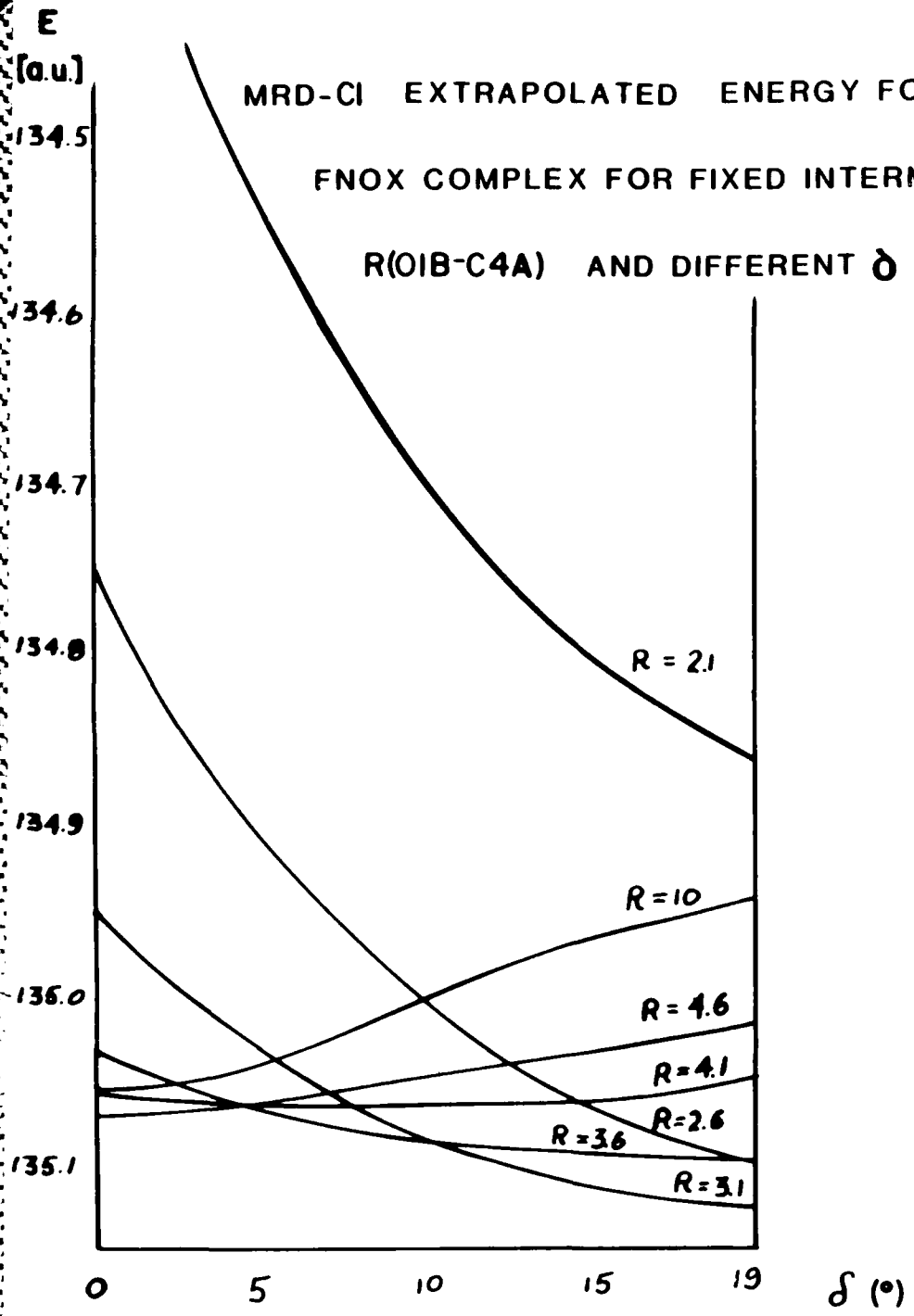
E
[a.u.]
MRD-CI EXTRAPOLATED ENERGY FOR OXETANE-PROTONATED
FNOX COMPLEX FOR FIXED INTERMOLECULAR DISTANCES
R(O1B-C4A) AND DIFFERENT δ ANGLE VALUES.
134.5
134.6
134.7
134.8
134.9
136.0
135.1
R = 2.1
R = 10
R = 4.6
R = 4.1
R = 2.6
R = 3.6
R = 3.1
0
5
10
15
19
δ (°)

Figure II-10

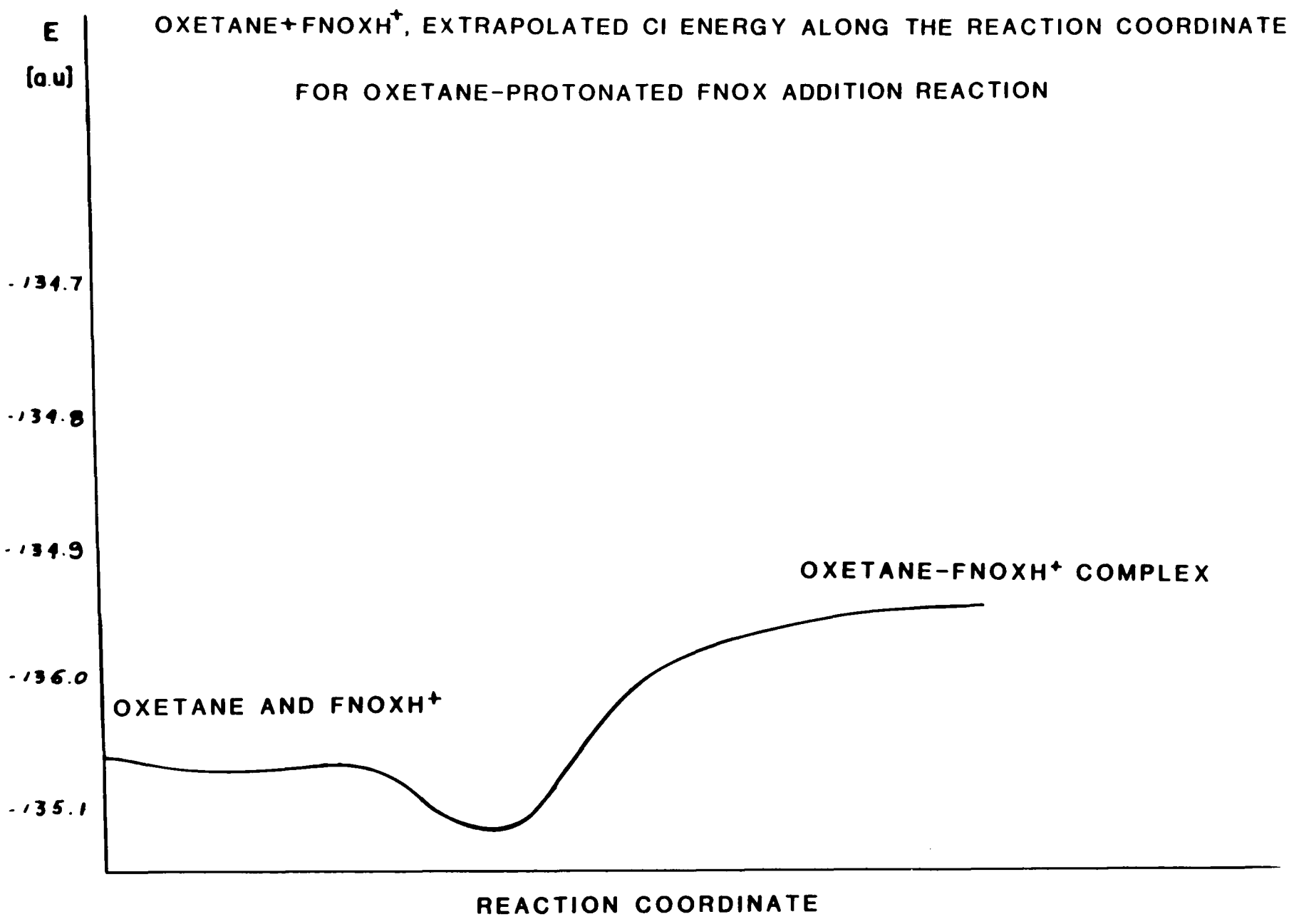
OXETANE+FNOXH+, EXTRAPOLATED CI ENERGY ALONG THE REACTION COORDINATE
FOR OXETANE-PROTONATED FNOX ADDITION REACTION
E
(a.u)
-134.7
-134.8
-134.9
-136.0
-135.1
OXETANE-FNOXH+ COMPLEX
OXETANE AND FNOXH+
REACTION COORDINATE

Figure II-11

THE POTENTIAL ENERGY SURFACE FOR OXETANE APPROACHING PROTONATED FNOX.

THE DASHED LINE IS THE REACTION COORDINATE. THE VALUES ON THE GRAPH

CORRESPOND TO EXTRAPOLATED MRD-CI ENERGY BY EQUATION E = 135.0+a (a.u.)

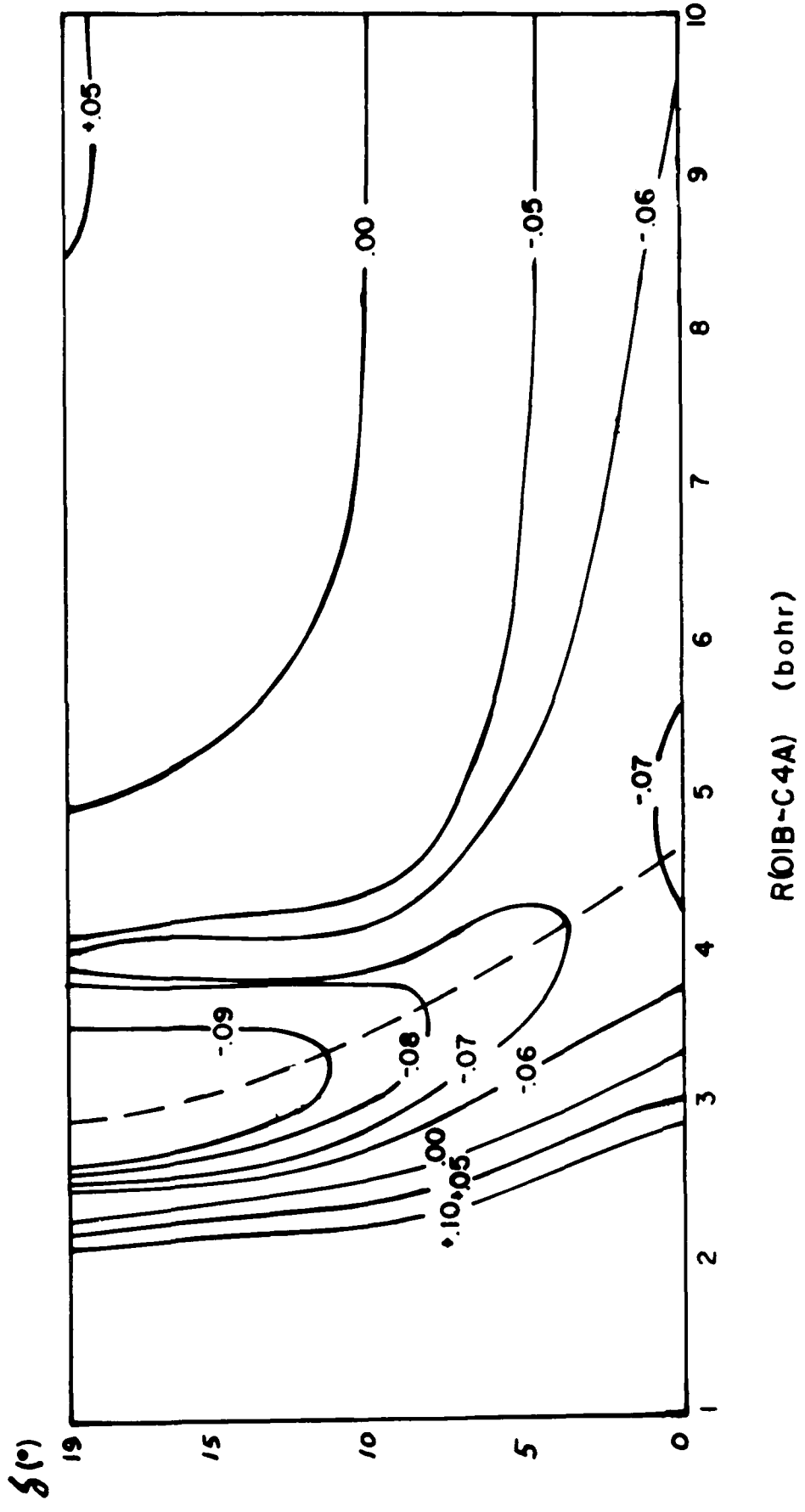

TABLE II - 7

OXET + $FNOXH^+$

SCF AND CI ENERGY (a.u.) FOR DIFFERENT VALUES OF ANGLE BETWEEN TWO RINGS (ALPHA)

(FULLY CLOSED GEOMETRY)

α (^{o})	-0	-45	-55
SCF	-134.40904	-134.56213	-134.56319
CI	-134.59884	-134.75371	-134.75493
EX	-134.60698	-134.76151	-134.76290
DAV	-134.61009	-134.76467	-134.76608

α (^{o})	-65	90 (-90)	-135
SCF	-134.55734	-134.43763	-134.25124
CI	-134.74906	-134.62844	-134.43975
EX	-134.75688	-134.63601	-134.44762
DAV	-134.76006	-134.63916	-134.45070

TABLE II - 8

A

OXET + $FNOXH^+$

$\delta = 0^o$ (FULLY CLOSED)

ENERGIES (a.u.)

R(O1B-C4A) (bohrs)	2.1	2.6	3.1
SCF	-134.110905	-134.563192	-134.762800
CI	-134.302148	-134.754932	-134.950999
EX	-134.310289	-134.762896	-134.958205
DAV	-134.313487	-134.766081	-134.961110
c^2	.965	.964	.965
GS	.907	.907	.907

R(O1B-C4A) (bohrs)	3.6	4.1	4.6
SCF	-134.847935	-134.878792	-134.887225
CI	-135.031883	-135.060623	-135.067424
EX	-135.038693	-135.065956	-135.072717
DAV	-135.041224	-135.068729	-135.074857
c^2	.967	.962	.969
gs	.907	.902	.906

R(O1B-C4A) (bohrs)	7.1	10.0
SCF	-134.882235	-134.877230
CI	-135.062520	-135.058033
EX	-135.066463	-135.061843
DAV	-135.068503	-135.063898
c^2	.970	.970
gs	.905	.904

TABLE II - 9

B

OXET + $FNOXH^+$

$\delta = 5^o$

ENERGIES (a.u.)

R(01B-C4A) (bohrs)	2.1	2.6	3.1
SCF	-134.370920	-134.727815	-134.847435
CI	-134.553873	-134.914168	-135.033105
EX	-134.560230	-134.921401	-135.040733
DAV	-134.563793	-134.932963	-135.043589
c^2	.961	.967	.964
gs	.908	.906	.905

R(01B-C4A) (bohrs)	3.6	4.1	4.6
SCF	-134.882307	-134.887248	-134.883394
CI	-135.065067	-135.068662	-135.063898
EX	-135.070494	-135.074395	-135.068526
DAV	-135.074265	-135.077118	-135.071054
c^2	.957	.964	.965
gs	.904	.903	.901

R(01B-C4A) (bohrs)	7.1	10.0
SCF	-134.868181	-134.862798
CI	-135.049391	-135.044737
EX	-135.052791	-135.048036
DAV	-135.055166	-135.050435
c^2	.965	.965
gs	.899	.898

TABLE II - 10

C

OXET + $FNOXH^+$

$\delta = 10^o$

ENERGIES (a.u.)

R(01B-C4A) (bohrs)	2.1	2.6	3.1
SCF	-134.535644	-134.830287	-134.899875
CI	-134.711865	-135.010989	-135.082938
EX	-134.717174	-135.016806	-135.088818
DAV	-134.719132	-135.018927	-135.091260
c^2	.971	.970	.967
gs	.910	.907	.904

R(01B-C4A) (bohrs)	3.6	4.1	4.6
SCF	-134.899562	-134.882823	-134.866316
CI	-135.080986	-135.060244	-135.040898
EX	-135.086011	-135.065866	-135.045438
DAV	-135.088703	-135.068135	-135.048004
c^2	.964	.968	.963
gs	.901	.906	.903

R(01B-C4A) (bohrs)	7.1	10.0
SCF	-134.837119	-134.831005
CI	-135.010516	-135.005397
EX	-135.014918	-135.009072
DAV	-135.017270	-135.011458
c^2	.964	.967
gs	.900	.900

TABLE II - 11

D

OXET + $FNOXH^+$

$\delta = 15^o$

ENERGIES (a.u.)

R(O1B-C4A) (bohrs)	2.1	2.6	3.1
SCF	-134.635098	-134.889992	-134.930457
CI	-134.806808	-135.066946	-135.111510
EX	-134.811851	-135.072539	-135.117082
DAV	-134.813663	-135.074458	-135.119276
c^2	.973	.972	.968
gs	.913	.909	.904

R(O1B-C4A) (bohrs)	3.6	4.1	4.6
SCF	-134.909566	-134.878881	-134.853019
CI	-135.091031	-135.057257	-134.026524
EX	-135.096412	-135.062585	-134.030965
DAV	-135.098936	-135.065315	-134.033521
c^2	.965	.962	.962
GS	.899	.898	.900

R(O1B-C4A) (bohrs)	7.1	7.1
SCF	-134.810279	-134.810279
CI	-135.977164	-134.977164
EX	-135.980338	-134.980388
DAV	-135.982137	-134.982137
c^2	.969	.969
gs	.904	.904

TABLE II - 12

E

OXET + $FNOXH^+$

$\delta = 19^o$(FULLY OPEN)

ENERGIES (a.u.)

R(01B-C4A) (bohrs)	2.1	2.6	2.9
SCF	-134.685867	-134.914697	-134.940369
CI	-134.856194	-135.090774	-135.119754
EX	-134.861224	-135.095386	-135.125109
DAV	-134.863028	-135.097236	-135.127119
c^2	.973	.972	.970
gs	.915	.910	.907

R(01B-C4A) (bohrs)	3.1	3.6	4.6
SCF	-134.937775	-134.905172	-134.866571
CI	-135.118956	-135.088558	-135.048086
EX	-135.123972	-135.092678	-135.052252
DAV	-135.126087	-135.095123	-135.055025
c^2	.969	.965	.961
gs	.904	.897	.894

R(01B-C4A) (bohrs)	4.6	7.1	10.0
SCF	-134.835066	-134.782966	-134.775784
CI	-135.011475	-134.948137	-135.942239
EX	-135.014585	-134.951378	-135.945234
DAV	-135.017295	-134.952855	-135.946753
c^2	.960	.973	.972
gs	.895	.905	.904

TABLE II - 13

FNOX + $OXETH^+$

$\delta = 0^o$ (FULLY CLOSED)

SCF ENERGY (a.u.) FOR DIFFERENT VALUES OF ANGLE BETWEEN TWO RINGS (α)

α (°)	SCF
-90	-134.573887
-45	-134.566354
0	-134.556369
45	-134.566333
90	-134.573804

3'. 3-Fluoro-3-nitrooxetane (FNOX) + protonated oxetane ($OXETH^+$).

a'. Determination of the pathway for 3-fluoro-3-nitrooxetane (FNOX) and protonated oxetane ($OXETH^+$) addition.

The addition of 3-fluoro-3-nitrooxetane (FNOX) to protonated oxetane ($OXETH^+$) also has the features of an S_N2 reaction and the approach prescibed utilizes these to the greatest extent.

The geometry of the reacting system.

The reaction of FNOX with $OXETH^+$ is assumed to be S_N2 type reaction with molecule B attacking molecule A (Figure II-13) along the O_{1B}-C_{4A}-O_{1A} line. Because essential structural changes are expected to appear relative to the plane of FNOX ring the angle alpha between the two rings was determined for R(O1B-C4A) = 2.6 bohrs and was used for all other geometries.

b'. Method of calculation

There is little difference in energy with changes in α, the angle between the rings, Table II-13, "FNOX + $OXETH^+$, δ = 0° (fully closed), SCF Energy for Different Values of Angle Between Two Rings (α)". The method of calculation is the same as described for OXET + $FNOXH^+$ in the previous section.

c'. Results for FNOX + $OXETH^+$.

The ring opening starts when FNOX approaches to oxetane H^+ for R(O_{1B}-C_{4A}) = 4.6 bohrs. Next, both: O_{1B}-C_{4A} and C_{4A}-O_{1A} change simultaneously until the complex reaches the stabilization point at R(O_{1B}-C_{4A}) = 2.9 bohrs and $\delta = 19^o$ (fully open). The stabilization energy for the complex is -.00915 a.u. = -5.74 kcal/mol. The estimated activation energy is 6.27 kcal/mol.

The energies for angle α between rings do not vary significantly.

The potential energy surfaces and reaction potential map are presented in Figures II-14 to Figure II-17.

Figure II-14: "MRD-CI Extrapolated Energy For FNOX Approaching Protonated Oxetane For Fixed Angle δ And Different Intermolecular Distances R(O1B-C4A)"

Figure II-15: "MRD-CI Extrapolated Energy For FNOX-Protonated Oxetane Complex For Fixed Intermolecular Distances R(O1B-C4A) and Different δ Angle Values"

Figure II-16: "FNOX-$OXETH^+$ Extrapolated CI Energy Along the Reaction Coordinate For FNOX-protonated Oxetane Addition Reaction"

Figure II-17: "The Potential Energy Surface For FNOX Approaching Protonated Oxetane"

The detailed Tables of results follow:

Table II-14: "FNOX + $OXETH^+$, δ = 0° (fully closed) Energies (a.u.) as a function of R(O1B-C4A)"

Table II-15: "FNOX + $OXETH^+$, δ = 5° Energies (a.u.) as a function of R(O1B-C4A)"

Table II-16: "FNOX + $OXETH^+$, δ = 10° Energies (a.u.) as a function of R(O1B-C4A)"

Table II-17: "FNOX + $OXETH^+$, δ = 15° Energies (a.u.) as a function of R(O1B-C4A)"

Table II-18: "FNOX + $OXETH^+$, δ = 19° (fully open) Energies (a.u.) as a function of R(O1B-C4A)"

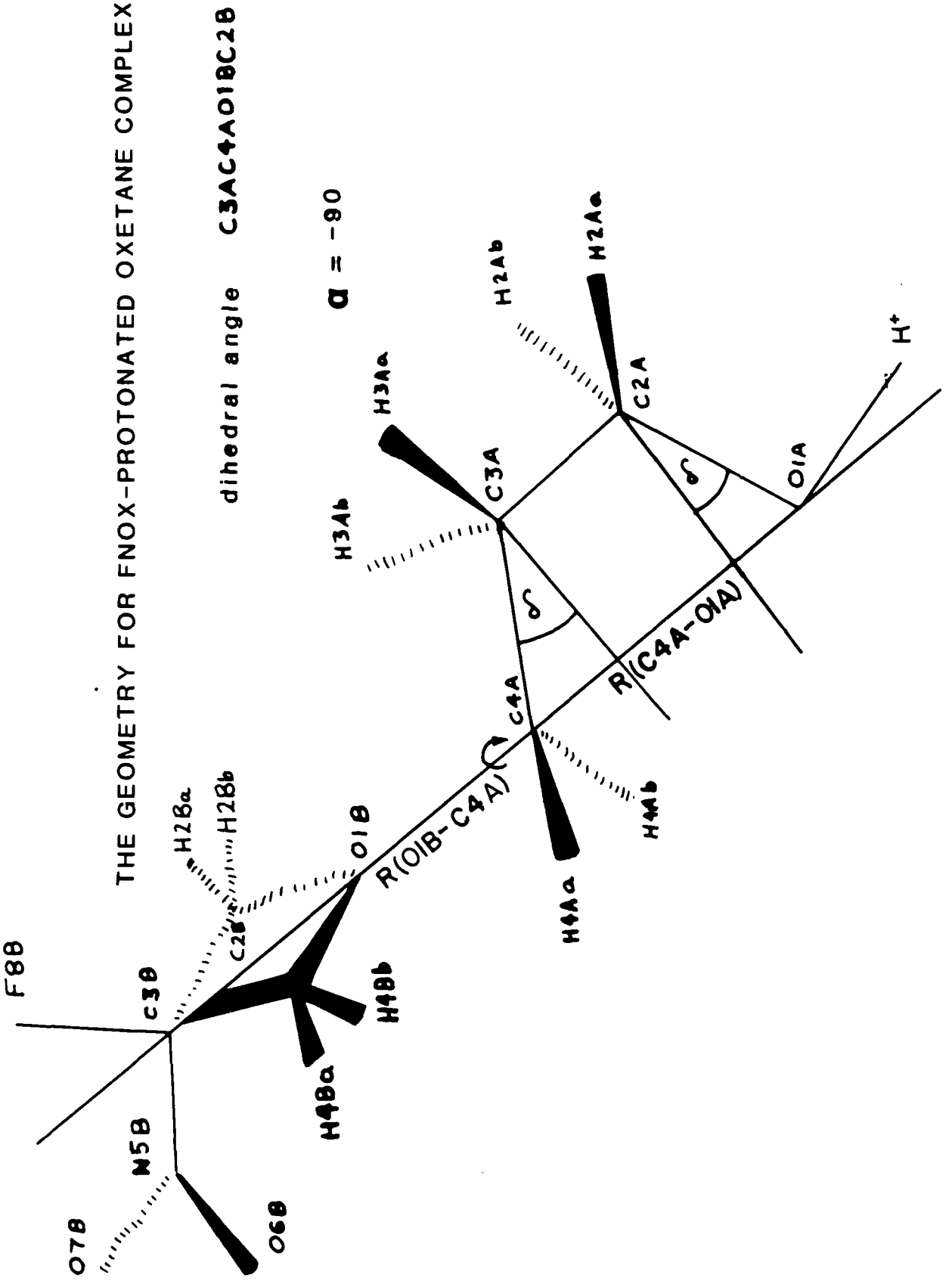
THE GEOMETRY FOR FNOX-PROTONATED OXETANE COMPLEX
dihedral angle C3AC4AO1BC2B
α = -90
F8B
C3B
H2Ba
H2Bb
C2B
O1B
R(O1B-C4A)
H4Bb
H4Ba
N5B
O7B
O6B
C4A
H4Aa
H4Ab
R(C4A-O1A)
C3A
H3Aa
H3Ab
H2Ab
H2Aa
C2A
O1A
H+

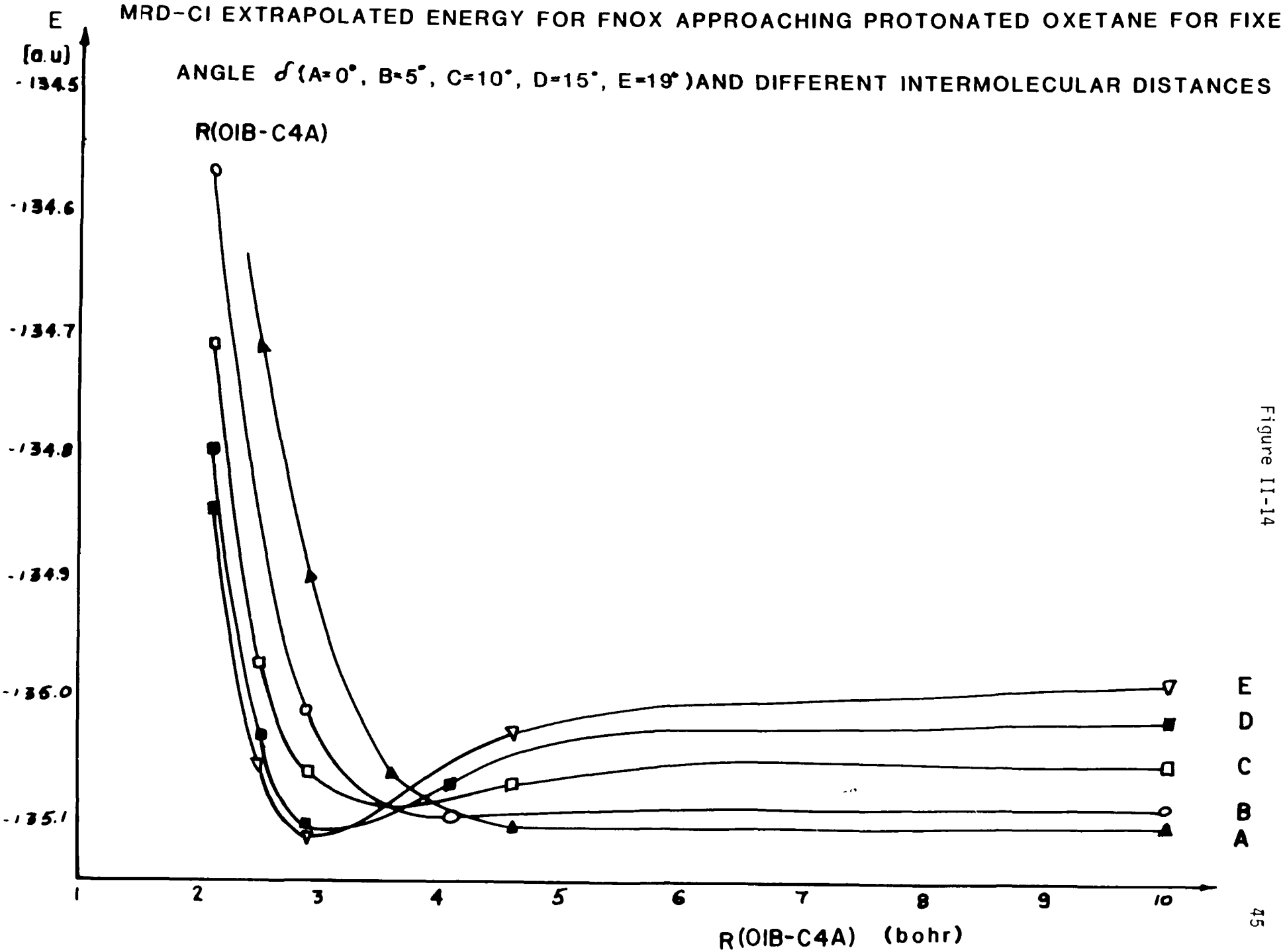
E
(a.u)
-134.5
-134.6
-134.7
-134.8
-134.9
-136.0
-135.1
MRD-CI EXTRAPOLATED ENERGY FOR FNOX APPROACHING PROTONATED OXETANE FOR FIXED
ANGLE δ (A=0°, B=5°, C=10°, D=15°, E=19°) AND DIFFERENT INTERMOLECULAR DISTANCES
R(OIB-C4A)
E
D
C
B
A
1
2
3
4
5
6
7
8
9
10
R(OIB-C4A) (bohr)

Figure II-14

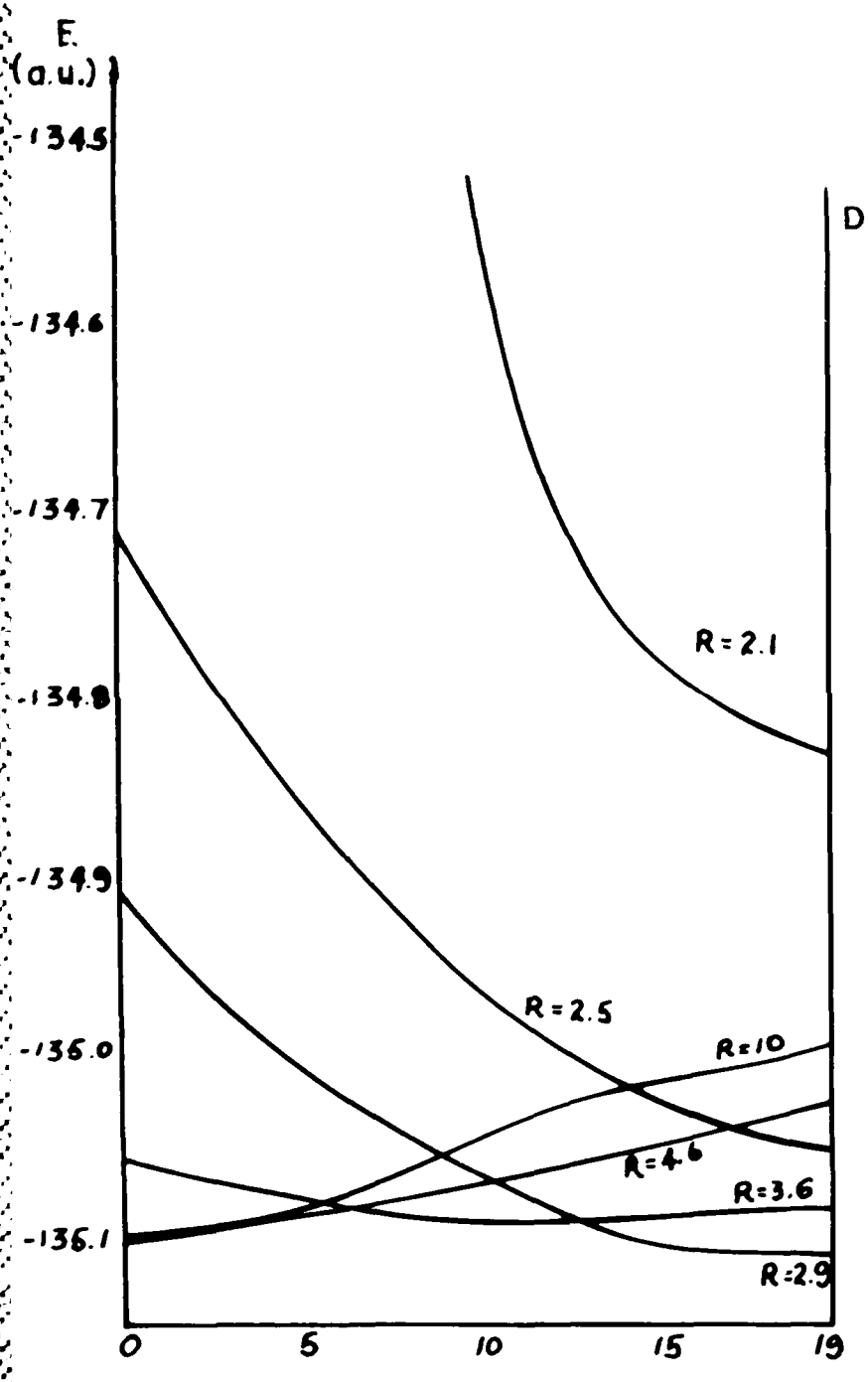

MRD-CI EXTRAPOLATED ENERGY FOR FNOX-PROTONATED OXETANE COMPLEX FOR FIXED INTERMOLECULAR DISTANCES R(O1B-C4A) AND DIFFERENT δ ANGLE VALUES

Figure II-15

TABLE II - 13

FNOX + $OXETH^+$

$\delta = 0^o$ (FULLY CLOSED)

SCF ENERGY (a.u.) FOR DIFFERENT VALUES OF ANGLE BETWEEN TWO RINGS (α)

α (°)	SCF
-90	-134.573887
-45	-134.566354
0	-134.556369
45	-134.566333
90	-134.573804

TABLE II - 14

A

FNOX + $OXETH^+$

$\delta = 0^o$ (FULLY CLOSED)

ENERGIES (a.u.)

R(O1B-C4A) (bohrs)	2.1	2.5	2.9
SCF	-134.131955	-134.511150	-134.71439
CI	-134.328233	-134.706202	-134.905989
EX	-134.336047	-134.713390	-134.912682
DAV	-134.339619	-134.716688	-134.915661
c^2	.962	.963	.964
gs	.904	.905	.905

R(O1B-C4A) (bohrs)	3.6	4.1	4.6
SCF	-134.870168	-134.906321	-134.918159
CI	-135.055303	-135.088869	-135.099405
EX	-135.061614	-135.094212	-135.104669
DAV	-135.064059	-135.096435	-135.106795
c^2	.967	.968	.969
gs	.905	.905	.905

R(O1B-C4A) (bohrs)	10.0
SCF	-134.917271
CI	-135.099207
EX	-135.103049
DAV	-135.105145
c^2	.969
gs	.903

TABLE II - 15

B

FNOX + $OXETH^+$

$\delta = 5^o$

ENERGIES (a.u.)

R(O1B-C4A) (bohrs)	2.1	2.9	3.6
SCF	-134.371600	-134.817032	-134.899072
CI	-134.559469	-135.003579	-135.081621
EX	-134.566346	-135.010938	-135.087747
DAV	-134.568878	-135.013692	-135.090412
c^2	.968	.965	.964
gs	.905	.905	.904

R(O1B-C4A) (bohrs)	4.1	10.0
SCF	-134.912246	-134.904573
CI	-135.093753	-135.086645
EX	-135.098762	-135.090328
DAV	-135.101315	-135.092754
c^2	.965	.965
gs	.902	.898

TABLE II - 16

C

FNOX + $OXETH^+$

$\delta = 10^o$

ENERGIES (a.u.)

R(O1B-C4A) (bohrs)	2.1	2.5	2.9
SCF	-134.523543	-134.785323	-134.879961
CI	-134.703562	-134.967402	-135.062094
EX	-134.709561	-134.973213	-135.067821
DAV	-134.711637	-134.875357	-135.070119
c^2	.971	.970	.968
gs	.908	.907	.905

R(O1B-C4A) (bohrs)	3.6	4.1	4.6
SCF	-134.909633	-134.903107	-134.894288
CI	-135.087083	-135.077655	-135.067303
EX	-135.092434	-135.082991	-135.072249
DAV	-135.094867	-135.085375	-135.074560
c^2	.965	.965	.964
gs	.905	.904	.901

R(O1B-C4A) (bohrs)	10.0
SCF	-134.874769
CI	-135.048181
EX	-135.051947
DAV	-135.054272
c^2	.964
gs	.901

TABLE II - 17

D

FNOX + $OXETH^+$

$\delta = 15^o$

ENERGIES (a.u.)

R(O1B-C4A) (bohrs)	2.1	2.6	3.6
SCF	-134.616620	-134.917116	-134.914524
CI	-134.791828	-135.096343	-135.090622
EX	-134.797443	-135.101219	-135.096394
DAV	-134.799299	-135.103258	-135.098661
c^2	.972	.970	.967
gs	.911	.906	.904

R(O1B-C4A) (bohrs)	4.1	10.0
SCF	-134.89416562	-134.847906
CI	-135.066025	-135.015423
EX	-135.070201	-135.018739
DAV	-135.072315	-135.020467
c^2	.967	.967
gs	.905	.903

TABLE II - 18

E

FNOX + $OXETH^+$

$\delta = 19^o$ (FULLY OPEN)

ENERGIES (a.u.)

R(O1B-C4A) (bohrs)	2.1	2.5	2.9
SCF	-134.665293	-134.875744	-134.928616
CI	-134.838385	-135.052121	-135.107297
EX	-134.843237	-135.056507	-135.112204
DAV	-134.845089	-135.058348	-135.114180
c^2	.973	.972	.970
gs	.913	.910	.907

R(O1B-C4A) (bohrs)	3.6	4.6	10.0
SCF	-134.906366	-134.854626	-134.818210
CI	-135.083692	-135.023718	-134.984149
EX	-135.087620	-135.027136	-134.986463
DAV	-135.089794	-135.028994	-134.987900
c^2	.967	.969	.973
gs	.903	.904	.904

Figure II-16

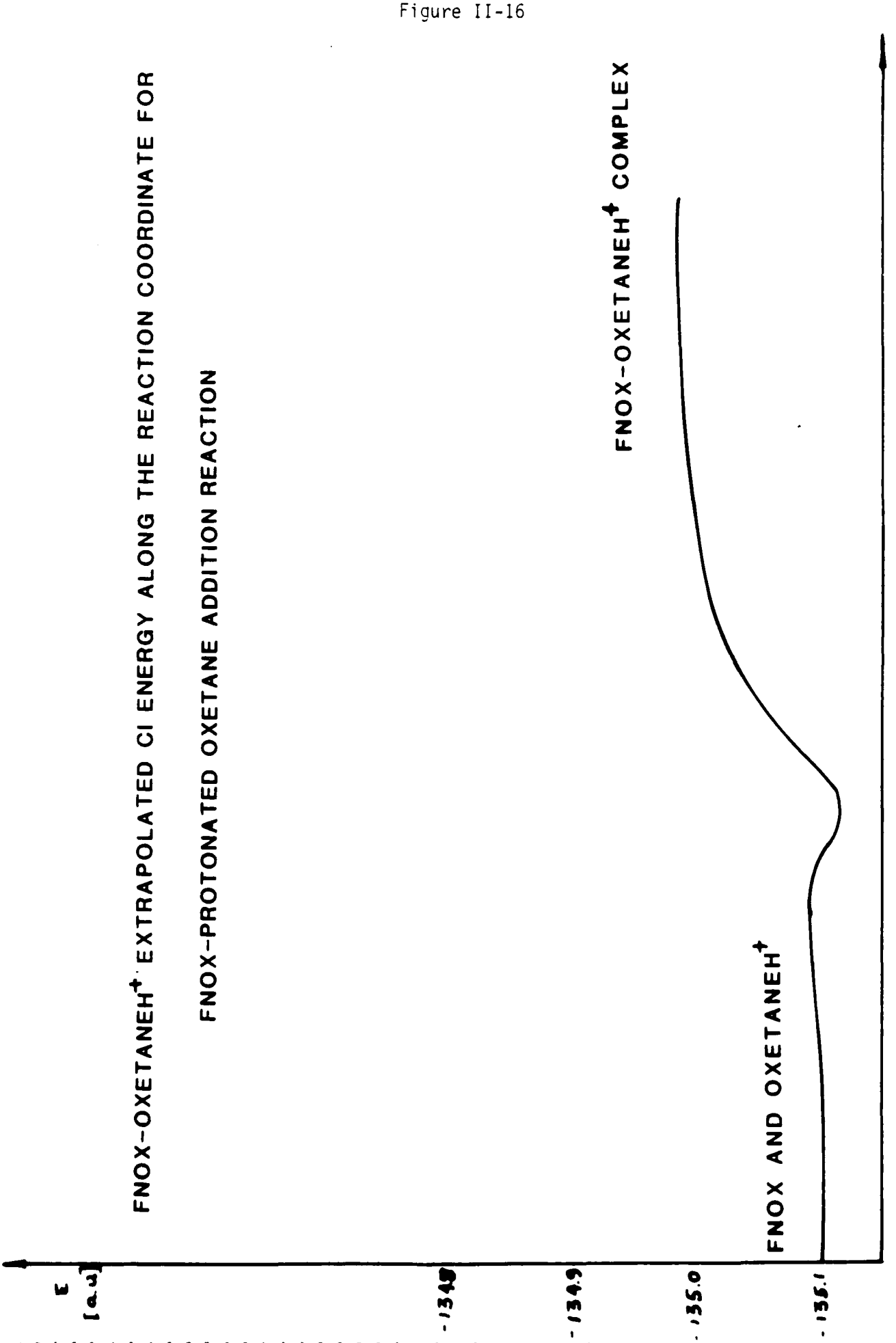
FNOX-OXETANEH+ EXTRAPOLATED CI ENERGY ALONG THE REACTION COORDINATE FOR
FNOX-PROTONATED OXETANE ADDITION REACTION
FNOX-OXETANEH+ COMPLEX
FNOX AND OXETANEH+
E [a.u.]
-134.8
-134.9
-135.0
-135.1
REACTION COORDINATE

THE POTENTIAL ENERGY SURFACE FOR FNOX APPROACHING PROTONATED OXET. THE DASHED LINE IS THE REACTION COORDINATE. THE VALUES ON THE GRAPH CORRESPOND TO EXTRAPOLATED MRD-CI ENERGY BY EQUATION E=-71.5+a (a.u.)

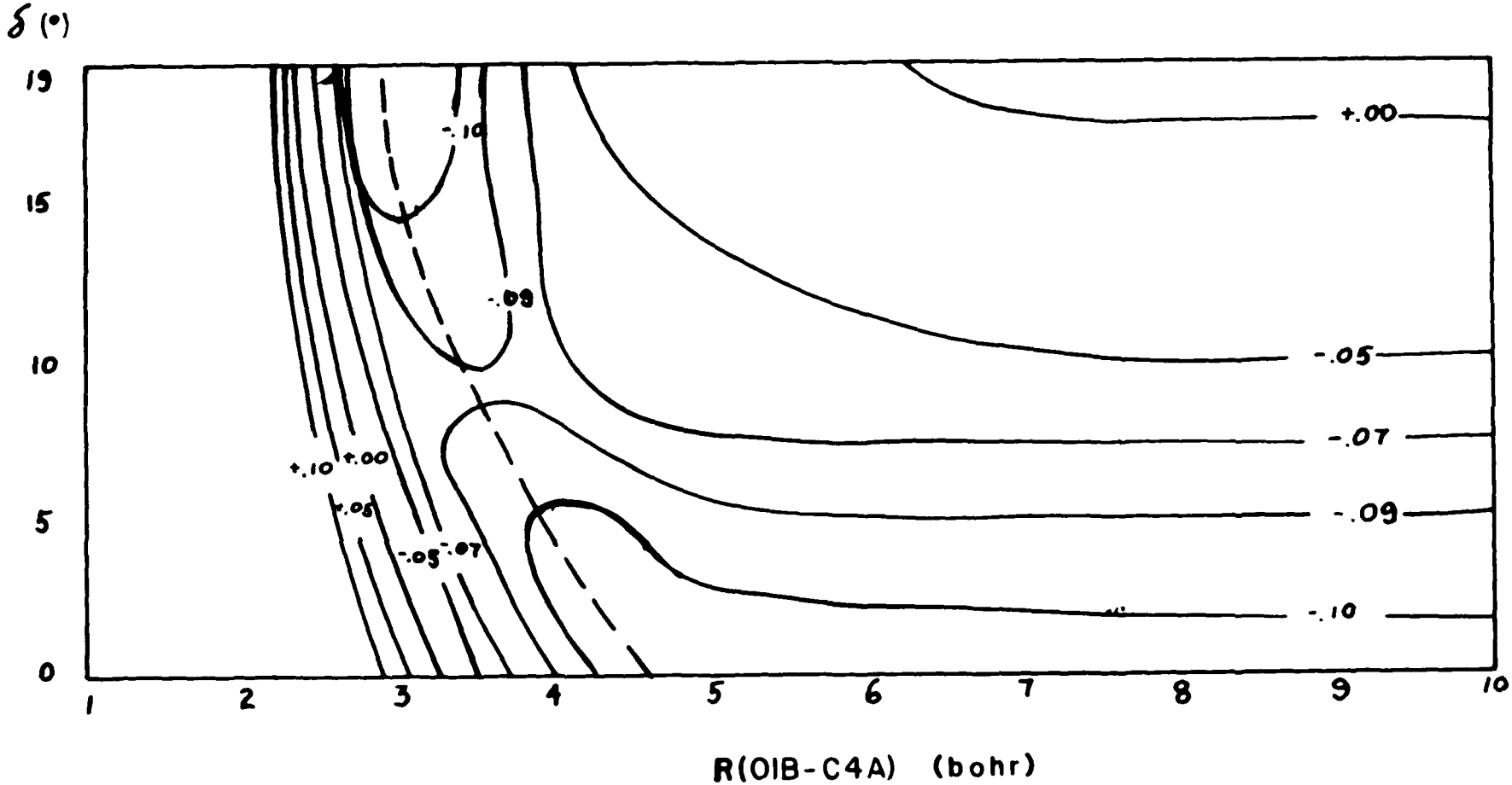

Figure II-17

4'. 3-Fluoro-3-nitrooxetane (FNOX) and protonated 3-fluoro-3-nitrooxetane ($FNOXH^+$)

a'. Determination of the pathway for 3-fluoro-3-nitrooxetane ($FNOXH^+$)

The addition of 3-fluoro-3-nitrooxetane (FNOX) to protonated 3-fluoro-3-nitrooxetane ($FNOXH^+$) also has the features of an S_N2 reaction and the approach presented utilizes these to the greatest extent.

The geometry of the reacting system. The reaction of FNOX with $FNOXH^+$ is assumed to be S_N2 type reaction with molecule B attacking molecule A (Figure II-18) along the O_{1B}-C_{4A}-O_{1A} line. Because essential structural changes are expected to appear relative to the plane of FNOX ring the angle alpha between the two rings was determined for R(O1B-C4A) = 2.6 bohrs and was used for all other geometries.

The optimal α angle was determined to be 55° (Table II-19), "FNOX + $FNOXH^+$, SCF Energy for Various Values of α Angle".

b'. Method of calculation

The method of calculation is the same as described for OXET + $FNOXH^+$ in section 2'.

c'. Results for FNOX + $FNOXH^+$

The ring opening again starts when FNOX approaches $FNOXH^+$ for R(O1B-C4A) = 4.6 bohrs. Again next both: O_{1B}-C_{4A} and C_{4A}-O_{1A} change simultaneously until the stabilization point at $R(O_{1B}\text{-}C_{4A})$ = 2.9 bohrs and δ = 19° (fully open)

The stabilization energy for the complex is -.03156 a.u. = -19.80 kcal/mol. Approximate activation energy .005 a.u. = 3.13 kcal/mol. The potential energy surfaces and reaction potential map are presented in Figures II-19 to II-22.

Figure II-19: "MRD-CI Extrapolated Energy For FNOX Approaching Protonated FNOX For Fixed Angle δ and Different Intermolecular Distances R(O1B-C4A)"

Figure II-20: "MRD-CI Extrapolated Energy For FNOX-FNOX Protonated Complex For Fixed Intermolecular Distances R(O1B-C4A) and Different δ Angle

Values"

Figure II-21: "FNOX-$FNOXH^+$, Extrapolated CI Energy Along the Reaction Coordinate for FNOX Protonated FNOX Addition Reaction"

Figure II-22: "The Potential Energy Surface for FNOX Approaching Protonated FNOX"

The detailed Tables of results follow:

Table II-20: "FNOX + $FNOXH^+$, $\delta \approx 0°$ (fully closed) Energies (a.u.) as a function of R(O1B-C4A)"

Table II-21: "FNOX + $FNOXH^+$, $\delta \approx 5°$ Energies (a.u.) as a function of R(O1B-C4A)"

Table II-22: "FNOX + $FNOXH^+$, $\delta \approx 10°$ Energies (a.u.) as a function of R(O1B-C4A)"

Table II-23: "FNOX + $FNOXH^+$, $\delta \approx 15°$ Energies (a.u.) as a function of R(O1B-C4A)"

Table II-24: "FNOX + $FNOXH^+$, $\delta \approx 19°$ (fully open) Energies (a.u.) as a function of R(O1B-C4A)"

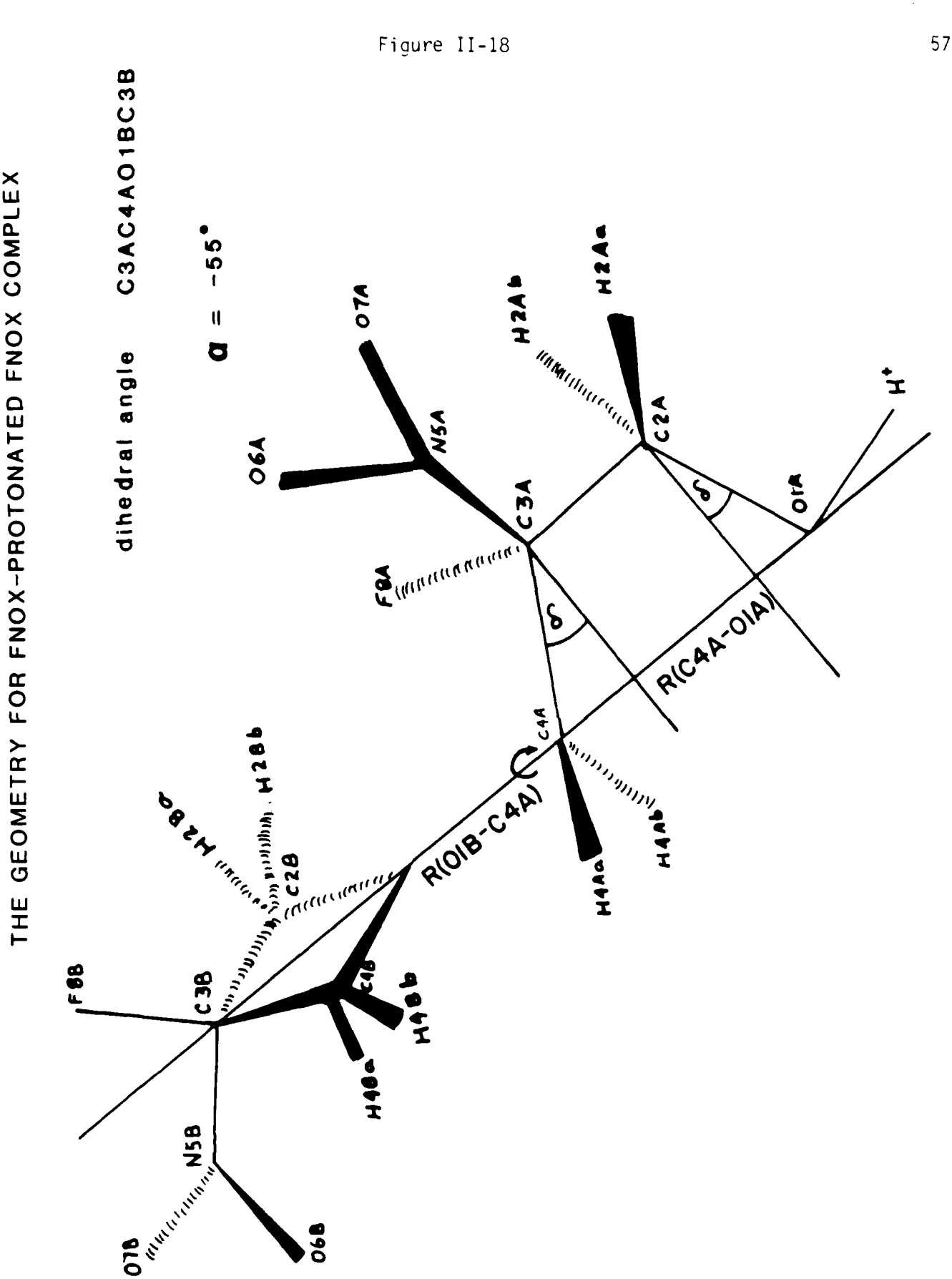
THE GEOMETRY FOR FNOX-PROTONATED FNOX COMPLEX
dihedral angle C3AC4AO1BC3B
α = -55°
O7A
O6A
N5A
H2Ab
H2Aa
C2A
C3A
H+
O1A
F8A
δ
δ
R(C4A-O1A)
C4A
R(O1B-C4A)
H4Aa
H4Ab
H2Ba
H2Bb
C2B
F8B
C3B
C4B
H4Bb
H4Ba
N5B
O7B
O6B

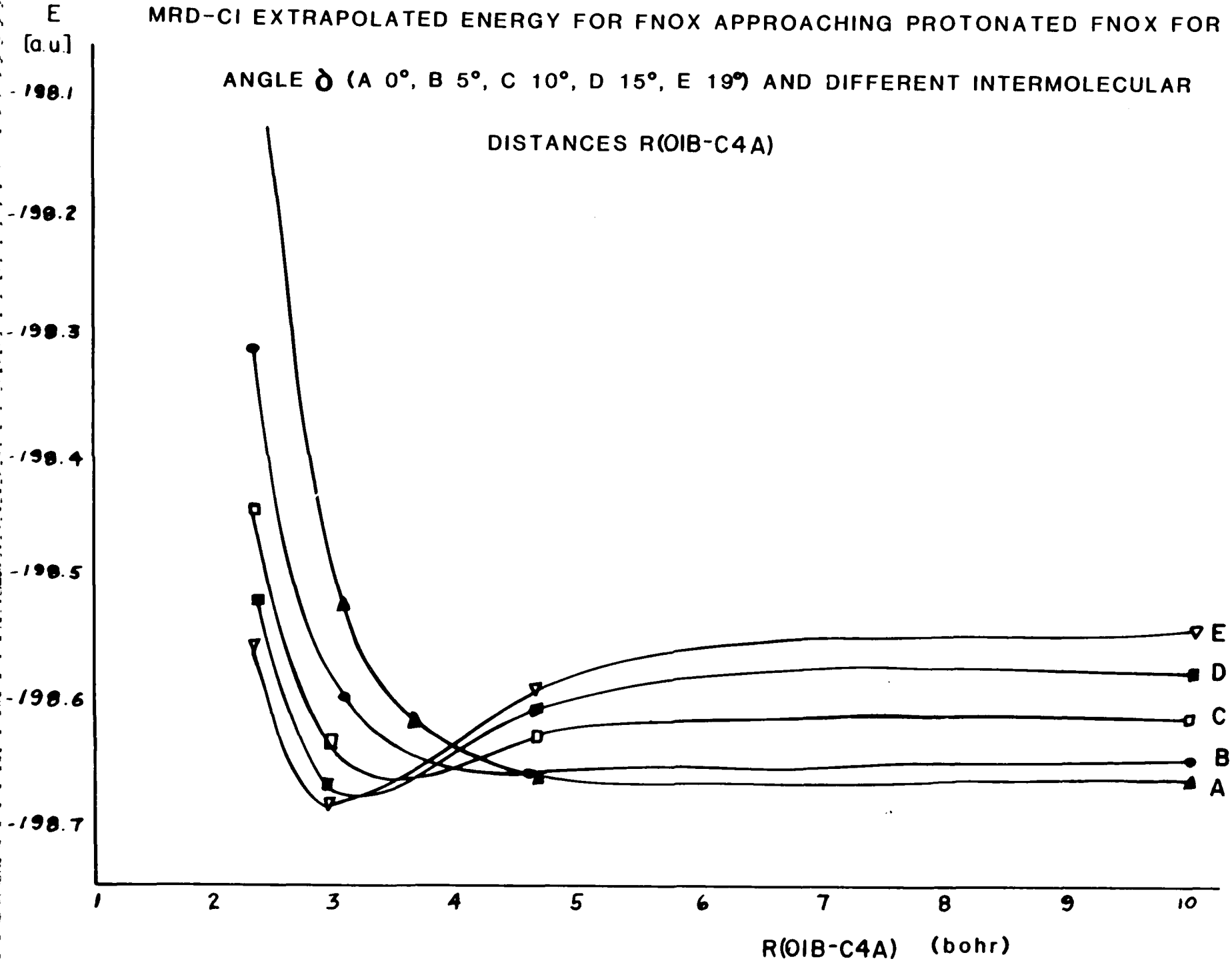
E
[a.u.]
MRD-CI EXTRAPOLATED ENERGY FOR FNOX APPROACHING PROTONATED FNOX FOR FIXED
ANGLE δ (A 0°, B 5°, C 10°, D 15°, E 19°) AND DIFFERENT INTERMOLECULAR
DISTANCES R(OIB-C4A)
-198.1
-198.2
-198.3
-198.4
-198.5
-198.6
-198.7
1
2
3
4
5
6
7
8
9
10
R(OIB-C4A) (bohr)
E
D
C
B
A

Figure II-19

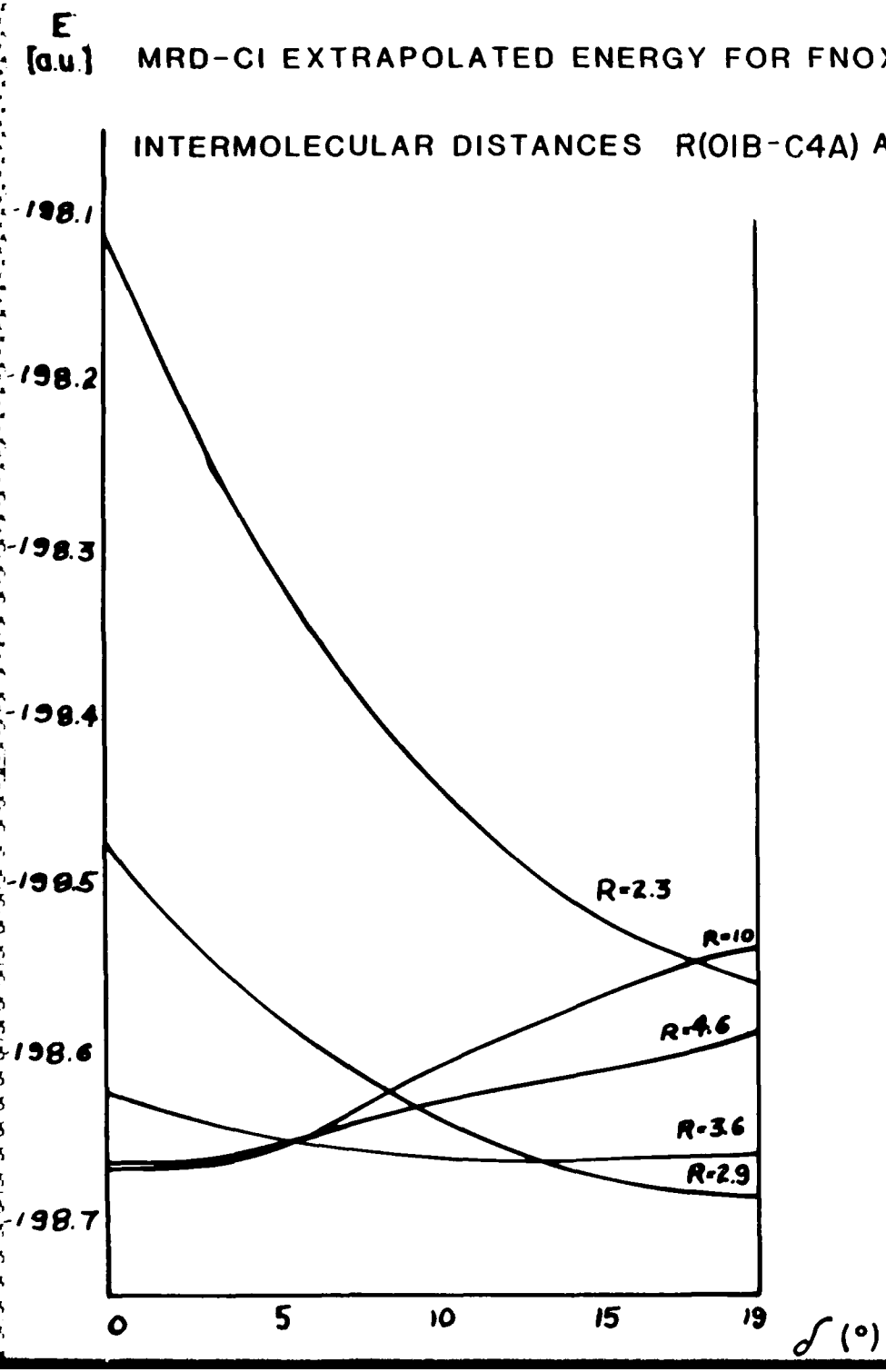
E
(a.u.)
MRD-CI EXTRAPOLATED ENERGY FOR FNOX - FNOX PROTONATED COMPLEX FOR FIXED
INTERMOLECULAR DISTANCES R(01B-C4A) AND DIFFERENT δ ANGLE VALUES
-198.1
-198.2
-198.3
-198.4
-198.5
-198.6
-198.7
R=2.3
R=10
R=4.6
R=3.6
R=2.9
0
5
10
15
19
δ (°)

Figure II-20

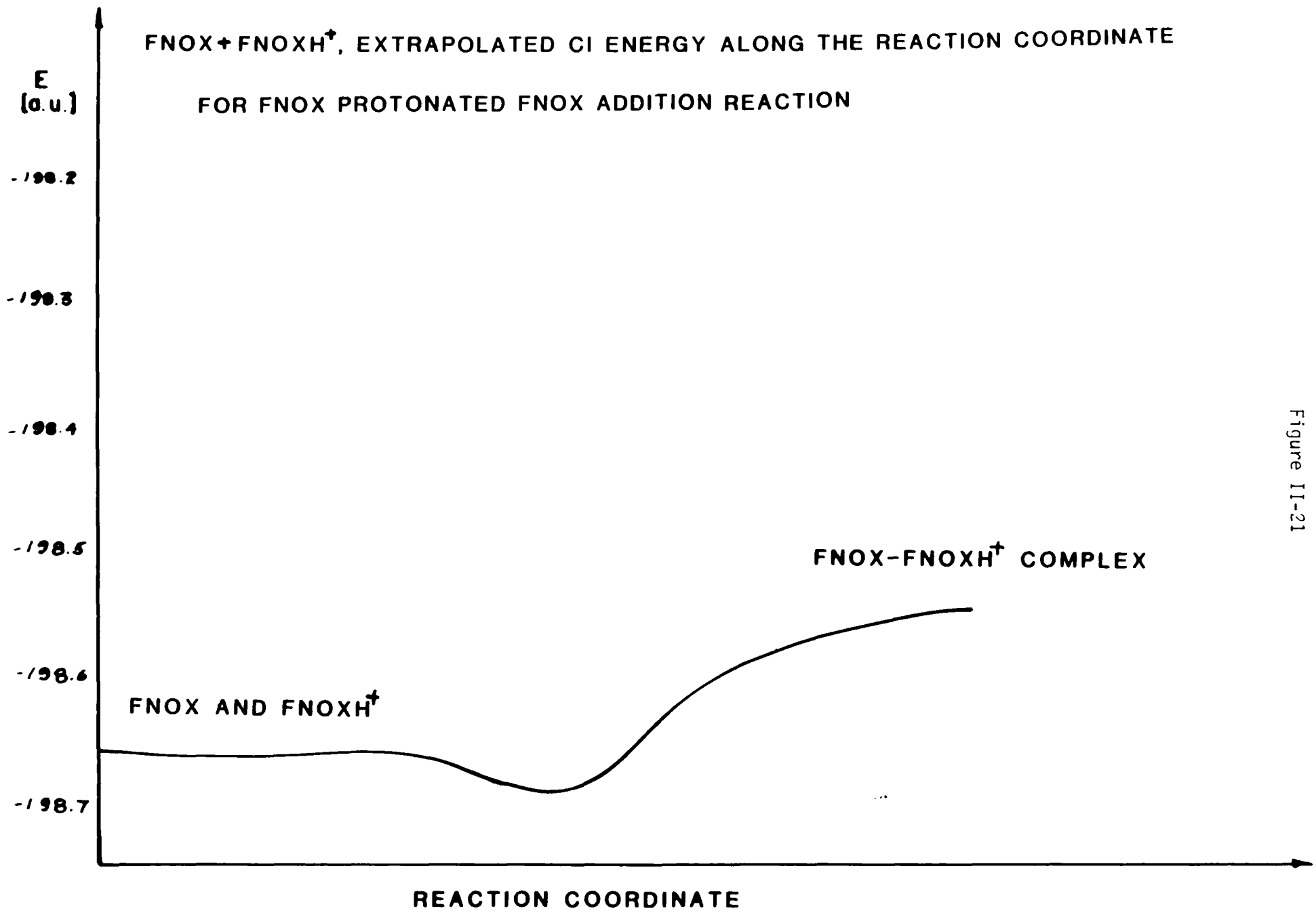
FNOX+FNOXH+, EXTRAPOLATED CI ENERGY ALONG THE REACTION COORDINATE
FOR FNOX PROTONATED FNOX ADDITION REACTION
E
(a.u.]
-198.2
-198.3
-198.4
-198.5
-198.6
-198.7
FNOX-FNOXH+ COMPLEX
FNOX AND FNOXH+
REACTION COORDINATE

Figure II-21

Figure II-22

THE POTENTIAL ENERGY SURFACE FOR FNOX APPROACHING PROTONATED FNOX. THE DASHED LINE IS THE REACTION COORDINATE. THE VALUES ON THE GRAPH CORRESPOND TO EXTRAPOLATED MRD-CI ENERGY BY EQUATION E -198.6+a (a.u.)

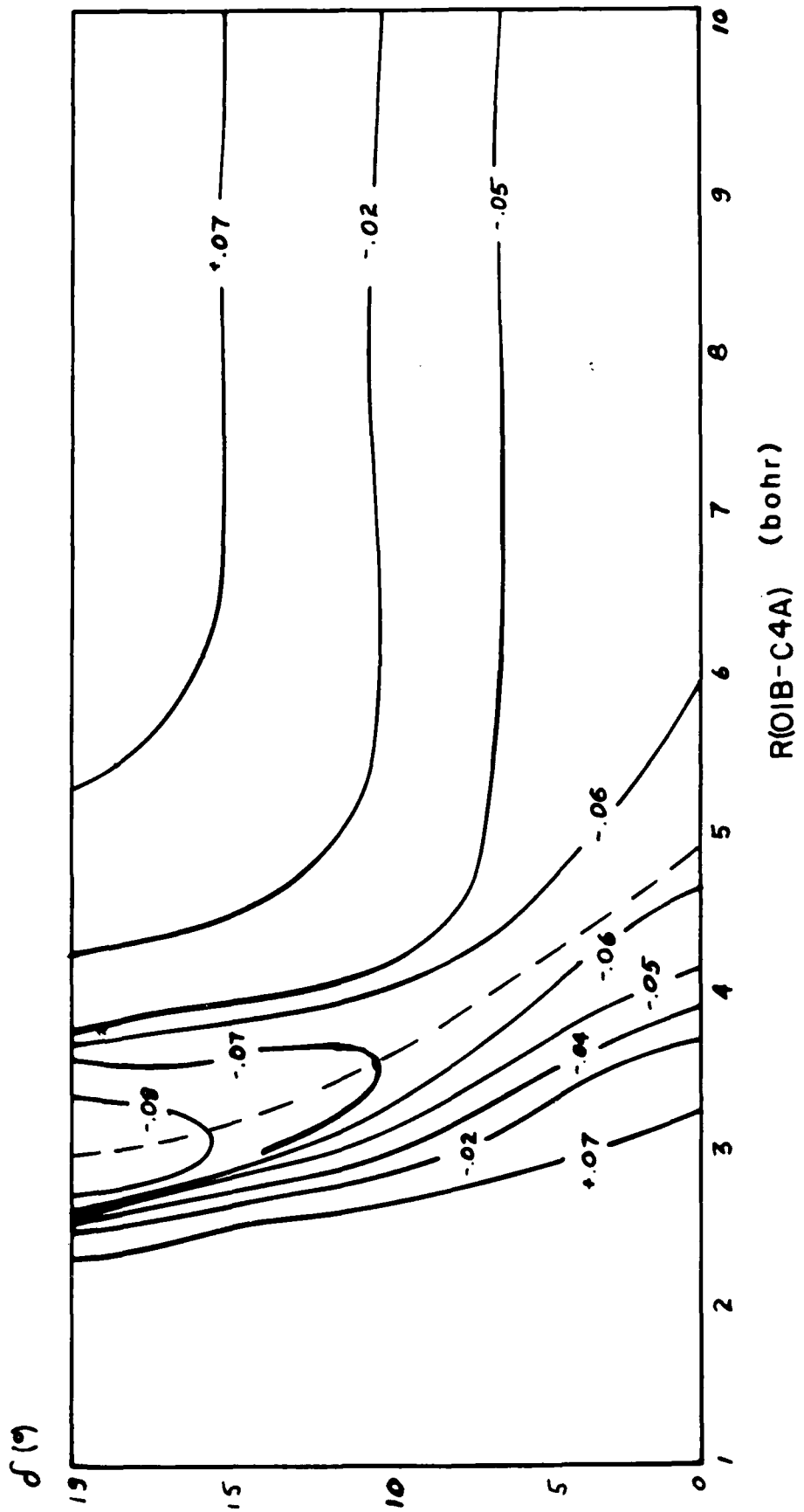

TABLE II - 19

$FNOX + FNOXH^+$
SCF ENERGY (a.u.) FOR VARIOUS VALUES OF α ANGLE

α (^{o})	ENERGY	
0	-198.181177	
45	-198.281031	
55	-198.281216	MINIMUM
65	-198.276447	
90	-198.199361	
135	-198.079309	
180	-198.182049	
225	-198.280452	
235	-198.280818	
245	-198.276348	
270	-198.199587	

TABLE II - 20

A

FNOX + $FNOXH^+$

$\delta = 0^o$ (FULLY CLOSED)

ENERGIES (a.u.)

R(O1B-C4A) (bohrs)	2.3	2.9	3.6
SCF	-197.910863	-198.281216	-198.435192
CI	-198.103109	-198.470845	-198.618954
EX	-198.111535	-198.477910	-198.625229
DAV	-198.114770	-198.480888	-198.627675
c^2	.964	.964	.967
gs	.906	.906	.906

R(O1B-C4A) (bohrs)	4.6	7.1	10.0
SCF	-198.480690	-198.418577	-198.479303
CI	-198.634550	-198.661953	-198.656760
EX	-198.638251	-198.665930	-198.660445
DAV	-198.639642	-198.667978	-198.662301
c^2	.974	.969	.971
gs	.915	.904	.906

TABLE II - 21

B

$FNOX + FNOXH^+$

$\delta = 5^o$

ENERGIES (a.u.)

R(01B-C4A) (bohrs)	2.3	2.9	3.6
SCF	-198.128612	-198.389364	-198.465030
CI	-198.313697	-198.575069	-198.647397
EX	-198.320611	-198.582967	-198.653065
DAV	-198.323023	-198.585722	-198.655796
c^2	.968	.965	.964
gs	.907	.906	.904

R(01B-C4A) (bohrs)	4.6	10.0
SCF	-198.474937	-198.464728
CI	-198.655547	-198.646778
EX	-198.660043	-198.650079
DAV	-198.662521	-198.652485
c^2	.965	.965
gs	.901	.898

TABLE II - 22

C

$FNOX + FNOXH^+$

$\delta = 10^o$

ENERGIES (a.u.)

R(01B-C4A) (bohrs)	2.3	2.9	3.6
SCF	-198.265018	-198.456342	-198.477340
CI	-198.443306	-198.638345	-198.656431
EX	-198.448377	-198.644268	-198.661916
DAV	-198.450357	-198.646572	-198.664543
c^2	.971	.968	.934
gs	.909	.905	.903

R(01B-C4A) (bohrs)	4.6	10.0
SCF	-198.454554	-198.432698
CI	-198.628227	-198.607392
EX	-198.633078	-198.611131
DAV	-198.635537	-198.613549
c^2	.964	.963
gs	.903	.899

TABLE II - 23

D

$FNOX + FNOXH^+$

$\delta = 15^o$

ENERGIES (a.u.)

R(O1B-C4A) (bohrs)	2.3	2.9	3.6
SCF	-198.346074	-198.495395	-198.483930
CI	-198.520243	-198.674606	-198.662553
EX	-198.525408	-198.679879	-198.667532
DAV	-198.527228	-198.681927	
c^2	.972	.970	.966
gs	.912	.906	.902

R(C4A-O1B) (bohrs)	4.6	10.0
SCF	-198.437954	-198.404983
CI	-198.608248	-198.569461
EX	-198.612647	-198.572663
DAV	-198.614829	-198.574290
c^2	.966	.970
gs	.904	.905

TABLE II - 24

E

FNOX + $FNOXH^+$

$\delta = 19^o$ (FULLY OPEN)

ENERGIES (a.u.)

R(O1B-C4A) (bohrs)	2.3	2.9	3.6
SCF	-198.384740	-198.507770	-198.477497
CI	-198.557601	-198.686766	-198.657925
EX	-198.562331	-198.692012	-198.661934
DAV	-198.564119	-198.694011	-198.664266
c^2	.973	.970	.966
gs	.913	.906	.900

R(O1B-C4A) (bohrs)	4.6	10.0
SCF	-198.417703	-198.377272
CI	-198.589036	-198.540339
EX	-198.592776	-198.543087
DAV	-198.594981	-198.544440
c^2	.965	.973
gs	.902	.906

(b). Population Analyses

Gerry Manser had expressed considerable interest in how the charges (corresponding to the gross atomic populations) on the O_{1A} (oxygen of protonated oxetane ring), C_{4A} (the α carbon of the protonated oxetane ring) and O_{1B} (oxygen of the oxetane ring) varied as a function of substituent and reaction pathway.

In last year's ONR Annual Report 1986, Table III Page 24, showed that that as oxetane and protonated oxetane approached each other that the intra-ring TOP of the C_{4A}-O_{1A} in the protonated ring got smaller as the oxetane ring approached, indicating a tendency for the protonated ring to open and the inter-ring TOP O_{1B}-C_{4A} got larger indicating bond formation.

On the following pages we have Tables II-25 to II-28 of the MRD-CI gross atomic populations and total overlap populations (C_{4A}-O_{4A}) and (O_{1B}-C_{4A}) for the systems OXET + $OXETH^+$, OXET + $FNOXH^+$, FNOX + $OXETH^+$ and FNOX + $FNOXH^+$ at representative intermediate inter-ring distance O_{1B}-C_{4A} distance of 3.6 bohrs.

i) It is apparent from the TOP's in the tables that the two rings are repulsive when the protonated oxetane (or substituted protonated oxetane) ring is closed.

ii) the protonated oxetane (or substituted protonated oxetane) will open upon approach of the oxetane (or substituted oxetane) along the appropriate reaction pathway.

iii) The O_{1B}-C_{4A} interring bond becomes stronger as the protonated (A) ring opens.

The behavior of these TOP's is indicative of the same conclusion as that from the MRD-CI energy calculations.

TABLES II-25,26,27,28

GROSS ATOMIC POPULATIONS for O1A, C4A, O1B and TOTAL OVERLAP POPULATIONS for C4A-O1A and O1B-C4A bonds for different value δ and R(O1A-C4B) = 3.6 bohrs

OXETANE + OXETANE H^+

	Gross Atomic populations			Total Overlap populations	
δ (°)	O1A	C4A	O1B	C4A-O1A	O1B-C4A
0 (fully closed)	6.385	4.160	6.350	0.290	-0.116
5	6.411	6.134	6.336	0.193	0.052
10	6.445	4.118	6.316	0.074	0.192
15	6.452	4.129	6.298	0.006	0.278
19 (fully open)	6.443	4.157	6.285	-0.010	0.317

OXETANE + FNOX H^+

	Gross Atomic populations			Total Overlap populations	
δ (°)	O1A	C4A	O1B	C4A-O1A	O1B-C4A
0 (fully closed)	6.385	4.160	6.350	0.290	-0.116
5	6.404	4.148	6.332	0.186	0.086
10	6.441	4.137	6.298	0.070	0.224
15	6.447	4.149	6.271	0.008	0.304
19 (fully open)	6.436	4.173	6.254	-0.002	0.342

FNOX + OXETANE H^+

	Gross Atomic populations			Total Overlap populations	
δ (°)	O1A	C4A	O1B	C4A-O1A	O1B-C4A
0 (fully closed)	6.384	4.157	6.336	0.309	-0.135
05	6.407	4.129	6.327	0.215	0.028
10	6.443	4.107	6.314	0.089	0.163
15	6.453	4.114	6.300	0.012	0.249
19 (fully closed)	6.445	4.139	6.290	-0.009	0.296

FNOX + FNOX H^+

	Gross Atomic populations			Total Overlap populations	
δ (°)	O1A	C4A	O1B	C4A-O1A	O1B-C4A
0 (fully closed)	6.383	4.167	6.346	0.310	-0.126
05	6.405	4.141	6.327	0.213	0.055
10	6.440	4.123	6.301	0.089	0.198
15	6.448	4.128	6.279	0.015	0.284
19 (fully closed)	6.438	4.150	6.263	-0.005	0.328

(2). AMMO + $OXETH^+$, OXET + $AMMOH^+$, AMMO + $AMMOH^+$

The reactions AMMO + $OXETH^+$, OXET + $AMMOH^+$ and AMMO + $AMMOH^+$ were treated as S_N2 reactions as the previous cases described in detail in the earlier section. The optimal α angles were determined to be 90° for each of those systems involving AMMO (3-azidomethyl-3-methyloxetane and/or protonated AMMO ($AMMOH^+$). The subsequent MRD-CI calculations were run at this α angle.

The same localized skeletal molecular orbitals (both occupied and virtual) were included explicitly in the MRD-CI as for the previous cases. This approach makes it meaningful to compare reaction energies between various systems.

For these cases involving AMMO and/or $AMMOH^+$, the ring opening of the protonated ring ($OXETH^+$ or $AMMOH^+$) starts for $R(O_{1B}-C_{4A})$ = 4.6 bohrs. Next, both: $O_{1B}-C_{4A}$ and $C_{4A}-O_{1A}$ change simultaneously until the stabilization point at $R(O_{1B}-C_{4A})$ = 2.9 bohrs and δ = 19° (fully open).

(a). Energies

1'. 3-azidomethyl-3-methyloxetane (AMMO) + protonated oxetane ($OXETH^+$)

a'. Results

The stabilization point R(O1B-C4A) = 2.9 bohrs, δ = 19° (fully open) with the stabilization energy -0.043262 a.u. = -27.37 kcal/mole.

The potential energy surfaces and reaction potential map are presented in Figures II-23 to II-26.

Figure II-23: "MRD-CI Extrapolated Energy for AMMO Approaching Protonated Oxetane For Fixed Angle δ and Different Intermolecular Distances R(O1B-C4A)"

Figure II-24: "MRD-CI Extrapolated Energy For AMMO-Protonated Oxetane Complex for Fixed Intermolecular Distances R(O1B-C4A) and Different δ Angle Values"

Figure II-25: "AMMO + $OXETH^+$, Extrapolated CI Energy Along the Reaction Coordinate For AMMO Protonated Oxetane Addition Reaction."

Figure II-26: "The Potential Energy Surface For AMMO Approaching Protonated OXET, MRD-CI Extrapolated"

The detailed Tables of results follow in Tables II-29 - II-33:

Table II-29: "AMMO + $OXETH^+$ δ = 0° (fully closed), Energies (a.u.) as a function of R(O1B-C4A)"

Table II-30: "AMMO + $OXETH^+$ δ = 5°, Energies (a.u.) as a function of R(O1B-C4A)"

Table II-31: "AMMO + $OXETH^+$ δ = 10°, Energies (a.u.) as a function of R(O1B-C4A)"

Table II-32: "AMMO + $OXETH^+$ δ = 15°, Energies (a.u.) as a function of R(O1B-C4A)"

Table II-33: "AMMO + $OXETH^+$ δ = 19° (fully open), Energies (a.u.) as a function of R(O1B-C4A)"

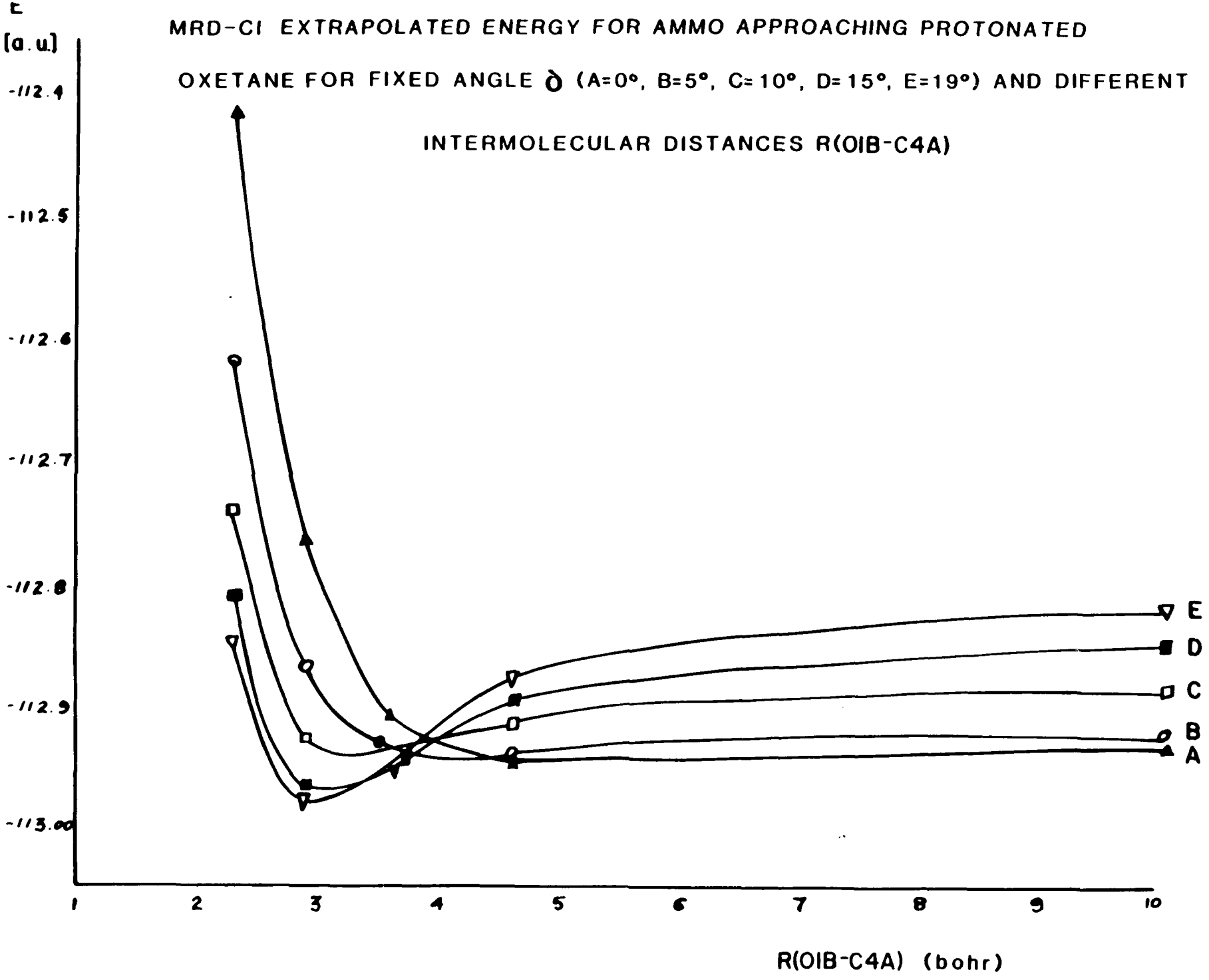
E
[a.u]
MRD-CI EXTRAPOLATED ENERGY FOR AMMO APPROACHING PROTONATED
OXETANE FOR FIXED ANGLE δ (A=0°, B=5°, C=10°, D=15°, E=19°) AND DIFFERENT
INTERMOLECULAR DISTANCES R(OIB-C4A)
-112.4
-112.5
-112.6
-112.7
-112.8
-112.9
-113.00
1
2
3
4
5
6
7
8
9
10
E
D
C
B
A
R(OIB-C4A) (bohr)

Figure II-23

Figure II-24

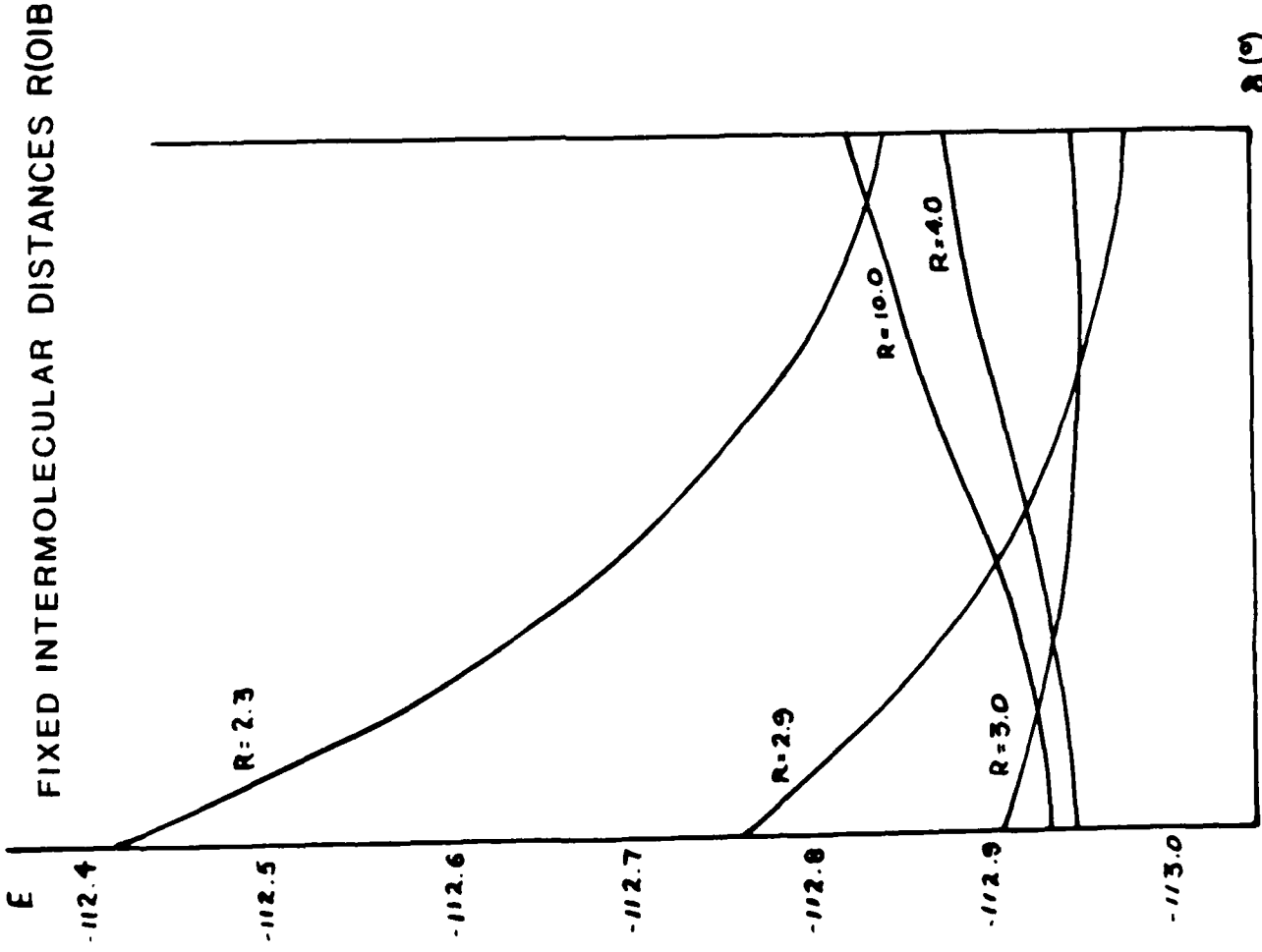
MRD-CI EXTRAPOLATED ENERGY FOR AMMO-PROTONATED OXETANE COMPLEX FOR
FIXED INTERMOLECULAR DISTANCES R(OIB-C4A)AND DIFFERENT δ ANGLE VALUES
E
-112.4
-112.5
-112.6
-112.7
-112.8
-112.9
-113.0
R=2.3
R=2.9
R=3.0
R=4.0
R=10.0
0
5
10
15
δ(°)

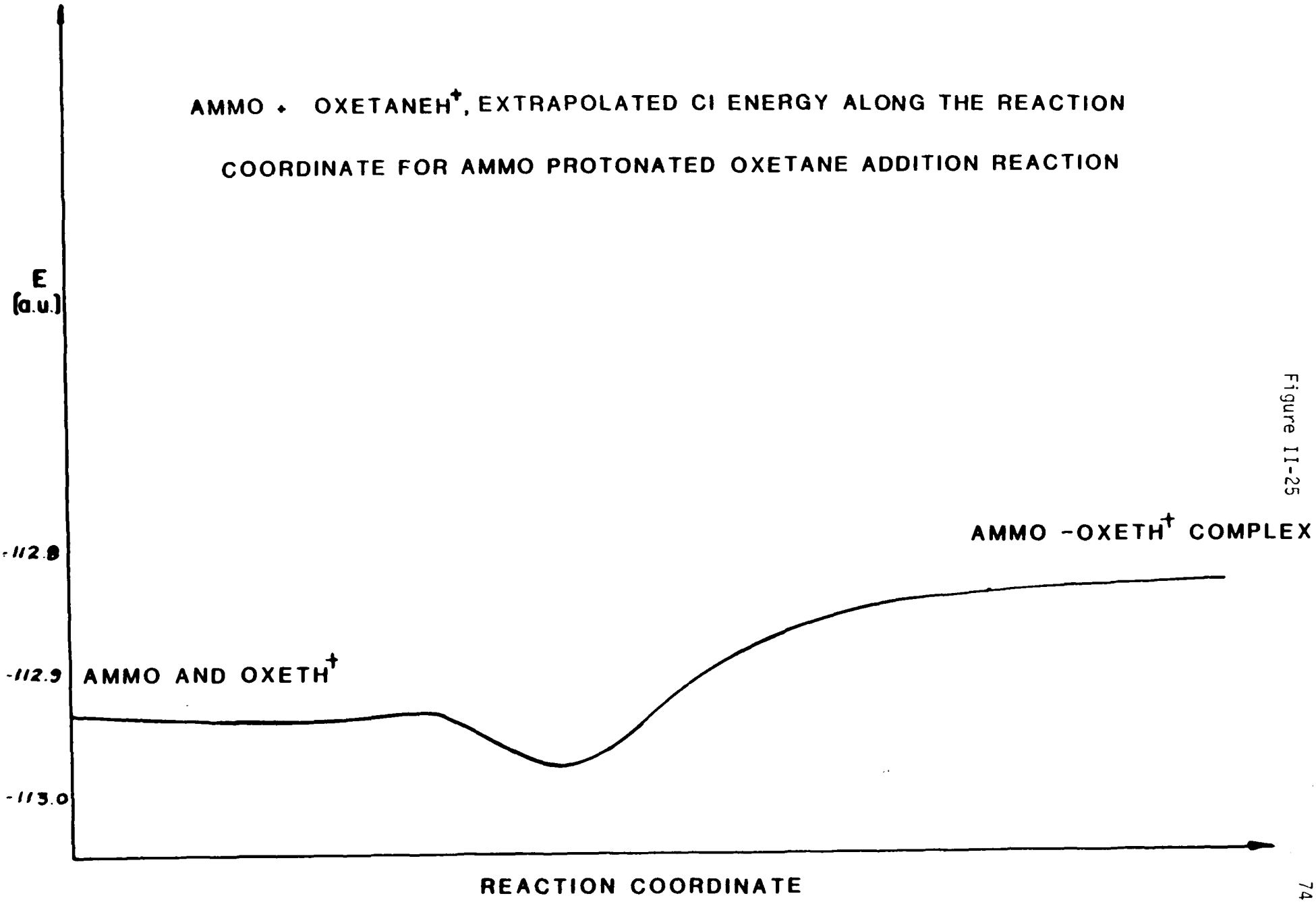
AMMO • OXETANEH+, EXTRAPOLATED CI ENERGY ALONG THE REACTION COORDINATE FOR AMMO PROTONATED OXETANE ADDITION REACTION
E (a.u.)
-112.8
AMMO -OXETH+ COMPLEX
-112.9
AMMO AND OXETH+
-113.0
REACTION COORDINATE

Figure II-25

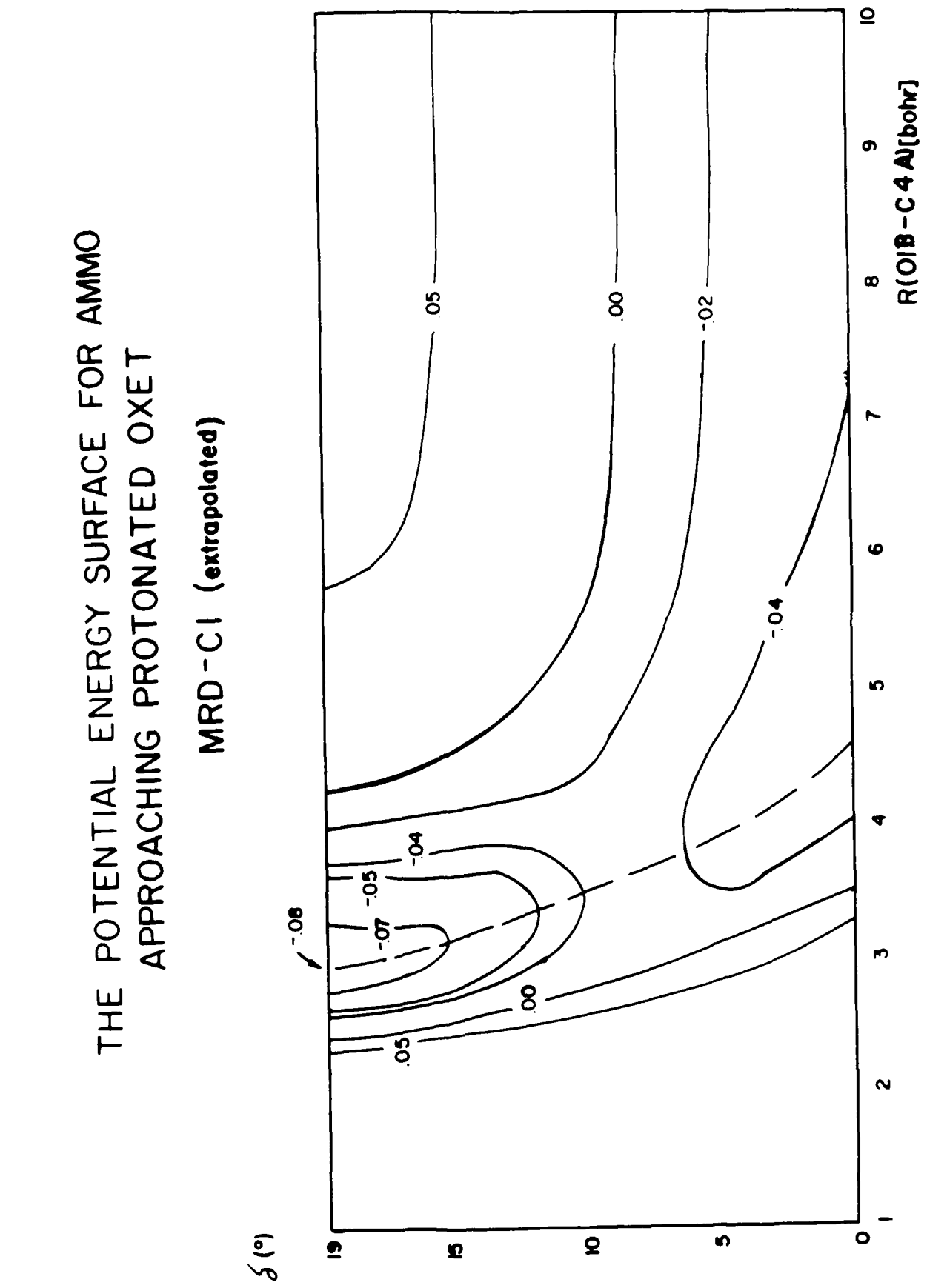
THE POTENTIAL ENERGY SURFACE FOR AMMO
APPROACHING PROTONATED OXET
MRD-CI (extrapolated)
δ(°)
R(OIB-C4A)[bohr]
.05
.00
-.02
-.04
-.05
-.07
-.08
-.04
.00
.05
19
15
10
5
0
1
2
3
4
5
6
7
8
9
10

TABLE II-39

A

AMMO + OXETH$^+$

δ = 0^o (FULLY CLOSED)

ENERGIES (a.u.)

R(O1B-C4A) (bohrs)	2.3	2.9	3.6
SCF	-112.212402	-112.567419	-112.715933
CI	-112.407367	-112.758700	-112.901015
EX	-112.415741	-112.765499	-112.907699
DAV	-112.419053	-112.768486	-112.910196
c^2	.964	.964	.967
GS	.905	.906	.905

R(O1B-C4A) (bohrs)	4.6	10.0
SCF	-112.758393	-112.750039
CI	-112.939447	-112.931844
EX	-112.944701	-112.935694
DAV	-112.946828	-112.937779
c^2	.969	.969
gs	.905	.903

TABLE II-30

B

AMMO + $OXETH^+$

$\delta = 5^o$

ENERGIES (a.u.)

R(O1B-C4A) (bohrs)	2.3	2.9	3.6
SCF	-112.422599	-112.675770	-112.748987
CI	-112.610259	-112.862895	-112.931570
EX	-112.617265	-112.871022	-112.937359
DAV	-112.619748	-112.873804	-112.940058
c^2	.968	.966	.965
gs	.906	.905	.905

R(O1B-C4A) (bohrs)	4.6	10.0
SCF	-112.755698	-112.737486
CI	-112.936221	-112.919347
EX	-112.941127	-112.923042
DAV	-112.943611	-112.925452
c^2	.965	.965
gs	.901	.898

TABLE II-31

C

AMMO + $OXETH^+$

$\delta = 10^o$

ENERGIES (a.u.)

R(O1B-C4A) (bohrs)	2.3	2.9	3.6
SCF	-112.553838	-112.742890	-112.764062
CI	-112.734576	-112.925800	-112.943298
EX	-112.740024	-112.931127	-112.949404
DAV	-112.742076	-112.933420	-112.951970
c^2	.971	.968	.965
gs	.908	.905	.904

R(O1B-C4A) (bohrs)	4.6	10.0
SCF	-112.707936	-112.738741
CI	-112.912073	-112.881148
EX	-112.917085	-112.884915
DAV	-112.919438	-112.887215
c^2	.965	.965
gs	.904	.901

TABLE II-32

D

AMMO + $OXETH^+$

$\delta = 15^o$

ENERGIES (a.u.)

R(O1B-C4A) (bohrs)	2.3	2.9	3.6
SCF	-112.632473	-112.782382	-112.772218
CI	-112.808287	-112.962256	-112.950352
EX	-112.813023	-112.967384	-112.955341
DAV	-112.814859	-112.969441	-112.957658
c^2	.972	.970	.966
gs	.911	.906	.903

R(O1B-C4A) (bohrs)	4.6	10.0
SCF	-112.724061	-112.632473
CI	-112.894278	-112.808287
EX	-112.898511	-112.813023
DAV	-112.900595	-112.814859
c^2	.967	.973
gs	.904	.911

TABLE II-33

E

AMMO + $OXETH^+$

$\delta = 19^o$(FULLY OPEN)

ENERGIES (a.u.)

R(01B-C4A) (bohrs)	2.3	2.9	3.6
SCF	-112.6704978	-112.795132	-112.7661185
CI	-112.844764	-112.974426	-112.946071
EX	-112.849093	-112.979312	-112.950276
DAV	-112.850878	-112.981302	-112.952574
c^2			
gs	.973	.971	.967
	.912	.907	.901

R(01B-C4A) (bohrs)	4.6	10.0
SCF	-112.703459	-112.65156
CI	-112.875073	-112.817392
EX	-112.878483	-112.819742
DAV	-112.880629	-112.821163
c^2		
gs	.966	.973
	.902	.905

2'. Oxetane (OXET) + protonated 3-azidomethyl-3-methyloxetane ($AMMOH^+$)

a'. Results

The stabilization point R(O1B-C4A) = 2.9 bohrs and 19° (fully open) with the stabilization energy -0.02386 a.u. = -14.97 kcal/mole.

The potential energy surfaces and the reaction potential map are presented in Figures II-27 to II-29. The detailed tables of results follow in Tables II-34 to II-38.

Figure II-27: "MRD-CI Extrapolated Energy for OXET Approaching Protonated AMMO For Fixed Angle δ and Different Intermolecular Distances R(O1B-C4A)"

Figure II-28: "MRD-CI Extrapolated Energy for OXET-Protonated AMMO Complex For Fixed Intermolecular Distances R(O1B-C4A) and Different δ Values"

Figure II-29: "The Potential Energy Surface For OXET Approaching Protonated AMMO"

Table II-34: "OXET + $AMMOH^+$ δ = 0° (fully closed) Energies (a.u.) as a function of R(O1B-C4A)"

Table II-35: "OXET + $AMMOH^+$ δ = 5° Energies (a.u.) as a function of R(O1B-C4A)"

Table II-36: "OXET + $AMMOH^+$ δ = 10° Energies (a.u.) as a function of R(O1B-C4A)"

Table II-37: "OXET + $AMMOH^+$ δ = 15° Energies (a.u.) as a function of R(O1B-C4A)"

Table II-38: "OXET + $AMMOH^+$ δ = 19° (fully open) Energies (a.u.) as a function of R(O1B-C4A)"

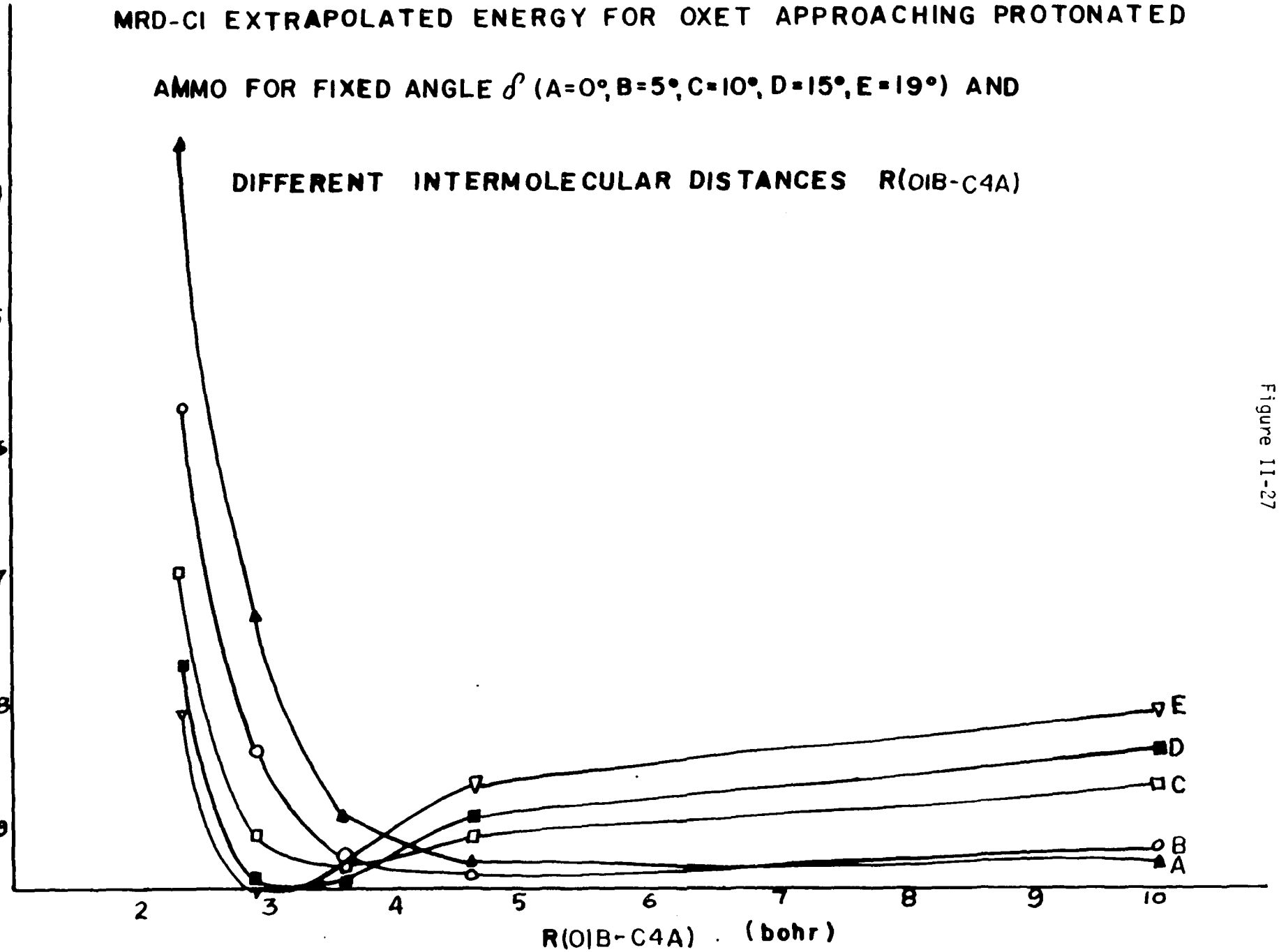
MRD-CI EXTRAPOLATED ENERGY FOR OXET APPROACHING PROTONATED AMMO FOR FIXED ANGLE δ (A=0°, B=5°, C=10°, D=15°, E=19°) AND DIFFERENT INTERMOLECULAR DISTANCES R(O1B-C4A)
E (a.u.)
-112.4
-112.5
-112.6
-112.7
-112.8
-112.9
2
3
4
5
6
7
8
9
10
R(O1B-C4A) (bohr)
E
D
C
B
A

Figure II-27

Figure II-28

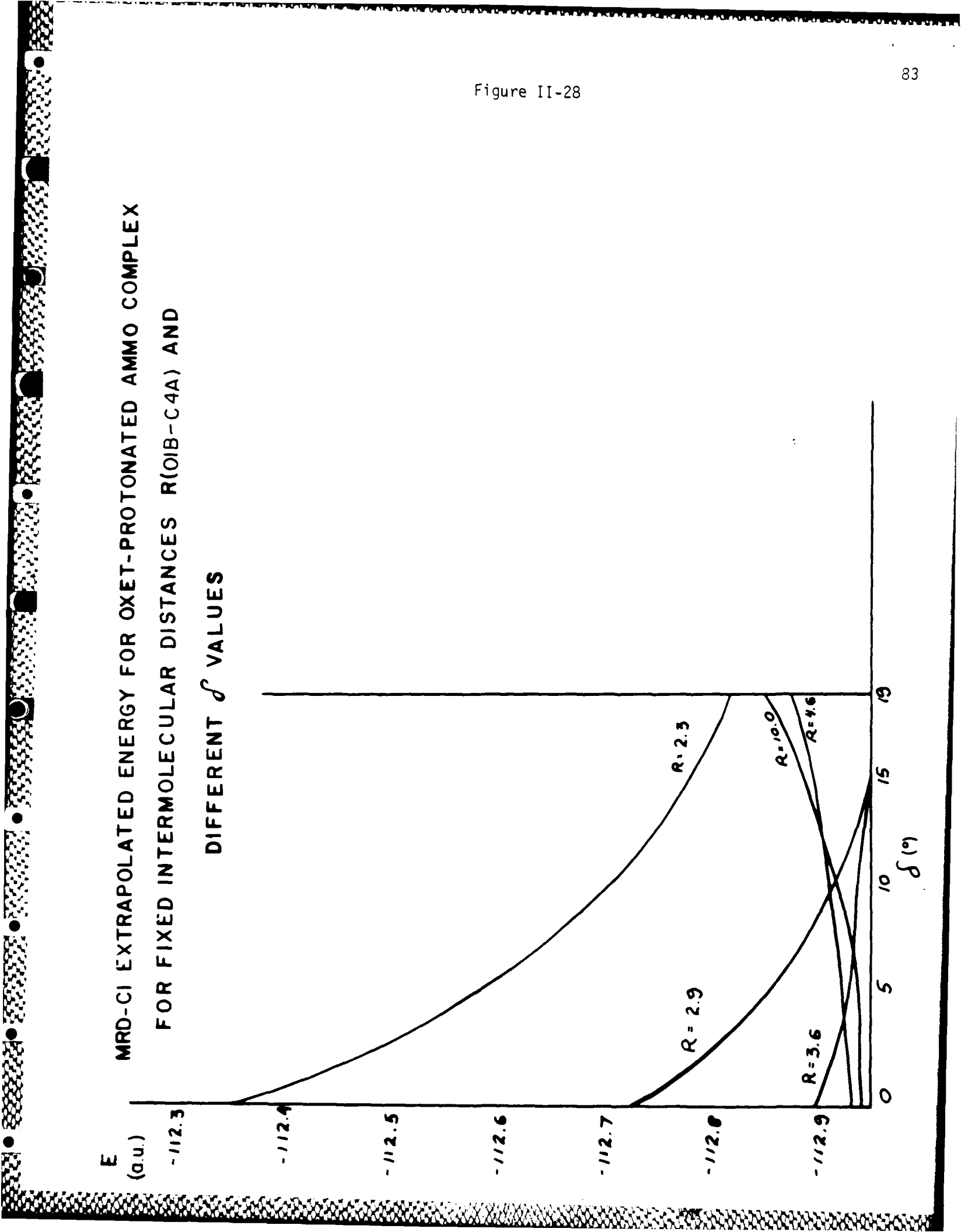
MRD-CI EXTRAPOLATED ENERGY FOR OXET-PROTONATED AMMO COMPLEX
FOR FIXED INTERMOLECULAR DISTANCES R(OIB-C4A) AND
DIFFERENT δ VALUES
E (a.u.)
-112.3
-112.4
-112.5
-112.6
-112.7
-112.8
-112.9
R=2.3
R=2.9
R=3.6
R=4.6
R=10.0
0
5
10
15
δ(°)

Figure II-29

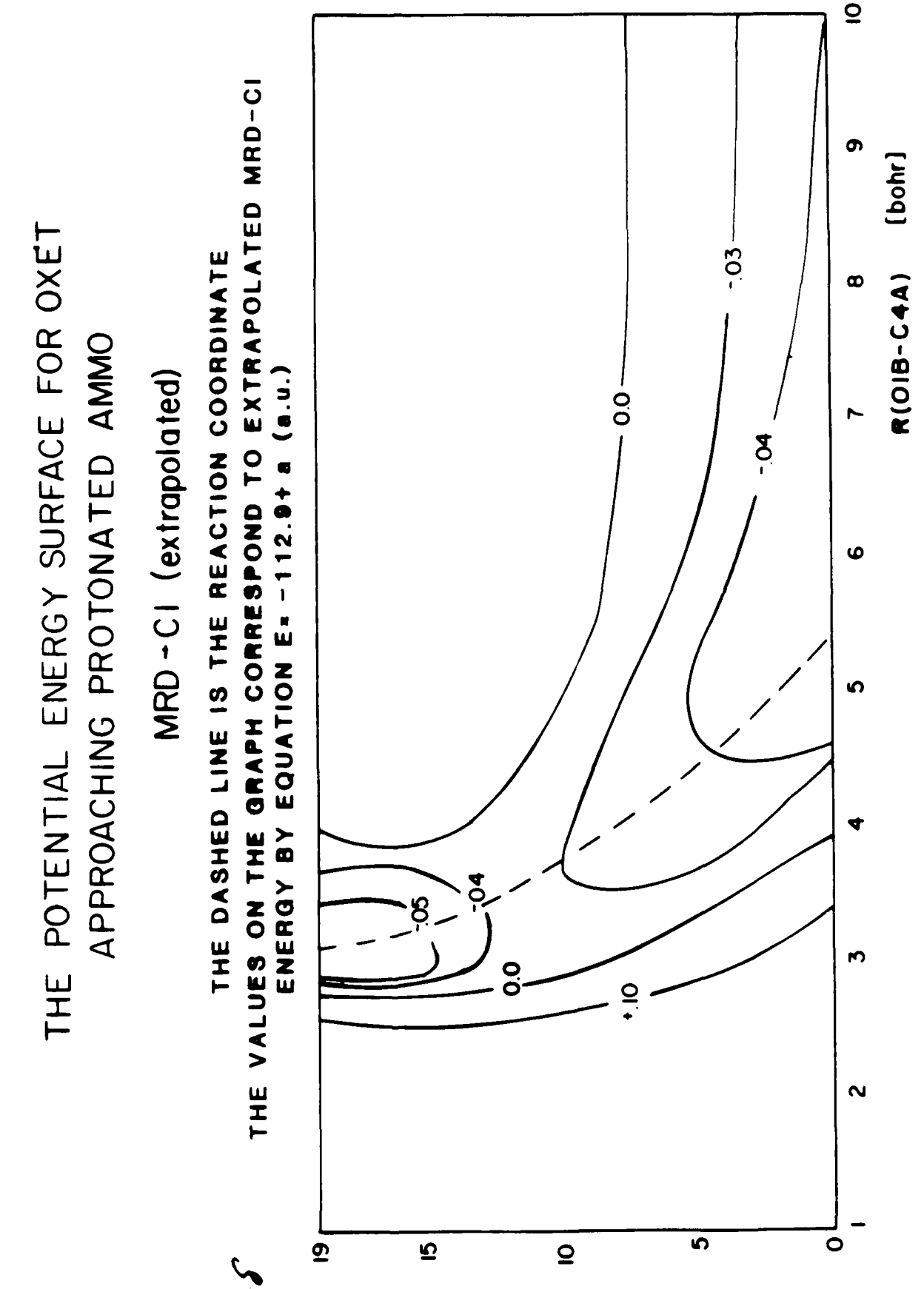
THE POTENTIAL ENERGY SURFACE FOR OXET
APPROACHING PROTONATED AMMO
MRD-CI (extrapolated)
THE DASHED LINE IS THE REACTION COORDINATE
THE VALUES ON THE GRAPH CORRESPOND TO EXTRAPOLATED MRD-CI
ENERGY BY EQUATION E= -112.9+ a (a.u.)
-.05
-.04
0.0
+.10
0.0
-.04
-.03
R(OIB-C4A) [bohr]
19
15
10
5
0
1
2
3
4
5
6
7
8
9
10

TABLE II-34

A

OXET + $AMMOH^+$

$\delta = 0^o$
(fully closed)

ENERGIES (a.u.)

R(O1B-C4A) (bohrs)	2.3	2.9	3.6
SCF	-112.164132	-112.542090	-112.706134
CI	-112.358522	-112.732924	-112.890654
EX	-112.366976	-112.739502	-112.896460
DAV	-112.370250	-112.742435	-112.900469
c^2	.964	.9651	.9569
gs	.905	.906	.906

R(O1B-C4A) (bohrs)	4.6	10.0
SCF	-112.757479	-112.751545
CI	-112.938395	-112.933136
EX	-112.943841	-112.936887
DAV	-112.945962	-112.938947
c^2	.9696	.9696
gs	.9056	.904

TABLE II-35

B

OXET + $AMMOH^+$

$\delta = 5^o$

ENERGIES (a.u.)

R(O1B-C4A) (bohrs)	2.3	2.9	3.6
SCF	-112.380825	-112.654044	-112.740730
CI	-112.567865	-112.840616	-112.922895
EX	-112.574772	-112.848736	-112.928602
DAV	-112.577225	-112.851497	-112.932235
c^2	.9687	.965	.958
gs	.9067	.9057	.9048

R(O1B-C4A) (bohrs)	4.6	10.0
SCF	-112.755627	-112.739371
CI	-112.936087	-112.921221
EX	-112.940998	-112.924839
DAV	-112.943458	-112.927221
c^2	.965	.9655
gs	.9015	.898

TABLE II-36

C

OXET + $AMMOH^+$

$\delta = 10^o$

ENERGIES (a.u.)

R(01B-C4A) (bohrs)	2.3	2.9	3.6
SCF	-112.517118	-112.72324	-112.75546
CI	-112.697121	-112.905683	-112.927808
EX	-112.702417	-112.911346	-112.930962
DAV	-112.704430	-112.913639	-112.942933
c^2	.909	.9060	.9124
gs	.971	.9685	.9226

R(01B-C4A) (bohrs)	4.6	10.0
SCF	-112.73736	-112.70814
CI	-112.91068	-112.874988
EX	-112.915738	-112.876492
DAV	-112.91810	-112.891173
C^2	.904	.909
GS	.965	.9108

TABLE II-37

D

OXET + $AMMOH^+$

$\delta = 15^O$

ENERGIES (a.u.)

R(O1B-C4A) (bohrs)	2.3	2.9	3.6
SCF	-112.599563	-112.763765	-112.7622807
CI	-112.774975	-112.943217	-112.940000
EX	-112.779670	-112.948373	-112.944830
DAV	-112.781491	-112.950410	-112.947124
C^2	.973	.970	.9668
GS	.9118	.9071	.903

R(O1B-C4A) (bohrs)	4.6	10.0
SCF	-112.7198416	-112.677837
CI	-112.889931	-112.845810
EX	-112.894115	-112.849130
DAV	-112.896185	-112.850898
c^2	.9672	.9694
gs	.905	.9037

TABLE II-33

E

OXET + $AMMOH^+$

$\delta = 19^o$
(fully open)

ENERGIES (a.u.)

R(O1B-C4A) (bohrs)	2.3	2.9	3.6
SCF	-112.6397454	-112.77667165	-112.7547122
CI	-112.811422	-112.953525	-112.932275
EX	-112.818284	-112.960747	-112.938784
DAV	-112.820049	-112.962721	-112.941037
c^2	0.97329334	0.97090597	0.96709588
gs	0.913082	0.90737	0.9018638

R(O1B-C4A) (bohrs)	4.6	10.0
SCF		-112.6445043
CI	-112.866056	-112.810255
EX	-112.871591	-112.813953
DAV	-112.873703	-112.815439
c^2	0.96659015	0.97269997
gs	0.90336874	0.90455537

3'. 3-Azidomethyl-3-methyloxetane (AMMO) + protonated 3-azidomethyl-3-methyloxetane

a'. Results

To check that the optimum α angle for AMMO + $AMMOH^+$ was 90° we ran the SCF calculations as a function of α.

Table II-39, "AMMO + $AMMOH^+$, SCF Energies, α Angle Dependence" The stabilization point R(C4A-O1B) = 2.9 bohrs and δ = 19° (fully open) with stabilization energy = -0.02408 a.u. = -15.11 kcal/mol. The estimated activation energy is 6.27 kcal/mol.

The potential energy surfaces and the reaction potential map are presented in Figures II-30 to II-33. The detailed tables of results follow in Tables II-40 - II-43.

Figure II-30: "Extrapolated Energy For AMMO Approaching Protonated AMMO For Fixed Angle δ And Different Intermolecular Distances R(O1BC4A)"

Figure II-31: "MRD-CI Extrapolated Energy For AMMO-AMMO Protonated Complex For Fixed Intermolecular Distances R(O1B-C4A) And Different δ Angle Values"

Figure II-32: "AMMO-$AMMOH^+$ Extrapolated CI Energy Along the Reaction Coordinate For AMMO Protonated AMMO Addition Reaction"

Figure II-33: "The Potential Energy Surface For AMMO Approaching Protonated AMMO"

Table II-40: "AMMO + $AMMOH^+$, δ = 0° (fully closed) Energies (a.u.) as a function of R(O1B-C4A)"

Table II-41: "AMMO + $AMMOH^+$, δ = 5° Energies (a.u.) as a function of R(O1B-C4A)"

Table II-42: "AMMO + $AMMOH^+$, δ = 10° Energies (a.u.) as a function of R(O1B-C4A)"

Table II-43: "AMMO + $AMMOH^+$, δ = 15° Energies (a.u.) as a function of R(O1B-C4A)"

Table II-44: "AMMO + $AMMOH^+$, δ = 19° (fully open) Energies (a.u.) as a function of R(O1B-C4A)"

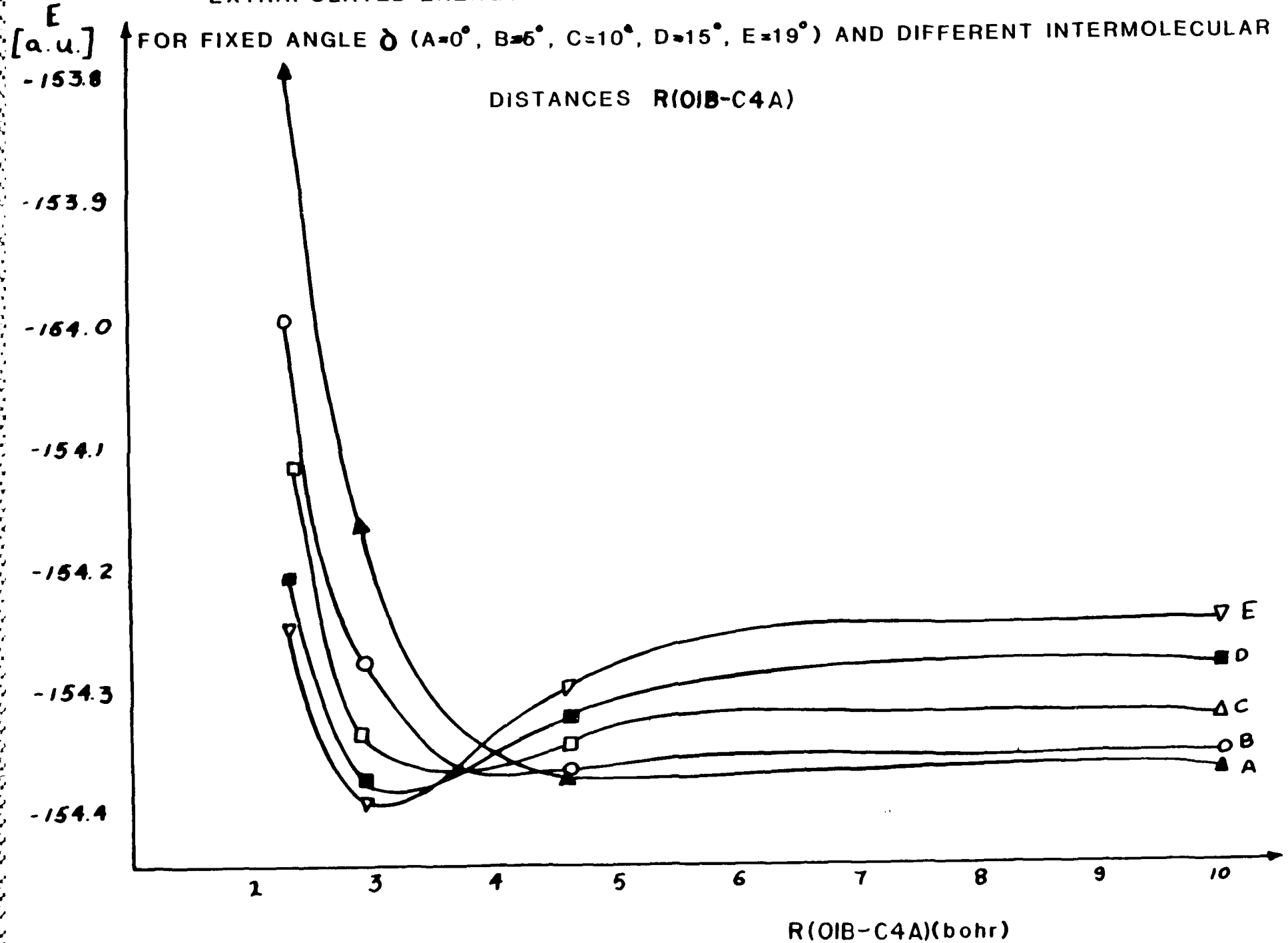
EXTRAPOLATED ENERGY FOR AMMO APPROACHING PROTONATED AMMO
FOR FIXED ANGLE δ (A=0°, B=6°, C=10°, D=15°, E=19°) AND DIFFERENT INTERMOLECULAR
DISTANCES R(OIB-C4A)
E
[a.u.]
-153.8
-153.9
-154.0
-154.1
-154.2
-154.3
-154.4
1
3
4
5
6
7
8
9
10
R(OIB-C4A)(bohr)
E
D
C
B
A

Figure II-30

Figure II-31

MRD-CI EXTRAPOLATED ENERGY FOR AMMO-AMMO PROTONATED COMPLEX FOR FIXED INTERMOLECULAR DISTANCES AND DIFFERENT δ ANGLE VALUES R(QB-C4A)

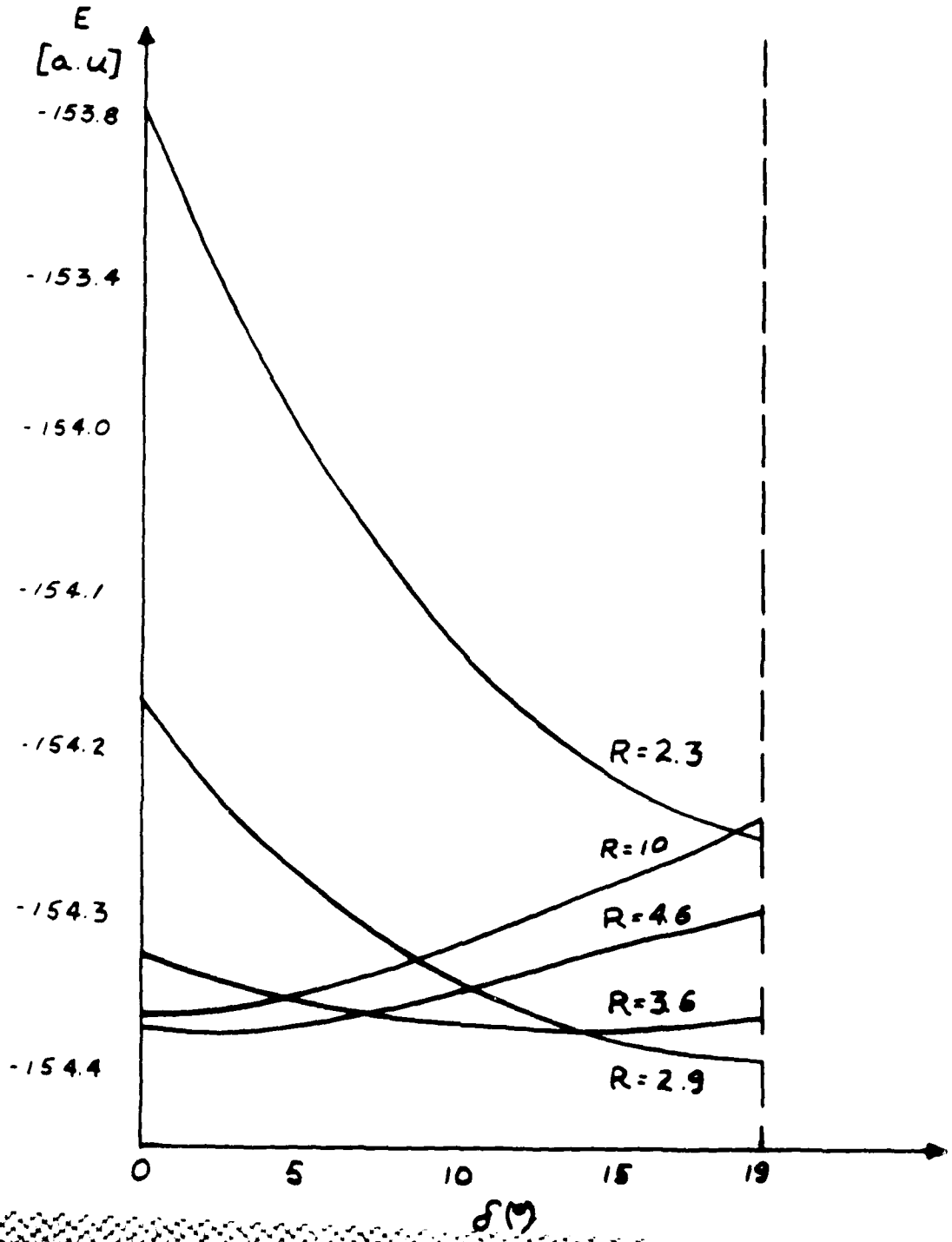

AD-A195 127 QUANTUM CHEMICAL INVESTIGATIONS OF THE MECHANISM OF CATIONIC POLYMERIZATI (U) JOHNS HOPKINS UNIV BALTIMORE MD J J KAUFMAN 15 NOV 87 TR-8 N00014-80-C-0003 2/2

UNCLASSIFIED F/G 7/3 NL

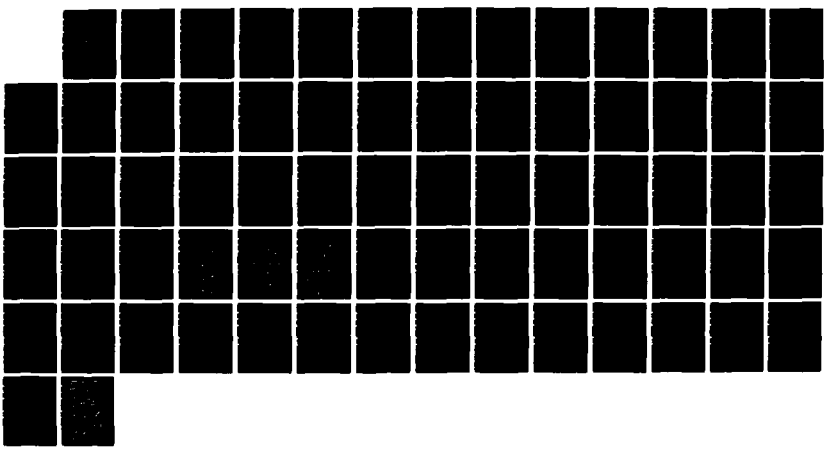

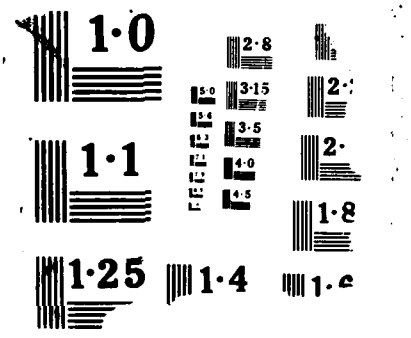
1·0
1·1
1·25
1·4
2·8
3·15
3·5
4·0
4·5
2·
1·8

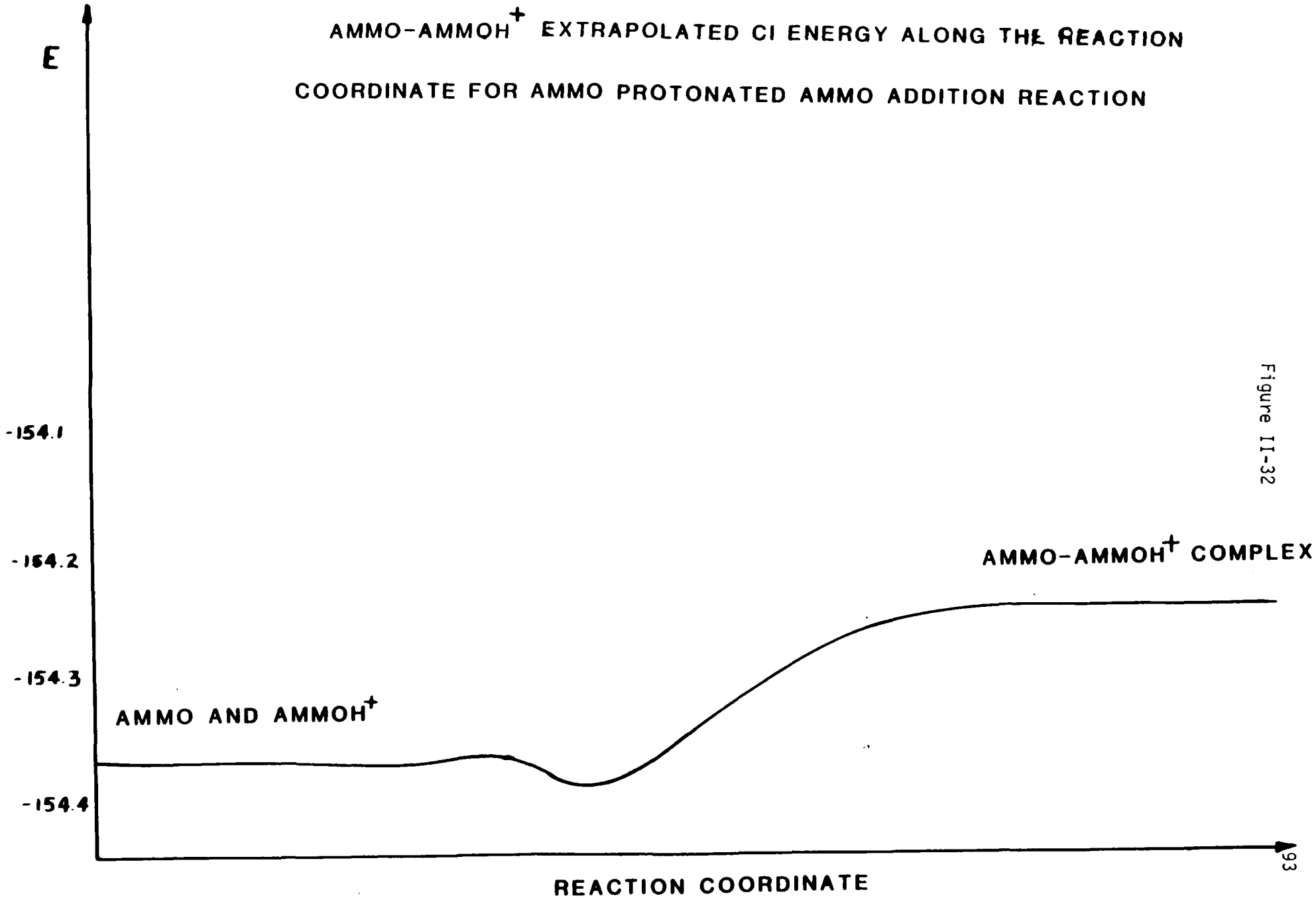
AMMO-AMMOH+ EXTRAPOLATED CI ENERGY ALONG THE REACTION COORDINATE FOR AMMO PROTONATED AMMO ADDITION REACTION
E
-154.1
-154.2
-154.3
-154.4
AMMO AND AMMOH+
AMMO-AMMOH+ COMPLEX
REACTION COORDINATE
93

Figure II-32

Figure II-33

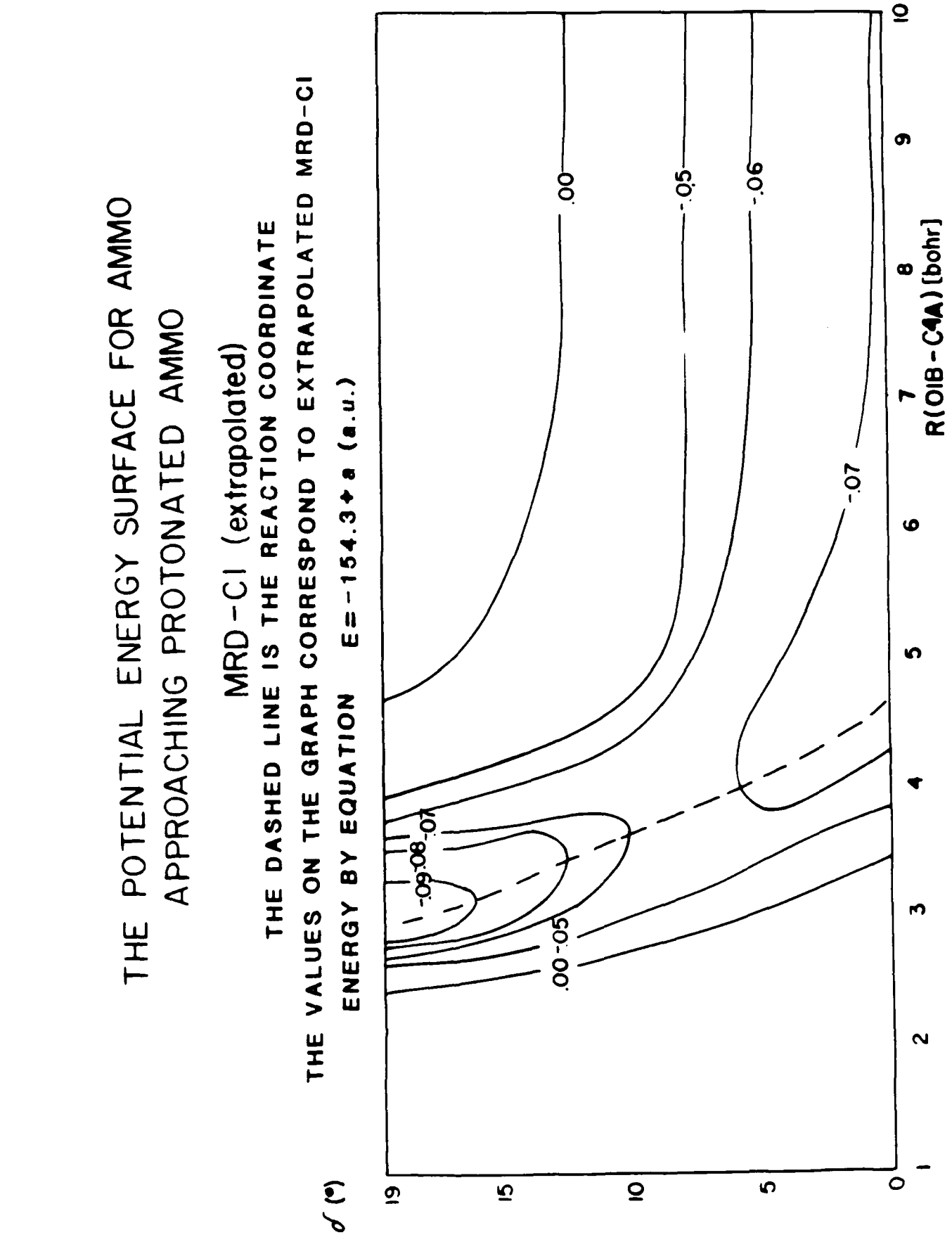
THE POTENTIAL ENERGY SURFACE FOR AMMO APPROACHING PROTONATED AMMO
MRD-CI (extrapolated)
THE DASHED LINE IS THE REACTION COORDINATE
THE VALUES ON THE GRAPH CORRESPOND TO EXTRAPOLATED MRD-CI ENERGY BY EQUATION E=-154.3+a (a.u.)
.00
-.05
-.06
-.07
-.09
-.08
-.07
.00
-.05
19
15
10
5
0
1
2
3
4
5
6
7
8
9
10
R(OIB-C4A) [bohr]
δ (°)

TABLE II-39

AMMO + $AMMOH^+$

α ANGLE DEPENDENCE

α (°)	SCF
0	-153.88041
90	-153.97455
180	-153.87978
270	-153.97535
305	-153.93036
315	-153.93097

TABLE II-[illegible]

AMMO + $AMMOH^+$

$\delta = 0^o$ (FULLY CLOSED)

ENERGIES (a.u.)

R(O1B-C4A) (bohrs)	2.3	2.9	3.6
SCF	-153.596296	-153.975355	-154.139594
CI	-153.790525	-154.165945	-154.324062
EX	-153.798841	-154.172725	-154.330693
DAV	-153.802098	-154.175653	-154.333130
c^2	0.964	0.965	0.967
gs	0.906	0.906	0.906

R(O1B-C4A) (bohrs)	4.6	10.0
SCF	-154.191083	-154.186025
CI	-154.371742	-154.367499
EX	-154.377200	-154.371299
DAV	-154.379303	-154.373342
c^2	0.970	0.970
gs	0.906	0.904

TABLE II-41

AMMO + $AMMOH^+$

$\delta = 5^o$

ENERGIES (a.u.)

R(O1B-C4A) (bohrs)	2.3	2.9	3.6
SCF	-153.814107	-153.951247	-154.174310
CI	-154.000988	-154.274199	-154.356484
EX	-154.007818	-154.282183	-154.362352
DAV	-154.010260	-154.284928	-154.365015
c^2	0.968	0.966	0.965
gs	0.907	0.906	0.905

R(O1B-C4A) (bohrs)	4.6	10.0
SCF	-154.189225	-154.173834
CI	-154.369528	-154.355578
EX	-154.374182	-154.359227
DAV	-154.376621	-154.36160
c^2	0.966	0.965
gs	0.902	0.899

TABLE II-[illegible]

C

$AMMO + AMMOH^+$

$\delta = 10^o$

ENERGIES (a.u.)

R(O1B-C4A) (bohrs)	2.3	2.9	3.6
SCF	-153.951248	-154.157459	-154.189200
CI	-154.130896	-154.339691	-154.367479
EX	-154.136065	-154.345329	-154.373005
DAV	-154.138029	-154.347606	-154.375491
c^2	0.972	0.969	0.965
gs	0.809	0.906	0.904

R(O1B-C4A) (bohrs)	4.6	10.0
SCF	-154.170941	-154.142564
CI	-154.344119	-154.316851
EX	-154.349152	-154.320735
DAV	-154.351513	-154.323112
c^2	0.965	0.963
gs	0.904	0.900

TABLE II-43

AMMO + $AMMOH^+$

$\delta = 15^o$

ENERGIES (a.u.)

R(O1B-C4A) (bohrs)	2.3	2.9	3.6
SCF	-154.034207	-154.198300	-154.196284
CI	-154.209377	-154.376871	-154.374171
EX	-154.214183	-154.381482	-154.379496
DAV	-154.215995	-154.384939	-154.381804
c^2	0.973	0.959	0.967
gs	0.912	0.908	0.903

R(O1B-C4A) (bohrs)	4.6	10.0
SCF	-154.153651	-154.112237
CI	-154.323403	-154.280050
EX	-154.327627	-154.283300
DAV	-154.329684	-154.285057
c^2	0.967	0.968
gs	0.905	0.903

TABLE II-44

AMMO + $AMMOH^+$

$\delta = 19^o$(FULLY OPEN)

ENERGIES (a.u.)

R(O1B-C4A) (bohrs)	2.3	2.9	3.6
SCF	-154.074638	-154.211389	-154.188879
CI	-154.248331	-154.390422	-154.368442
EX	-154.253127	-154.395379	-154.373253
DAV	-154.254876	-154.337350	-154.375538
c^2	0.973	0.971	0.967
gs	0.913	0.907	0.901

R(O1B-C4A) (bohrs)	4.6	10.0
SCF	-154.130128	-154.078893
CI	-154.301398	-154.245371
EX	-154.305233	-154.248153
DAV	-154.307349	-154.249629
c^2	0.966	0.973
gs	0.903	0.904

(b). Recap of Reaction Energies for Cationic Polymerization of Energetic Oxetanes for Initiation and Reaction

Cationic polymerization has two major steps: initiation and propagation. Initiation is governed by the propensity for protonation of the oxetane. The three dimensional electrostatic molecular potential contour (EMPC) maps we calculated earlier are very indicative of the propensity of the energetic substituted oxetanes to initiate. These EMPC maps are also indicative of the propensity of the energetic substituted oxetanes to polymerize. For a more quantitative comparison of propensity to initiate we calculated the MRD-CI energies of protonation [ΔE(protonation)] for all the energetic substituted oxetanes we have studied.

The next step in cationic polymerization is reaction between the oxetane (or substituted oxetanes) and the protonated oxetane (or protonated substituted oxetane). We have calculated the MRD-CI stabilization energy [ΔE(addition)] for several series of reactants as a function of the angle (α) between the rings, the interring distance R(01B-C4A) and the angle (δ) of opening the protonated ring. The stabilization point for all of the pairs of reactants we have studied to date is R(01B-C4A) = 2.9 bohrs and δ = 19°. (See sketch page 8 for definition of δ angle)

In the Table (II-45) are tabulated the MRD-CI values for ΔE (protonation), ΔE (addition) and ΔE [ΔE (protonation) + ΔE (addition)] at the stabilization point for OXET (oxetane) + $OXETH^+$ (oxetane H^+), FNOX + $OXETH^+$, OXET + $FNOXH^+$, FNOX + $FNOXH^+$, AMMO + $OXETH^+$, OXET + $AMMOH^+$, and AMMO + $AMMOH^+$.

The calculated MRD-CI values for ΔE (protonation) indicate that FNOX gains less energy on protonation than OXET or AMMO. OXET and AMMO have close to the same protonation energy. However, our earlier EMPC maps which indicated that OXET had a larger volume within its -20 kcal isopotential contour would imply that oxetane would still have a somewhat greater tendency to protonate sooner (initiate sooner) than AMMO even though they both have similar ΔE (protonation).

The calculated ΔE values indicate that all combinations involving FNOX or $FNOXH^+$ are less favorable than those involving OXET or $OXETH^+$ and AMMO or $AMMOH^+$.

The most favorable reactions involve $OXETH^+$ reacting with OXET or AMMO rather than $AMMOH^+$ reacting with OXET or AMMO.

Our initial MRD-CI result on protonation of BAMO indicates it has a lower ΔE (protonation) than that of AMMO. Thus in a BAMO-AMMO mixture AMMO will tend to initiate first to form $AMMOH^+$. We are continuing MRD-CI

calculations for the potential surfaces of reactions involving BAMO and $BAMOH^+$ with various partners.

The results of calculations such as these will enable one both to understand and then to predict copolymerization preferences.

TABLE II-45

CATIONIC POLYMERIZATION INITIATION AND PROPAGATION

PROTONATED OXETANES ($OXETANEH^+$) + OXETANES
AB-INITIO MODPOT/VRDDO MRD-CI

ENERGIES (a.u.)

	ΔE(protonation)	ΔE(addition)	ΔE
OXETANE + $OXETANEH^+$	-0.31601	-0.04378	-0.35979
FNOX + $OXETANEH^+$	-0.31601	-0.01113	-0.32714
OXETANE + $FNOXH^+$	-0.27068	-0.06327	-0.33394
FNOX + $FNOXH^+$	-0.27068	-0.03157	-0.30225
AMMO + $OXETANEH^+$	-0.31601	-0.04362	-0.35963
AMMO + $AMMOH^+$	-0.31548	-0.02408	-0.33956
OXETANE + $AMMOH^+$	-0.31548	-0.02386	-0.33934
OXETANE + $BAMOH^+$	-0.30906		

(c). Population Analyses

Gerry Manser had expressed interest in the population analyses for the gross atomic populations on the carbon atom being attacked (C4A) in the protonated ring and the total overlap populations between C4A-O1A (in the protonated ring) and O1B-C4A (the bond being formed between the unprotonated ring and the protonated ring).

Following are detailed tables of this and the total overlap populations and gross atomic populations for the entire AMMO + $OXETH^+$, OXET + $AMMOH^+$, and AMMO + $AMMOH^+$ series as a function of the inter-ring distance R(O1B-C4A) and the angle of opening the protonated ring (δ). Tables II-46 - Table II-63

The general conclusions are:

1'. C2A and C4A (the α carbons in the original protonated ring) still carry about the same excess negative charge (~0.2 e) in spite of the fact that the protonated species carries a formal positive charge. The closeness of the charges on C2A and C4A in $OXETH^+$ and $AMMOH^+$ is commensurate with their similarities in pertinent energy quantities. As the protonated ring opens and the O1B of the unprotonated ring begins to form a bond with C_{4A}, there is little change in the charge on C_{4A}.

2'. O1A in the protonated ring ($OXETH^+$ or $AMMOH^+$) carries an excess negative charge of -0.37. O1B in the unprotonated ring (OXET or AMMO) carries an excess negative charge of -0.35. When the O1B-C4A bond forms, O1B still carries an excess negative charge of -0.29 in AMMO + $OXETH^+$ and excess negative charge of 0.32 in AMMO + $AMMOH^+$. When the C4A-O1A breaks, the O1A carries a little more negative charge (0.44 in AMMO + $OXETH^+$, 0.45 in AMMO + $AMMOH^+$) in both protonated partners.

3'. Total overlap populations are a very sensitive criteria of the incipient making and breaking of bonds. The largest TOP's occur when the energy is a minimum. As the protonated and unprotonated oxetane (energetic substituted oxetane)rings approach

    a'. the interring TOP (C4A-O1A) begins to get smaller even when the protonated ring is still fully closed. This indicates that the C4A-O1A bond wants to lengthen.

b'. The TOP (O1B-C4A) begins to be noticeable at 4.6 bohrs and gets larger as the rings approach closer provided that the protonated ring is open by at least $\delta = 5°$. The strongest TOP(O1B-C4A) occurs (as anticipated) at the most stable point energetically R(O1B-C4A) = 2.9 bohrs and $\delta = 19°$.

TABLE II-46

AMMO + OXETH$^+$

Total Overlap Populations
Ab-Initio MODPOT/VRDDO

O1B-C4A

δ	0°		5°		10°		15°		19°	
R(bohrs)	SCF	CI	SCF	CI	SCF	CI	SCF	CI	SCF	CI
2.3	-0.191	-0.202	0.100	0.075	0.240	0.206	0.317	0.278	0.367	0.325
2.9	-0.226	-0.214	0.080	0.074	0.254	0.240	0.350	0.328	0.407	0.481
3.6	-0.124	-0.015	0.052	0.059	0.240	0.206	0.270	0.276	0.318	0.318
4.6	-0.021	-0.019	0.024	0.025	0.069	0.074	0.106	0.116	0.131	0.144
10.0	0.000	0.000	0.000	0.000	0.000	0.000	0.000	0.000	0.000	0.000

C4A-O1A

2.3	-0.026	-0.037	-0.040	-0.037	-0.040	-0.038	-0.030	-0.030	-0.022	-0.021
2.9	0.167	0.143	0.077	0.077	0.011	0.013	-0.013	-0.013	-0.016	-0.016
3.6	0.317	0.290	0.192	0.193	-0.040	-0.038	0.005	0.006	-0.011	-0.011
4.6	0.389	0.363	0.267	0.271	0.119	0.134	0.024	0.031	-0.005	-0.004
10.0	0.422	0.392	0.306	0.307	0.153	0.175	0.427	0.398	-0.001	0.004

TABLE II-47

AMMO + OXETH$^+$

Gross Atomic Populations
Ab-Initio MODPOT/VRDDO

$\delta = 0°$ (fully closed)

R(bohrs)	2.3		2.9		3.6		4.6		10.0	
	SCF	CI	SCF	CI	SCF	CI	SCF	CI	SCF	CI
O1A	6.448	6.387	6.461	6.394	6.460	6.386	6.452	6.375	6.444	6.367
C2A	4.240	4.264	4.227	4.252	4.213	4.238	4.203	4.228	4.196	4.221
C3A	4.458	4.450	4.440	4.437	4.439	4.439	4.441	4.443	4.446	4.449
C4A	4.078	4.092	4.122	4.143	4.146	4.160	4.171	4.178	4.192	4.198
H2Aa	0.739	0.739	0.727	0.727	0.715	0.715	0.707	0.707	0.700	0.700
H2Ab	0.740	0.740	0.728	0.728	0.716	0.716	0.707	0.707	0.700	0.700
H4Aa	0.745	0.754	0.730	0.742	0.711	0.723	0.698	0.710	0.699	0.711
H4Ab	0.746	0.755	0.731	0.743	0.711	0.723	0.699	0.711	0.700	0.711
H^+	0.586	0.608	0.556	0.576	0.529	0.549	0.512	0.531	0.500	0.520
O1B	6.358	6.300	6.376	6.318	6.402	6.352	6.413	6.373	6.381	6.347
C2B	4.249	4.272	4.247	4.260	4.250	4.270	4.252	4.272	4.250	4.276
C3B	4.043	4.043	4.038	4.038	4.038	4.038	4.040	4.039	4.042	4.042
C4B	4.258	4.281	4.256	4.274	4.260	4.278	4.262	4.280	4.260	4.276
H2Ba	0.731	0.731	0.744	0.744	0.757	0.757	0.766	0.766	0.772	0.772
H2Bb	0.728	0.728	0.744	0.744	0.758	0.758	0.767	0.767	0.775	0.775
H4Ba	0.733	0.733	0.745	0.745	0.758	0.758	0.767	0.767	0.773	0.773
H4Bb	0.732	0.732	0.747	0.747	0.761	0.761	0.771	0.771	0.779	0.779

TABLE II-48

AMMO + $OXETH^+$

Gross Atomic Populations
Ab-Initio MODPOT/VRDDO

$\delta = 5°$

R(bohrs)	2.3		2.9		3.6		4.6		10.0	
	SCF	CI	SCF	CI	SCF	CI	SCF	CI	SCF	CI
O1A	6.476	6.424	6.484	6.425	6.481	6.411	6.471	6.390	6.461	6.373
C2A	4.253	4.273	4.246	4.265	4.234	4.252	4.223	4.237	4.215	4.228
C3A	4.443	4.441	4.440	4.442	4.445	4.451	4.449	4.458	4.453	4.465
C4A	4.090	4.096	4.107	4.125	4.110	4.135	4.115	4.113	4.136	4.154
H2Aa	0.753	0.753	0.742	0.742	0.730	0.730	0.719	0.719	0.711	0.711
H2Ab	0.753	0.753	0.743	0.743	0.730	0.730	0.720	0.720	0.711	0.711
H4Aa	0.751	0.760	0.733	0.744	0.705	0.718	0.684	0.699	0.678	0.694
H4Ab	0.753	0.761	0.733	0.745	0.705	0.719	0.684	0.700	0.678	0.695
H^+	0.624	0.647	0.599	0.621	0.570	0.589	0.548	0.563	0.536	0.547
O1B	6.356	6.293	6.370	6.304	6.398	6.339	6.415	6.371	6.382	6.348
C2B	4.215	4.241	4.221	4.242	4.236	4.254	4.248	4.268	4.250	4.268
C3B	4.043	4.042	4.040	4.040	4.040	4.040	4.040	4.040	4.042	4.042
C4B	4.224	4.249	4.231	4.250	4.245	4.262	4.257	4.276	4.260	4.276
H2Ba	0.721	0.721	0.733	0.733	0.749	0.749	0.763	0.763	0.772	0.772
H2Bb	0.719	0.719	0.733	0.733	0.750	0.750	0.764	0.764	0.775	0.775
H4Ba	0.722	0.722	0.735	0.735	0.751	0.751	0.764	0.764	0.773	0.773
H4Bb	0.722	0.722	0.737	0.737	0.753	0.753	0.767	0.767	0.779	0.779

TABLE II-49

AMMO + $OXETH^+$

Gross Atomic Populations
Ab-Initio MODPOT/VRDDO

δ = 10°

R(bohrs)	2.3		2.9		3.6		4.6		10.0	
	SCF	CI	SCF	CI	SCF	CI	SCF	CI	SCF	CI
O1A	6.487	6.444	6.495	6.448	6.487	6.444	6.495	6.430	6.488	6.411
C2A	4.263	4.278	4.259	4.275	4.263	4.278	4.240	4.253	4.234	4.240
C3A	4.437	4.437	4.442	4.447	4.437	4.437	4.457	4.467	4.460	4.473
C4A	4.119	4.118	4.120	4.129	4.119	4.118	4.072	4.084	4.075	4.086
H2Aa	0.761	0.761	0.753	0.753	0.761	0.761	0.731	0.731	0.721	0.721
H2Ab	0.761	0.761	0.753	0.753	0.761	0.761	0.731	0.731	0.721	0.721
H4Aa	0.741	0.749	0.725	0.736	0.741	0.749	0.668	0.683	0.654	0.669
H4Ab	0.742	0.750	0.726	0.737	0.742	0.750	0.669	0.684	0.654	0.669
H^+	0.646	0.671	0.630	0.655	0.646	0.671	0.590	0.609	0.574	0.590
O1B	6.363	6.297	6.366	6.295	6.363	6.297	6.414	6.363	6.383	6.349
C2B	4.193	4.220	4.204	4.224	4.193	4.220	4.241	4.260	4.250	4.269
C3B	4.043	4.043	4.042	4.042	4.043	4.042	4.041	4.040	4.042	4.041
C4B	4.202	4.229	4.213	4.232	4.202	4.229	4.251	4.268	4.260	4.277
H2Ba	0.714	0.714	0.725	0.725	0.714	0.714	0.758	0.758	0.772	0.772
H2Bb	0.714	0.714	0.725	0.726	0.714	0.714	0.759	0.759	0.775	0.775
H4Ba	0.715	0.715	0.726	0.726	0.715	0.715	0.759	0.759	0.773	0.773
H4Bb	0.717	0.717	0.729	0.729	0.717	0.717	0.762	0.762	0.778	0.778

TABLE II-50

AMMO + $OXETH^+$

Gross Atomic Populations
Ab-Initio MODPOT/VRDDO

δ = 15°

R(bohrs)	2.3		2.9		3.6		4.6		10.0	
	SCF	CI	SCF	CI	SCF	CI	SCF	CI	SCF	CI
O1A	6.483	6.445	6.489	6.450	6.494	6.452	6.496	6.451	6.448	6.370
C2A	4.269	4.281	4.268	4.280	4.264	4.276	4.257	4.266	4.176	4.201
C3A	4.435	4.437	4.444	4.450	4.455	4.466	4.463	4.474	4.043	4.047
C4A	4.150	4.146	4.146	4.149	4.116	4.130	4.063	4.065	4.183	4.188
H2Aa	0.764	0.764	0.757	0.757	0.748	0.748	0.737	0.738	0.705	0.705
H2Ab	0.764	0.765	0.757	0.758	0.749	0.749	0.738	0.738	0.709	0.709
H4Aa	0.733	0.740	0.722	0.732	0.696	0.711	0.664	0.678	0.704	0.715
H4Ab	0.735	0.741	0.723	0.733	0.697	0.712	0.665	0.679	0.709	0.720
H^+	0.655	0.681	0.654	0.672	0.633	0.660	6.407	6.348	0.504	0.524
O1B	6.373	6.306	6.363	6.291	6.378	6.301	4.235	4.250	6.383	6.349
C2B	4.179	4.207	4.192	4.214	4.211	4.224	4.041	4.041	4.251	4.269
C3B	4.043	4.043	4.043	4.043	4.043	4.043	4.244	4.257	4.042	4.042
C4B	4.188	4.216	4.201	4.222	4.220	4.232	0.753	0.753	4.260	4.276
H2Ba	0.710	0.711	0.720	0.720	0.734	0.734	0.754	0.754	0.772	0.773
H2Bb	0.711	0.711	0.721	0.721	0.735	0.735	0.754	0.754	0.775	0.775
H4Ba	0.712	0.712	0.721	0.721	0.735	0.735	0.754	0.754	0.773	0.773
H4Bb	0.714	0.714	0.724	0.724	0.738	0.738	0.757	0.757	0.778	0.778

TABLE II-51

AMMO + $OXETH^+$

Gross Atomic Populations
Ab-Initio MODPOT/VRDDO

δ = 19°(fully open)

R(bohrs)	2.3		2.9		3.6		4.6		10.0	
	SCF	CI	SCF	CI	SCF	CI	SCF	CI	SCF	CI
O1A	6.474	6.438	6.478	6.441	6.481	6.444	6.483	6.447	6.483	6.446
C2A	4.275	4.285	4.274	4.284	4.272	4.281	4.266	4.273	4.259	4.264
C3A	4.434	4.437	4.445	4.451	4.457	4.469	4.464	4.477	4.467	4.477
C4A	4.177	4.173	4.175	4.180	4.145	4.159	4.083	4.087	4.036	4.006
H2Aa	0.765	0.765	0.758	0.759	0.750	0.751	0.739	0.739	0.726	0.726
H2Ab	0.765	0.765	0.759	0.759	0.751	0.751	0.739	0.740	0.726	0.726
H4Aa	0.727	0.733	0.721	0.729	0.700	0.715	0.668	0.693	0.637	0.649
H4Ab	0.728	0.734	0.721	0.730	0.7014	0.715	0.669	0.684	0.637	0.649
H^+	0.658	0.684	0.650	0.677	0.642	0.669	0.630	0.658	0.617	0.645
O1B	6.381	6.314	6.360	6.287	6.368	6.287	6.398	6.332	6.385	6.349
C2B	4.171	4.199	4.185	4.207	4.204	4.217	4.230	4.240	4.250	4.269
C3B	4.044	4.044	4.044	4.044	4.044	4.044	4.042	4.042	4.042	4.041
C4B	4.179	4.208	4.193	4.215	4.213	4.2258	4.239	4.249	4.260	4.277
H2Ba	0.708	0.709	0.717	0.717	0.730	0.730	0.749	0.749	0.772	0.772
H2Bb	0.709	0.709	0.718	0.718	0.731	0.731	0.750	0.750	0.775	0.775
H4Ba	0.710	0.710	0.718	0.718	0.731	0.731	0.750	0.750	0.733	0.733
H4Bb	0.712	0.712	0.720	0.721	0.734	0.734	0.753	0.753	0.778	0.778

TABLE II-52

OXET + $AMMOH^+$

Total Overlap Populations
Ab-Initio MODPOT/VRDDO

O1B-C4A

δ	0°		5°		10°		15°		19°	
R(bohrs)	SCF	CI	SCF	CI	SCF	CI	SCF	CI	SCF	CI
2.3	-0.199	-0.209	0.098	0.073	0.243	0.209	0.323	0.285	0.376	0.334
2.9	0.174	0.150	0.074	0.068	0.253	0.238	0.323	0.331	0.412	0.387
3.6	-0.127	-0.119	0.047	0.053	0.075	0.189	0.269	0.275	0.319	0.320
4.6	-0.021	-0.020	0.023	0.023	0.066	0.070	0.104	0.113	0.129	0.141
10.0	0.000	0.000	0.000	0.000	0.000	0.000	0.000	0.000	0.000	0.000

C4A-O1A

2.3	-0.025	-0.036	-0.037	-0.033	-0.037	-0.035	-0.029	-0.028	-0.021	-0.021
2.9	-0.236	-0.224	0.085	0.086	0.016	0.019	-0.011	-0.010	-0.015	-0.015
3.6	0.325	0.299	0.202	0.202	0.182	0.182	0.009	0.011	-0.009	-0.009
4.6	0.396	0.370	0.275	0.279	0.128	0.144	0.031	0.039	-0.002	0.000
10.0	0.427	0.397	0.312	0.312	0.162	0.184	0.050	0.065	0.005	0.012

TABLE II-53

OXET + $AMMOH^+$

Gross Atomic Populations
Ab-Initio MODPOT/VRDDO

δ = 0° (fully closed)

R(bohrs)	2.3		2.9		3.6		4.6		10.0	
	SCF	CI	SCF	CI	SCF	CI	SCF	CI	SCF	CI
O1A	6.452	6.391	6.466	6.398	6.463	6.389	6.456	6.379	6.448	6.371
C2A	4.218	4.242	4.205	4.230	4.191	4.216	4.182	4.207	4.176	4.201
C3A	4.060	4.053	4.040	4.038	4.037	4.038	4.038	4.041	4.043	4.047
C4A	4.067	4.081	4.111	4.131	4.136	4.149	4.161	4.168	4.183	4.188
H2Aa	0.740	0.740	0.729	0.729	0.718	0.718	0.711	0.711	0.705	0.705
H2Ab	0.744	0.744	0.733	0.733	0.722	0.722	0.715	0.715	0.709	0.709
H4Aa	0.745	0.751	0.731	0.743	0.713	0.725	0.701	0.713	0.703	0.715
H4Ab	0.749	0.758	0.736	0.747	0.718	0.730	0.707	0.718	0.709	0.720
H^+	0.587	0.608	0.557	0.578	0.531	0.551	0.515	0.534	0.504	0.524
O1B	6.359	6.302	6.376	6.319	6.401	6.352	6.412	6.373	6.382	6.348
C2B	4.257	4.280	4.259	4.279	4.268	4.287	4.273	4.292	4.272	4.289
C3B	4.453	4.453	4.446	4.446	4.446	4.446	4.447	4.446	4.450	4.449
C4B	4.258	4.281	4.260	4.279	4.268	4.268	4.273	4.292	4.271	4.288
H2Ba	0.723	0.723	0.737	0.737	0.750	0.750	0.760	0.760	0.771	0.771
H2Bb	0.730	0.730	0.745	0.745	0.758	0.758	0.766	0.766	0.773	0.773
H4Ba	0.726	0.726	0.740	0.740	0.753	0.753	0.763	0.763	0.774	0.774
H4Bb	0.741	0.741	0.754	0.754	0.766	0.766	0.773	0.773	0.776	0.776

TABLE II-54

OXET + $AMMOH^+$

Gross Atomic Populations
Ab-Initio MODPOT/VRDDO

$\delta = 5°$

R(bohrs)	2.3		2.9		3.6		4.6		10.0	
	SCF	CI	SCF	CI	SCF	CI	SCF	CI	SCF	CI
O1A	6.484	6.431	6.492	6.432	6.488	6.417	6.478	6.395	6.468	6.379
C2A	4.230	4.251	4.221	4.242	4.209	4.227	4.198	4.214	4.192	4.206
C3A	4.048	4.046	4.043	4.045	4.046	4.053	4.049	4.059	4.053	4.065
C4A	4.077	4.083	4.093	4.112	4.097	4.120	4.104	4.121	4.126	4.144
H2Aa	0.754	0.754	0.744	0.744	0.733	0.733	0.724	0.724	0.718	0.718
H2Ab	0.758	0.758	0.748	0.748	0.737	0.737	0.728	0.728	0.722	0.722
H4Aa	0.757	0.765	0.739	0.751	0.713	0.726	0.693	0.708	0.689	0.705
H4Ab	0.751	0.760	0.733	0.745	0.706	0.719	0.686	0.702	0.682	0.698
H^+	0.627	0.649	0.602	0.624	0.574	0.592	0.553	0.566	0.539	0.551
O1B	6.357	6.294	6.371	6.305	6.397	6.340	6.415	6.371	6.383	6.348
C2B	4.224	4.249	4.236	4.255	4.255	4.272	4.269	4.289	4.273	4.289
C3B	4.451	4.451	4.447	4.447	4.446	4.446	4.447	4.446	4.450	4.449
C4B	4.224	4.250	4.236	4.256	4.255	4.272	4.269	4.289	4.271	4.288
H2Ba	0.712	0.712	0.725	0.725	0.742	0.742	0.757	0.767	0.771	0.771
H2Bb	0.718	0.719	0.732	0.733	0.749	0.749	0.763	0.763	0.773	0.773
H4Ba	0.715	0.715	0.728	0.728	0.745	0.745	0.760	0.760	0.774	0.774
H4Bb	0.729	0.729	0.741	0.741	0.757	0.757	0.769	0.769	0.776	0.776

TABLE II-55

OXET + $AMMOH^+$

Gross Atomic Populations
Ab-Initio MODPOT/VRDDO

$\delta = 10°$

R(bohrs)	2.3		2.9		3.6		4.6		10.0	
	SCF	CI	SCF	CI	SCF	CI	SCF	CI	SCF	CI
O1A	6.499	6.454	6.507	6.459	6.510	6.455	6.506	6.436	6.499	6.418
C2A	4.239	4.256	4.235	4.252	4.227	4.240	4.217	4.229	4.210	4.218
C3A	4.043	4.043	4.046	4.051	4.054	4.062	4.059	4.070	4.062	4.076
C4A	4.106	4.104	4.104	4.113	4.083	4.107	4.057	4.070	4.064	4.083
H2Aa	0.761	0.761	0.753	0.754	0.744	0.744	0.735	0.736	0.728	0.728
H2Ab	0.765	0.765	0.757	0.757	0.748	0.748	0.739	0.739	0.732	0.732
H4Aa	0.746	0.753	0.731	0.742	0.703	0.716	0.677	0.691	0.664	0.678
H4Ab	0.740	0.747	0.724	0.735	0.697	0.709	0.670	0.685	0.657	0.672
H^+	0.652	0.676	0.636	0.660	0.617	0.638	0.597	0.614	0.582	0.594
O1B	6.364	6.299	6.366	6.296	6.389	6.319	6.415	6.365	6.384	6.351
C2B	4.203	4.230	4.218	4.239	4.241	4.257	4.263	4.281	4.273	4.289
C3B	4.450	4.450	4.448	4.448	4.447	4.447	4.447	4.447	4.450	4.449
C4B	4.203	4.230	4.219	4.239	4.241	4.257	4.263	4.281	4.271	4.287
H2Ba	0.706	0.706	0.716	0.717	0.733	0.733	0.752	0.752	0.771	0.771
H2Bb	0.711	0.711	0.723	0.723	0.739	0.739	0.758	0.758	0.773	0.773
H4Ba	0.708	0.708	0.719	0.719	0.736	0.736	0.755	0.755	0.774	0.774
H4Bb	0.721	0.721	0.731	0.731	0.747	0.638	0.763	0.764	0.776	0.776

TABLE II-56

OXET + $AMMOH^+$

Gross Atomic Populations
Ab-Initio MODPOT/VRDDO

δ = 15°

R(bohrs)	2.3		2.9		3.6		4.6		10.0	
	SCF	CI	SCF	CI	SCF	CI	SCF	CI	SCF	CI
O1A	6.498	6.458	6.505	6.463	6.510	6.466	6.513	6.463	6.512	6.457
C2A	4.245	4.260	4.244	4.258	4.240	4.255	4.234	4.247	4.229	4.237
C3A	4.042	4.044	4.049	4.055	4.059	4.070	4.066	4.078	4.069	4.081
C4A	4.137	4.133	4.129	4.133	4.096	4.110	4.043	4.045	4.023	4.010
H2Aa	0.763	0.763	0.757	0.757	0.750	0.750	0.741	0.741	0.733	0.733
H2Ab	0.767	0.766	0.761	0.761	0.753	0.753	0.745	0.745	0.737	0.737
H4Aa	0.737	0.743	0.726	0.736	0.701	0.716	0.670	0.684	0.647	0.660
H4Ab	0.730	0.738	0.719	0.729	0.695	0.709	0.664	0.678	0.642	0.655
H^+	0.664	0.688	0.654	0.679	0.643	0.668	0.629	0.653	0.616	0.636
O1B	6.373	6.307	6.363	6.291	6.379	6.304	6.409	6.350	6.384	6.349
C2B	4.190	4.218	4.208	4.229	4.231	4.244	4.257	4.272	4.273	4.290
C3B	4.450	4.450	4.449	4.448	4.448	4.448	4.447	4.447	4.450	4.449
C4B	4.191	4.218	4.208	4.229	4.231	4.244	4.256	4.272	4.271	4.289
H2Ba	0.702	0.702	0.711	0.711	0.726	0.726	0.746	0.747	0.771	0.771
H2Bb	0.707	0.707	0.717	0.717	0.732	0.732	0.752	0.752	0.772	0.772
H4Ba	0.704	0.704	0.714	0.714	0.729	0.729	0.750	0.750	0.774	0.774
H4Bb	0.716	0.716	0.725	0.725	0.738	0.738	0.757	0.757	0.776	0.776

TABLE II-57

OXET + AMMOH$^+$

Gross Atomic Populations
Ab-Initio MODPOT/VRDDO

δ = 19° (fully open)

	2.3		2.9		3.6		4.6		10.0	
	SCF	CI	SCF	CI	SCF	CI	SCF	CI	SCF	CI
O1A	6.391	6.453	6.495	6.456	6.499	6.460	6.503	6.462	6.505	6.462
C2A	4.249	4.263	4.250	4.262	4.248	4.260	4.245	4.256	4.241	4.251
C3A	4.041	4.044	4.050	4.056	4.060	4.073	4.067	4.079	4.069	4.080
C4A	4.167	4.162	4.160	4.065	4.126	4.138	4.061	4.063	4.017	3.989
H2Aa	0.763	0.763	0.758	0.758	0.751	0.751	0.742	0.743	0.733	0.733
H2Ab	0.767	0.767	0.761	0.761	0.755	0.755	0.746	0.746	0.736	0.736
H4Aa	0.728	0.734	0.423	0.4731	0.403	0.717	0.671	0.686	0.641	0.654
H4Ab	0.722	0.728	0.716	0.725	0.697	0.711	0.666	0.681	0.637	0.650
H$^+$	0.669	0.693	0.662	0.687	0.654	0.680	0.644	0.670	0.632	0.658
O1B	6.381	6.314	6.361	6.288	6.369	6.290	6.401	6.336	6.385	6.350
C2B	4.183	4.211	4.201	4.224	4.224	4.237	4.252	4.263	4.273	4.290
C3B	4.450	4.450	4.449	4.449	4.449	4.449	4.448	4.448	4.450	4.449
C4B	4.183	4.212	4.201	4.224	4.224	4.236	4.251	4.263	4.271	4.289
H2Ba	0.700	0.700	0.708	0.708	0.721	0.721	0.742	0.742	0.771	0.771
H2Bb	0.704	0.704	0.713	0.713	0.726	0.726	0.747	0.747	0.772	0.772
H4Ba	0.702	0.702	0.711	0.711	0.724	0.724	0.745	0.745	0.774	0.774
H4Bb	0.713	0.713	0.721	0.721	0.733	0.733	0.752	0.752	0.775	0.775

TABLE II-58

AMMO + $AMMOH^+$

Total Overlap Populations
Ab-Initio MODPOT/VRDDO

O1B-C4A

δ	0°		5°		10°		15°		19°	
R(bohrs)	SCF	CI	SCF	CI	SCF	CI	SCF	CI	SCF	CI
2.3	-0.198	-0.210	0.099	0.074	0.245	0.208	0.326	0.287	0.379	0.337
2.9	-0.235	-0.233	0.245	0.208	0.256	0.241	0.356	0.334	0.415	0.389
3.6	-0.127	-0.118	0.048	0.054	0.184	0.191	0.271	0.277	0.321	0.322
4.6	-0.021	-0.020	0.023	0.023	0.067	0.070	0.104	0.113	0.130	0.142
10.0	0.000	0.000	0.000	0.000	0.000	0.000	0.000	0.000	0.000	0.000

C4A-O1A

2.3	-0.027	-0.038	-0.038	-0.035	-0.038	-0.041	-0.029	-0.029	-0.022	-0.021
2.9	0.173	0.149	-0.038	-0.041	0.015	0.018	-0.011	-0.011	-0.015	-0.015
3.6	0.325	0.299	0.201	0.202	0.075	0.081	0.009	0.010	-0.009	-0.009
4.6	0.396	0.370	0.276	0.279	0.128	0.114	0.031	0.039	-0.002	0.000
10.0	0.427	0.398	0.312	0.312	0.162	0.183	0.050	0.065	0.005	0.012

TABLE II-59

AMMO + $AMMOH^+$

Gross Atomic Populations
Ab-Initio MODPOT/VRDDO

$\delta = 0°$ (fully closed)

R(bohrs)	2.3		2.9		3.6		4.6		10.0	
	SCF	CI	SCF	CI	SCF	CI	SCF	CI	SCF	CI
O1A	6.453	6.391	6.466	6.398	6.463	6.389	6.456	6.379	6.448	6.370
C2A	4.218	4.242	4.205	4.230	4.190	4.216	4.182	4.207	4.176	4.201
C3A	4.060	4.053	4.040	4.038	4.037	4.038	4.038	4.041	4.043	4.047
C4A	4.069	4.083	4.112	4.132	4.136	4.149	4.161	4.168	4.183	4.188
H2Aa	0.741	0.741	0.729	0.729	0.718	0.718	0.711	0.711	0.705	0.705
H2Ab	0.744	0.745	0.733	0.733	0.722	0.722	0.715	0.715	0.709	0.709
H4Aa	0.746	0.756	0.732	0.743	0.713	0.726	0.702	0.713	0.704	0.715
H4Ab	0.749	0.758	0.736	0.747	0.718	0.730	0.707	0.718	0.709	0.720
H^+	0.588	0.609	0.558	0.579	0.531	0.551	0.515	0.534	0.504	0.524
O1B	6.363	6.305	6.380	6.322	6.403	6.355	6.414	6.375	6.383	6.349
C2B	4.239	4.263	4.241	4.260	4.249	4.269	4.253	4.273	4.251	4.269
C3B	4.047	4.047	4.040	4.040	4.039	4.039	4.040	4.039	4.042	4.042
C4B	4.244	4.268	4.247	4.266	4.256	4.275	4.261	4.279	4.260	4.276
H2Ba	0.741	0.741	0.754	0.754	0.765	0.765	0.771	0.771	0.772	0.773
H2Bb	0.730	0.730	0.744	0.744	0.765	0.756	0.765	0.765	0.775	0.775
H4Ba	0.734	0.734	0.748	0.748	0.761	0.761	0.768	0.768	0.773	0.773
H4Bb	0.734	0.734	0.747	0.747	0.759	0.759	0.768	0.768	0.778	0.778

TABLE II-60

AMMO + $AMMOH^+$

Gross Atomic Populations
Ab-Initio MODPOT/VRDDO

δ = 5°

R(bohrs)	2.3		2.9		3.6		4.6		10.0	
	SCF	CI	SCF	CI	SCF	CI	SCF	CI	SCF	CI
O1A	6.484	6.431	6.499	6.459	6.488	6.417	6.478	6.395	6.468	6.379
C2A	4.230	4.251	4.239	4.255	4.209	4.227	4.198	4.213	4.192	4.206
C3A	4.048	4.046	4.043	4.043	4.046	4.053	4.049	4.059	4.053	4.065
C4A	4.079	4.084	4.106	4.100	4.097	4.121	4.104	4.122	4.126	4.144
H2Aa	0.754	0.754	0.761	0.761	0.733	0.733	0.724	0.724	0.718	0.718
H2Ab	0.758	0.758	0.765	0.761	0.737	0.737	0.728	0.728	0.721	0.722
H4Aa	0.757	0.766	0.747	0.754	0.713	0.726	0.693	0.708	0.689	0.705
H4Ab	0.752	0.761	0.741	0.749	0.707	0.720	0.687	0.703	0.682	0.699
H^+	0.628	0.650	0.652	0.675	0.574	0.592	0.552	0.566	0.539	0.551
O1B	6.361	6.298	6.368	6.304	6.401	6.343	6.417	6.374	6.384	6.349
C2B	4.206	4.232	4.185	4.213	4.235	4.254	4.249	4.270	4.260	4.269
C3B	4.046	4.045	4.045	4.045	4.040	4.040	4.040	4.040	4.042	4.041
C4B	4.212	4.238	4.191	4.219	4.243	4.260	4.259	4.276	4.260	4.276
H2Ba	0.730	0.730	0.722	0.723	0.756	0.756	0.767	0.767	0.772	0.772
H2Bb	0.720	0.720	0.714	0.714	0.748	0.748	0.762	0.762	0.775	0.775
H4Ba	0.723	0.723	0.717	0.717	0.752	0.753	0.765	0.765	0.773	0.773
H4Bb	0.723	0.724	0.717	0.717	0.751	0.751	0.765	0.765	0.778	0.778

TABLE II-61

AMMO + $AMMOH^+$

Gross Atomic Populations
Ab-Initio MODPOT/VRDDO

$\delta = 10°$

R(bohrs)	2.3		2.9		3.6		4.6		10.0	
	SCF	CI	SCF	CI	SCF	CI	SCF	CI	SCF	CI
O1A	6.499	6.459	6.507	6.459	6.510	6.453	6.506	6.437	6.498	6.417
C2A	4.239	4.255	4.235	4.252	4.227	4.244	4.217	4.229	4.210	4.217
C3A	4.043	4.043	4.046	4.051	4.054	4.063	4.059	4.070	4.062	4.077
C4A	4.106	4.100	4.105	4.114	4.084	4.102	4.058	4.070	4.065	4.078
H2Aa	0.761	0.761	0.734	0.754	0.745	0.745	0.735	0.736	0.728	0.728
H2Ab	0.765	0.765	0.757	0.758	0.748	0.748	0.739	0.739	0.732	0.732
H4Aa	0.747	0.754	0.731	0.742	0.704	0.718	0.677	0.691	0.664	0.680
H4Ab	0.741	0.749	0.725	0.737	0.697	0.712	0.671	0.685	0.658	0.674
H^+	0.652	0.675	0.637	0.661	0.617	0.639	0.597	0.614	0.582	0.594
O1B	6.368	6.304	6.371	6.299	6.393	6.324	6.418	6.368	6.385	6.350
C2B	4.185	4.213	4.200	4.221	4.222	4.237	4.244	4.262	4.251	4.269
C3B	4.045	4.045	4.043	4.043	4.042	4.042	4.041	4.040	4.042	4.041
C4B	4.191	4.219	4.206	4.227	4.229	4.244	4.251	4.269	4.260	4.277
H2Ba	0.722	0.723	0.732	0.733	0.747	0.747	0.762	0.762	0.772	0.772
H2Bb	0.714	0.714	0.725	0.725	0.740	0.740	0.758	0.758	0.775	0.775
H4Ba	0.717	0.717	0.728	0.728	0.743	0.743	0.760	0.760	0.773	0.773
H4Bb	0.717	0.717	0.728	0.728	0.743	0.743	0.760	0.760	0.778	0.778

TABLE II-62

AMMO + $AMMOH^+$

Gross Atomic Populations
Ab-Initio MODPOT/VRDDO

$\delta = 15°$

R(bohrs)	2.3		2.9		3.6		4.6		10.0	
	SCF	CI	SCF	CI	SCF	CI	SCF	CI	SCF	CI
O1A	6.498	6.458	6.505	6.464	6.510	6.466	6.513	6.464	6.512	6.457
C2A	4.245	4.260	4.244	4.258	4.240	4.255	4.234	4.247	4.228	4.237
C3A	4.042	4.044	4.049	4.056	4.049	4.070	4.066	4.078	4.069	4.081
C4A	4.137	4.133	4.130	4.134	4.097	4.111	4.044	4.046	4.023	4.010
H2Aa	0.763	0.763	0.757	0.757	0.750	0.750	0.741	0.741	0.733	0.733
H2Ab	0.767	0.767	0.761	0.761	0.753	0.753	0.745	0.745	0.736	0.737
H4Aa	0.738	0.744	0.727	0.737	0.701	0.716	0.670	0.684	0.647	0.660
H4Ab	0.732	0.739	0.721	0.731	0.696	0.710	0.665	0.679	0.642	0.655
H^+	0.664	0.689	0.655	0.680	0.643	0.669	0.629	0.653	0.616	0.636
O1B	6.377	6.310	6.367	6.294	6.382	6.306	6.412	6.354	6.386	6.351
C2B	4.173	4.201	4.189	4.211	4.212	4.225	4.237	4.253	4.251	4.269
C3B	4.045	4.045	4.044	4.044	4.043	4.043	4.041	4.041	4.042	4.041
C4B	4.178	4.206	4.196	4.217	4.219	4.231	4.245	4.259	4.260	4.277
H2Ba	0.718	0.718	0.726	0.726	0.739	0.739	0.756	0.756	0.772	0.772
H2Bb	0.711	0.711	0.720	0.720	0.733	0.733	0.753	0.753	0.775	0.775
H4Ba	0.713	0.713	0.722	0.722	0.736	0.736	0.754	0.755	0.773	0.773
H4Bb	0.714	0.714	0.723	0.723	0.736	0.736	0.756	0.756	0.778	0.778

TABLE II-63

AMMO + $AMMOH^+$

Gross Atomic Populations
Ab-Initio MODPOT/VRDDO

δ = 19°(fully open)

R(bohrs)	2.3		2.9		3.6		4.6		10.0	
	SCF	CI	SCF	CI	SCF	CI	SCF	CI	SCF	CI
O1A	6.491	6.453	6.495	6.457	6.499	6.460	6.503	6.463	6.505	6.462
C2A	4.249	4.263	4.249	4.262	4.248	4.260	4.245	4.256	4.241	4.251
C3A	4.041	4.044	4.050	5.056	4.060	4.073	4.067	4.080	4.069	4.080
C4A	4.166	4.161	4.160	4.165	4.127	4.140	4.062	4.064	4.018	3.989
H2Aa	0.763	0.764	0.758	0.758	0.751	0.731	0.743	0.743	0.733	0.733
H2Ab	0.767	0.767	0.761	0.762	0.755	0.755	0.746	0.746	0.736	0.736
H4Aa	0.730	0.736	0.724	0.732	0.704	0.718	0.672	0.686	0.641	0.653
H4Ab	0.724	0.731	0.718	0.727	0.698	0.713	0.667	0.682	0.638	0.650
H^+	0.669	0.694	0.662	0.688	0.654	0.680	0.644	0.670	0.632	0.658
O1B	6.385	6.318	6.365	6.291	6.373	6.292	6.404	6.338	6.386	6.351
C2B	4.165	4.193	4.183	4.206	4.205	4.218	4.232	4.244	4.251	4.269
C3B	4.046	4.045	4.045	4.045	4.044	4.044	4.042	4.042	4.042	4.041
C4B	4.171	4.199	4.189	4.212	4.212	4.224	4.240	4.250	4.260	4.277
H2Ba	0.715	0.715	0.722	0.722	0.733	0.734	0.751	0.752	0.772	0.772
H2Bb	0.709	0.709	0.716	0.716	0.729	0.729	0.749	0.749	0.775	0.775
H4Ba	0.710	0.710	0.718	0.718	0.731	0.731	0.750	0.750	0.773	0.773
H4Bb	0.712	0.712	0.719	0.719	0.732	0.732	0.752	0.752	0.778	0.778

B. Ab-Initio MRD-CI Calculations of the Protonation of Oxetane

Protonation of oxetane (or substituted oxetane) is the initiation step in cationic polymerization.

We had long since pointed out the initiation protonation step in cationic polymerization is an ion-molecule reaction

$$A^+ + B \dashrightarrow AB^+ \qquad \text{(Type II)}$$

where the ionization potential of A (the hydrogen atom 13.6 eV) is higher than that of B (oxetane or any substituted oxetane) For ion-molecule reactions of Type I

$$A^+ + B \dashrightarrow AB^+ \qquad \text{(Type I)}$$

where the ionization potential of A is lower than that of B the reaction has the possibility to proceed along a single lowest potential energy surface which separates properly theoretically at the asymptotes of A^+ and B (since both A^+ and B are closd shell ground state systems). However, for ion-molecule reactions where the ionization potential of the molecule is less than 13.6 eV which is the case for all oxetanes and apparently all organic molecules) there has to be at least one potential energy surface arising from the asymptotes $A + B^+$ which is lower in energy at the asympotote and along at least part of the interaction potential energy surfaces.

A single determinant SCF calculation will definitely not separate properly at the asymptotes and is not sufficient to describe a protonation reaction of oxetanes or other organic molecules. Ab-initio MRD-CI calculations for the entire potential energy surface for ground and at least several excited states are necessary to describe protonation reactions. We had long stated this based on the fundamental physics involved. This past year we verified this convincingly, by accurate full valence electron ab-initio MRD-CI calculations for the ground and electronically excitd states for the proton attack on oxetane. We carried out the calculations for the linear attack of the proton to form an $O\text{-}H^+$ bond both for the in-plane attack and the out-of-plane attack.

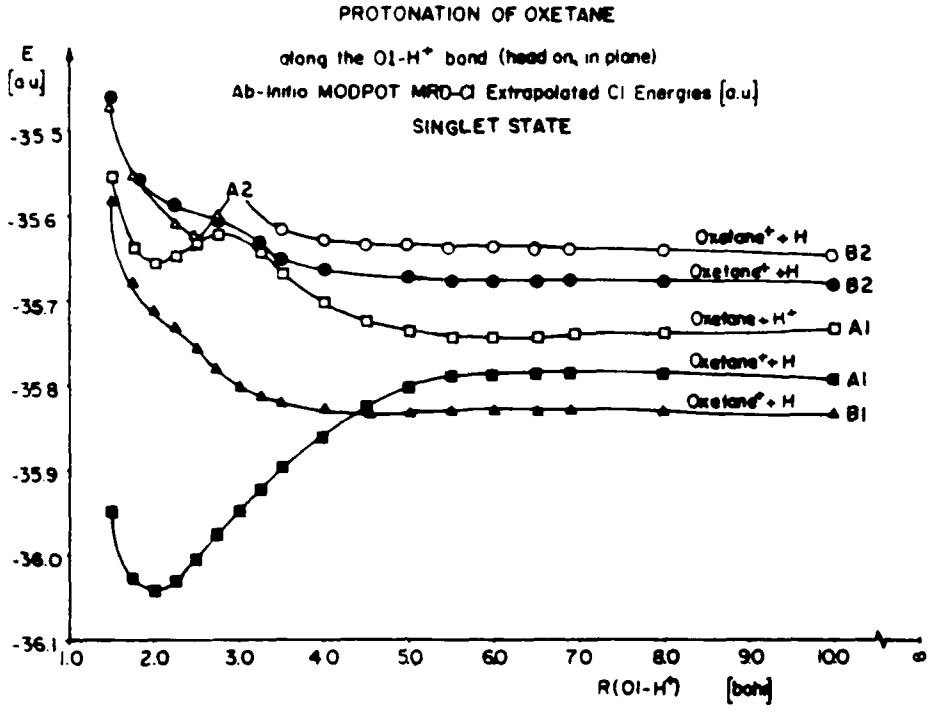

Our MRD-CI results confirmed our earlier geometry optimization results that the O-H^+ bond is in the plane of the oxetane ring even though the lone pairs on the original oxetane are out of plane. The results indicated an even greater complexity for the potential energy surfaces then we had originally hypothesized. The lowest energy root from 1.5 bohrs to 4.5 bohrs (including the equilibrium internuclear O-H^+ distance of protonated oxetane at 2.0 bohrs) is $^1A_1$. At 4.5 bohrs the lowest root becomes $^1B_1$ to an asymptote of oxetane$^+$(ground state, $^2B_1$) + H. At 4.5 bohrs the $^1A_1$ curve continues as the second root of the CI matrix smoothly to oxetane$^+$(first excited singlet state $^2A_1$) + H. The third root of the CI matrix, also a $^1A_1$ state, has a minimum at 2.0 bohrs, a hump at 2.75 bohrs and then continues down to the separated products oxetane(ground state) + H^+. The behavior of the next two higher roots of the CI matrix is also complicated. This implies that while the $^1A_1$ potential energy surface arising from or dissociating to oxetane (or substituted oxetane) + H^+ will always be one of two higher lying potential energy surfaces involving protonated oxetane (or protonated substituted oxetane), the exact relative position of that potential energy surface will be critically dependent on the explicit values

of the ionization potentials for the substituted oxetane (ground or excited states) and will also depend on the type of molecular orbital from which ionization had occurred (i.e. lone pair, bonding or non-bonding orbital). Thus the behavior upon protonation can be somewhat different for each individual substituted oxetane.

These findings have a profound significance. Thus MRD-CI calculations for the ground and a number of excited states will be necessary to describe protonation or deprotonation processes.

This behavior will hold true for all protonation reaction of organic molecules since their ionization potentials are less than 13.6 eV.) as well as protonation reactions involving molecules with ionization potentials lower than the ionization potential of the hydrogen atom, 13.6 eV. This multipotential surface behavior also holds true for deprotonation of these protonated species.

Thus the potential energy surfaces for protonation reactions are much more complicated than customarily assumed and moreover are crucially dependent not only on the lowest ionzation potentials of the molecules involved but also on the energies of their higher ionization potentials relative to the ionization potential of the hydrogen atom.

III. Ab-Initio MRD-CI Calculations for Breaking a Chemical Bond in a Molecule in a Crystal or Other Solid Environment

Breaking a >C-NO_2 or >N-NO_2 bond is the initial step in fractoemission of explosives and also the initial step leading to detonation of explosives. To describe properly breaking of a chemical bond in a molecule it is necessary to to carry out ab-initio MRD-CI (multireference double excitation configuration interaction) calculations of the isolated molecule. To describe properly breaking of a chemical bond in a molecule in a crystal or other solid environment it is necessary to carry out ab-initio MRD-CI calculations on the molecule surrounded by other molecules as in the crystal or solid arrangement. Even this generation of supercomputers still does not have the space to carry out such calculations on large nitroexplosive molecules especially since many of them (such as RDX and HMX) have a large number of molecules in the unit cell.

We had earlier derived and implemented and used successfully a method for dissociation of large molecules based on localized/local orbitals. The localized molecular orbitals. The localized molecular orbitals in the region of the bond breaking are included explicitly in the MRD-CI. The remainder of the occupied and virtual orbitals are folded into an "effective" CI Hamiltonian.

A. Methodology

MRD-CI calculations are absolutely necessary to describe bondbreaking processes correctly in the ground state and especially in the excited states.

The electronic challenge arose to extend our MRD-CI (multireference double excitation - configuration interaction) technique based on localized/local orbitals to the breaking of a chemical bond in a molecule in crystal (or other solid environment). This past year we have derived, implemented, and used successfully a procedure for doing this. We made the first presentation of results using this method spring 1987 at the ONR Workshop on Dynamic Deformation, Fracture and Transient Combustion of Energetic Compounds.

Our technique involves solving a quantum chemical ab-initio SCF explicitly for a system of a molecule surrounded by a number of other molecules (the unit reference cell or larger assemblage) in the multipole environment of yet more further out surrounding molecules. Multipoles in the environmental region affect the one-electron term in the Hamiltonian. This Hamiltonian is solved for the SCF for all the molecules in the space treated explicitly quantum chemically. The resulting canonical molecular orbitals are localized. All of the occupied and virtual localized orbitals in the region of interest are included explicitly in the MRD-CI and the remaining occupied localized orbitals are folded into an "effective" CI Hamiltonian. The advantage is that the transformations from integrals over atomic orbitals to integrals over molecular orbitals (the computer time-, computer core- and external storage - consuming part of the CI calculations) only have to be carried out for the localized molecular orbitals included explicitly in the MRD-CI calculations.

Space is broken up into three regions:

(C[B[A]B']C)

A Localized space treated explicitly in ab-initio MRD-CI calculations. (This can be an entire molecule or the localized dissociation region of a large molecule.)

B + A + B' Space treated explicitly quantum chemically (ab-initio SCF) for supermolecule B A B'

C + C' Space represented by multipoles of additional molecules taken into account by inclusion of multipole interactions (up through quadrupoles) into one-electron part of SCF Hamiltonian.

This method is completely general. The space treated explicitly quantum chemically and the surrounding space can have defects, deformations, dislocations, impurities, dopants, edges and surfaces, boundaries, etc.

To be able to carry out such MRD-CI calculations for breaking a chemical bond in a molecule or a crystal (or other solid environment) represents a significant breakthrough.

The desirable optimal computational strategies we have developed over the years for ab-initio calculations on large molecules and molecular systems is what makes these computations tractable for us: MODPOT - ab-initio effective core model potentials which enable calculation of the valence electrons only explicitly, yet accurately; VRDDO - a charge-conserving integral prescreening evaluation, especially effective for spatially extended systems; MERGE - to save and reuse integrals from common fragments or molecules, which enables us to build up larger and larger clusters very efficiently and a special SCF technique which allows us to use the SCF wave functions from smaller clusters as a start to get rapid convergence for larger clusters.

Test results on 5 unit cells of H_2 (for dissociating the H_2 molecule in the center cell treated by this method) verified the validity of this new technique.

B. Calculations Carried Out for Nitromethanes:

We have been carrying out extensive test calculations by this new technique for the dissociation of the $H_3C - NO_2$ bond in nitromethane for various numbers of molecules treated explicitly on the SCF in the multipole field of varying numbers of additional CH_3NO_2 molecules as in the crystal arrangement followed by localization and ab-initio MRD-CI calculations on breaking the $CH_3 - NO_2$ bond in a specific nitromethane molecule. Since this

technique is new we are carrying out extensive testing to ascertain how many molecules must be treated in each region for reliable results.

One of the pertinent questions we posed initially for decomposition of molecules in crystals was did it take more or less energy to break the bond when the molecule was in a crystal compared to breaking the bond of an isolated molecule. The MRD-CI results for breaking the $H_3C - NO_2$ bond of nitromethane in the presence of multipoles of other nitromethane molecules compared to the MRD-CI results for breaking the $H_3C - NO_2$ bond in an isolated nitromethane molecule indicate that it takes more energy to break the $H_3C - NO_2$ bond when nitromethane is in the field of the additional nitromethane molecules.

We have also investigated such MRD-CI calculations treating different numbers of nitromethane molecules explicitly in the SCF calculation and varying the numbers of the external nitromethane molecules contributing to the multipole field.

Several different choices of the arrangement of nitromethane molecules was also considered picking different pieces from the experimental crystal structure of nitromethane.

The ab-initio MRD-CI calculations have been carried out for R_{C-N} distances for the H_3C-NO_2 molecule being dissociated of 2.4, 2.8, 3.0, 3.2, 3.6, 4.4 and 5.6 bohrs for each choice of nitromethane system description.

C. Detailed Results of Calculations Carried Out for Nitromethane: Various Choices of Size and Description of System.

All Figures and Tables appear at the end of this section starting on page 136

1. The Model Case

To test the proposed approach the model cluster has been selected from real nitromethane crystal. The model cluster includes:

a. reference molecule (A)

b. two closest neighbors (B) to reference molecule (these two molecules are the most important for decomposition of C - N bond in the reference molecule)

c. two far-lying molecules (C) having big influence on the B region (Fig III-1, "The Cluster of 5 Nitromethanes Chosen For Model Calculations)".

To test how good is the representation of a molecule by multipoles, calculations for two different geometries of the cluster have been performed. (See Figure III-1) First full SCF calculation for three nitromethane molecules with the reference nitromethane molecule at position A and two more nitromethane molecules at positions B compared to SCF calculation for the reference nitromethane molecule at position A and two nitromethane molecules represented by multipoles at position B. Second, full SCF calculation for three nitromethane molecules with the reference molecule at position A and two nitromethane molecules at position C compared to SCF calculation for the reference nitromethane molecule at position A and two nitromethane molecules represented by multipoles at position C. These results are presented in Table III-1, "Energies For Equilibrium Geometry (R_{CN} = 3.0 bohrs), Bond Dissociation Energy and Relative Error For Two Geometries For the Cluster of 3 Nitromethane Molecules". The results show that the multipole representation is extremely reliable compared to full ab-initio SCF results for the three nitromethane molecules. The relative error on the MRD-CI calculated C-N dissociation energy when the two nitromethane molecules in the C position are represented by their multipole effects is only 0.027%. The relative error when the two closer nitromethane molecules in the B positions are represented by their multipole effects is still only 1.14%.

Table III-2, "Total Energies, Reduced Energies, and Bond Dissociation Energies For Model Cluster of Nitromethane Molecules Within Different Approaches", has more extensive results for the E_{SCF}, $E_{CI,EX}$ and C-N bond dissociation energy for:

5 nitromethanes	full SCF
3 nitromethanes	full SCF in field of 2 multipoles
3 nitromethanes	full SCF
1 nitromethane	full SCF in field of 4 multipoles
1 nitromethane	full SCF in field of 2 multipoles in B positions
1 nitromethane	single free molecule full SCF

Table III-2a, "Total Energies and Bond Dissociation Energies (Corresponding to R_{CN} = 5.6 bohrs and $R_{CN} = \infty$) For Model Cluster of Nitromethane Molecules Within Different Approaches", presents results for R_{CN} = 5.6 bohrs and $R_{CN} = \infty$ for the same descriptions of the nitromethane cluster as in Table III-2.

The bond dissociation energy of a molecule in a crystal, (or other solid) in contrast to the bond dissociation energy in a free molecule, includes interactions with other molecules in the crystal or other solid. The energy of the cluster before the decomposition can be written

$$\varepsilon_1 = E_A + E_B + E_{AB} + E_{AC} + E_{CB} + E_{ABC},$$

(A,B,C correspond to spaces of cluster, Fig III-1. where here B space = B + B';
C = C + C') and after decomposition

$$\varepsilon_2 = \tilde{E}_A + E_B + E_{BC} + \ldots$$

where E_A, $\tilde{E}_A$ energy of molecule A before and after decomposition

E_B energy of molecules B

($E_B = E_B + E_{B'} + E_{BB'}$ in our case)

E_{ij} two body interactions

E_{ijk} th ee body interactions

The bond dissociation energy

$$\Delta E = \varepsilon_1 - \varepsilon_2 = \varepsilon_1 - E_A - E_B$$

Assuming the decomposition of the bond to infinity, E_A is a energy of completely decomposed free molecule and E_B is an energy of the cluster

without A molecule.

The value

$$E_R(r) = \varepsilon_1(r) - \bar{E}_B,$$

is called the reduced energy and represents the energy of reference molecule in the field of other spaces of the crystal. The $E_R(r)$ can be used to compare energy surfaces (reaction surfaces) in different assumed models. These calculations have also been carried out as a function of R_{C-N}. Table III-3, "The Decomposition Pathway for C-N Bond in Nitromethane Crystal (Model Cluster) For Different Approaches"

2. Real Cluster - Extended Cluster and Alternative Extended Cluster

The cluster of 13 molecules has been chosen to represent the real crystal. Within this cluster the distance between atoms C_1 and N_2 of reference molecule and C or N atom in neighbor molecules is smaller than 10 bohrs. Since only 5 nitromethanes can be treated quantum mechanically at present due to computer disc limitations (which limits the size of the transformation from atomic orbitals to molecular orbitals for the MRD-CI calculation), the selection of 4 molecules around the reference molecule was necessary. Two choices have been tried. First: four molecules closest to reference molecule (Fig. III-2, "The Cluster of 5 Nitromethanes From Extended Cluster") and second four molecules having atoms which are the closest to C-N bond (Fig. III-3, "The Cluster of 5 Nitromethanes From Extended Cluster (Alternative Choice"). Eight remaining molecules were represented by multipoles. Multipoles were generated in crystal orbital calculation), by the crystal orbital part (XTLORB) of our POLY-CRYST program (for ab-initio calculations on polymers and crystals) taking advantage of repeated symmetry units for one unit cell and then decomposed into point charges.

a. Extended Cluster

Figure III-2

Table III-4: "Total Energies, Reduced Energies, and Bond Dissociation Energies for Extended Cluster of Nitromethane Molecules Within Different Approaches (energy in a.u., equilibrium distance R = 3.0 bohrs)"

Table III-4a: "Total Energies, Reduced Energies, and Bond Dissociation Energies (corresponding to R_{CN} = 5.6 bohrs and $R_{CN} = \infty$) For Extended Cluster of Nitromethane Molecules Within Different Approaches"

b. Extended Cluster (Alternative Choice)

Figure III-3

Table III-5 "Total Energies, Reduced Energies, and Bond Dissociation Energies for Extended Cluster of Nitromethane Molecules (Alternative Choice) Within Different Approaches (energy in a.u., equilibrium distance R = 3.0 bohrs)

Table III-5a: "Total Energies, Reduced Energies, and Bond Dissociation Energies (corresponding to R_{CN} = 5.6 bohrs and $R_{CN} = \infty$) For Extended Cluster of Nitromethane Molecules (Alternative Choice) Within Different Approaches"

For both the extended cluster and the extended cluster (alternative choice) these calculations have also been carried out as a function of R_{C-N}.

Table III-6: "The Decomposition Pathway for C-N bond in Nitromethane Crystal (Extended Cluster) for Different Approaches."

Table III-7: "The Decomposition Pathway for C-N bond in Nitromethane Crystal (Extended Cluster, Alternative Choice) For Different Approaches"

3. Crystal Orbital Calculations For Model Nitromethane Cluster

To check the goodness of the model cluster approximation for crystalline nitromethane we carried out ab-initio crystal orbital calculations (XTLORB) using our POLY-CRYST program. The POLY-CRYST program calculates ab-initio crystal orbitals for the unit reference cell (or unit reference polymer segment) taking advantage of the translational symmetry in a crystal and the translational/rotational symmetry in a polymer. This POLY-CRYST program incorporates as options all the desirable computational strategies we had derived over the years for calculations on large molecules: Ab-initio MODPOT, VRDDO, and MERGE. (See description page 128 III. Section A. Methodology Ab-Initio MODPOT/VRDDO/MERGE.) These XTLORB calculations were carried out for three cells of 4 nitromethane molecules/unit cell (from the model cluster). These XTLORB calculations were carried out integrating over 3 $\vec{k}$ points and over 5 $\vec{k}$ points. Results (Table III-8, "Nitromethane - Crystal Orbital Calculations for Model Cluster") showed the XTLORB calculations for nitromethane integrating over only 3 $\vec{k}$ points were essentially already converged. This demonstrates that for molecular crystals integration over far fewer $\vec{k}$ points is necessary for convergence than for atomic, interatomic or ionic crystals. These XTLORB calculations were then carried out for 3 cells of three nitromethane molecules/unit cell (taking one central molecule away from the cluster). The difference in the XTLORB total energies between the 4 nitromethane molecules/unit cell and the 3 nitromethane molecules/unit cell (Table III-8.)

$$E_R = E_4 - E_3 = -48.06091 \text{ a.u.}$$

corresponds very closely to the reduced energy per nitromethane molecule,

$$E_R = -48.06057 \text{ a.u.}$$

calculated from explicit SCF calculations on the model nitromethane cluster in the multipole field of farther out nitromethane molecules for the model cluster.

Thus, the multipole approximation for describing the effect of further out molecules on the SCF cluster energies is quite good.

D. Conclusions

To be able to carry out such MRD-CI calculations for breaking a chemical bond in a molecule or a crystal (or other solid environment) represents a significant breakthrough.

Describing the processes and mechanisms of breaking chemical bonds in an energetic molecule when the molecule is in a crystal or other solid environment leads to an understanding of the initiation of energetic reactions and subsequent processes leading to detonation and also leads to an understanding of fractoemission processes.

The results confirm the preliminary results of our original MRD-CI test calculations for breaking the $H_3C - NO_2$ bond in a single nitromethane in the multipole field of 6 other nitromethane molecules, namely that it takes more energy to break the $H_3C - NO_2$ bond when the nitromethane molecule is in a crystal or solid environment in the presence of other nitromethane molecules. However, to reach the convergent value it is necessary to take into account a number of nitromethane molecules explicitly in the SCF and a number more nitromethane molecules in the surrounding multipole space. We are continuing our investigations in this area.

Our development has led to crucial understanding of the initial steps leading to detonation. We plan to explore the application of our techniques to the subsequent events taking place after the initial bond breaking.

We plan to carry out such calculations for breaking the $>C-NO_2$ and $>N-NO_2$ bond breaking in larger energetic molecules such as RDX and other energetic compounds. This method is very applicable for such calculations. Carrying out such calculations on larger molecules will be dependent on the computer core, disc storage and time available. However, computers are getting faster and their memories and peripheral storage are getting larger. The next generation of computers which is already past the drawing board stage are ideally suited for such calculations.

THE CLUSTER OF 5 NITROMETHANES CHOSEN FOR MODEL CALCULATIONS.

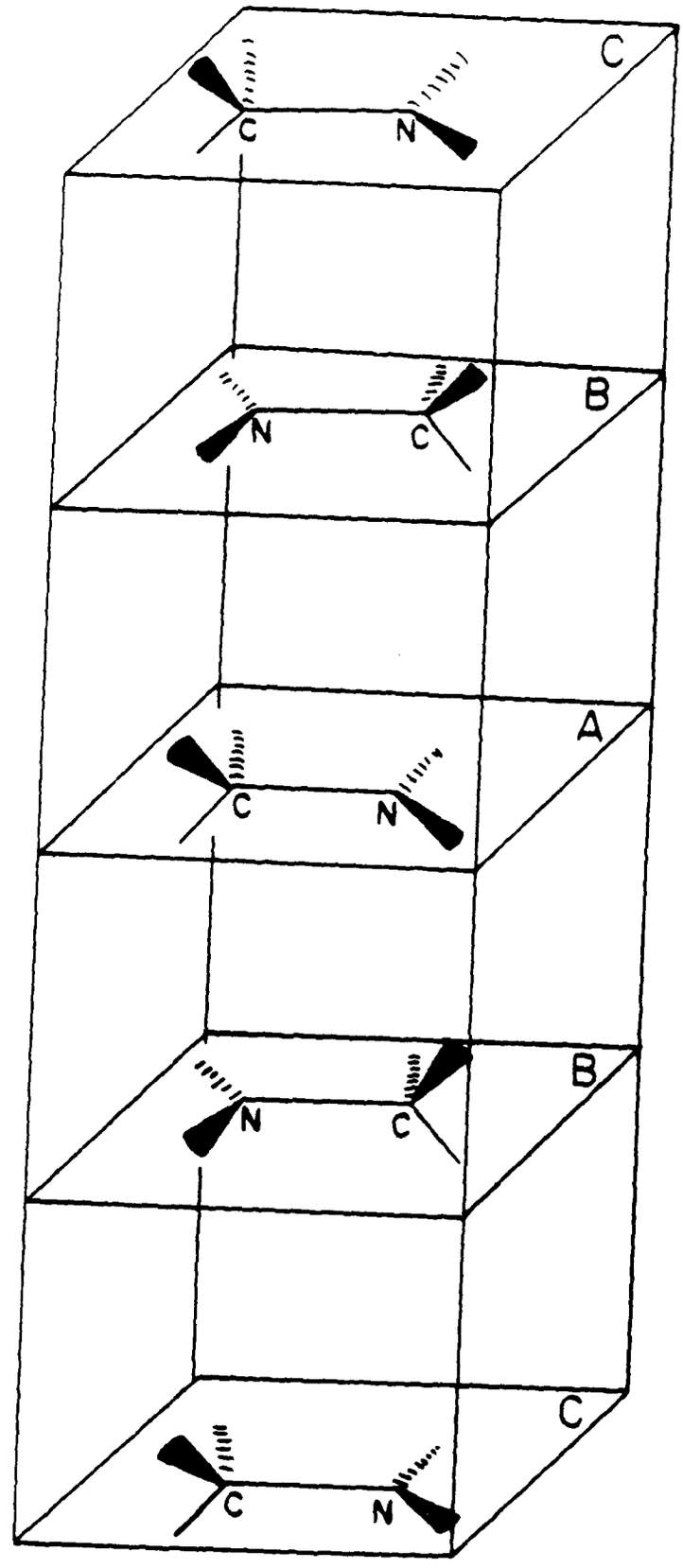

Figure III-1

THE CLUSTER OF 5 NITROMETHANES
FROM EXTENDED CLUSTER

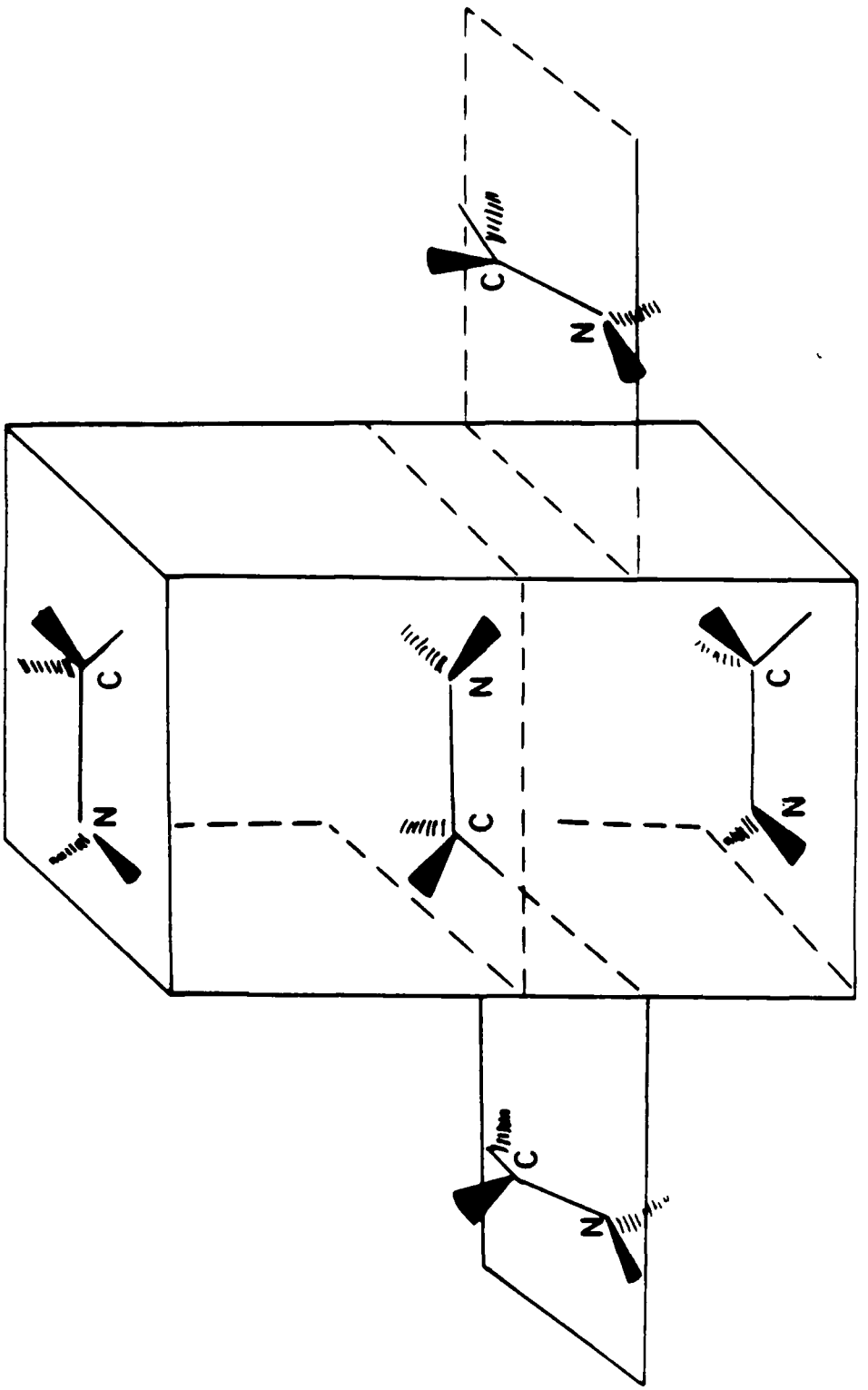

Figure III-2

THE CLUSTER OF 5 NITROMETHANES FROM EXTENDED CLUSTER (ALTERNATIVE CHOICE)

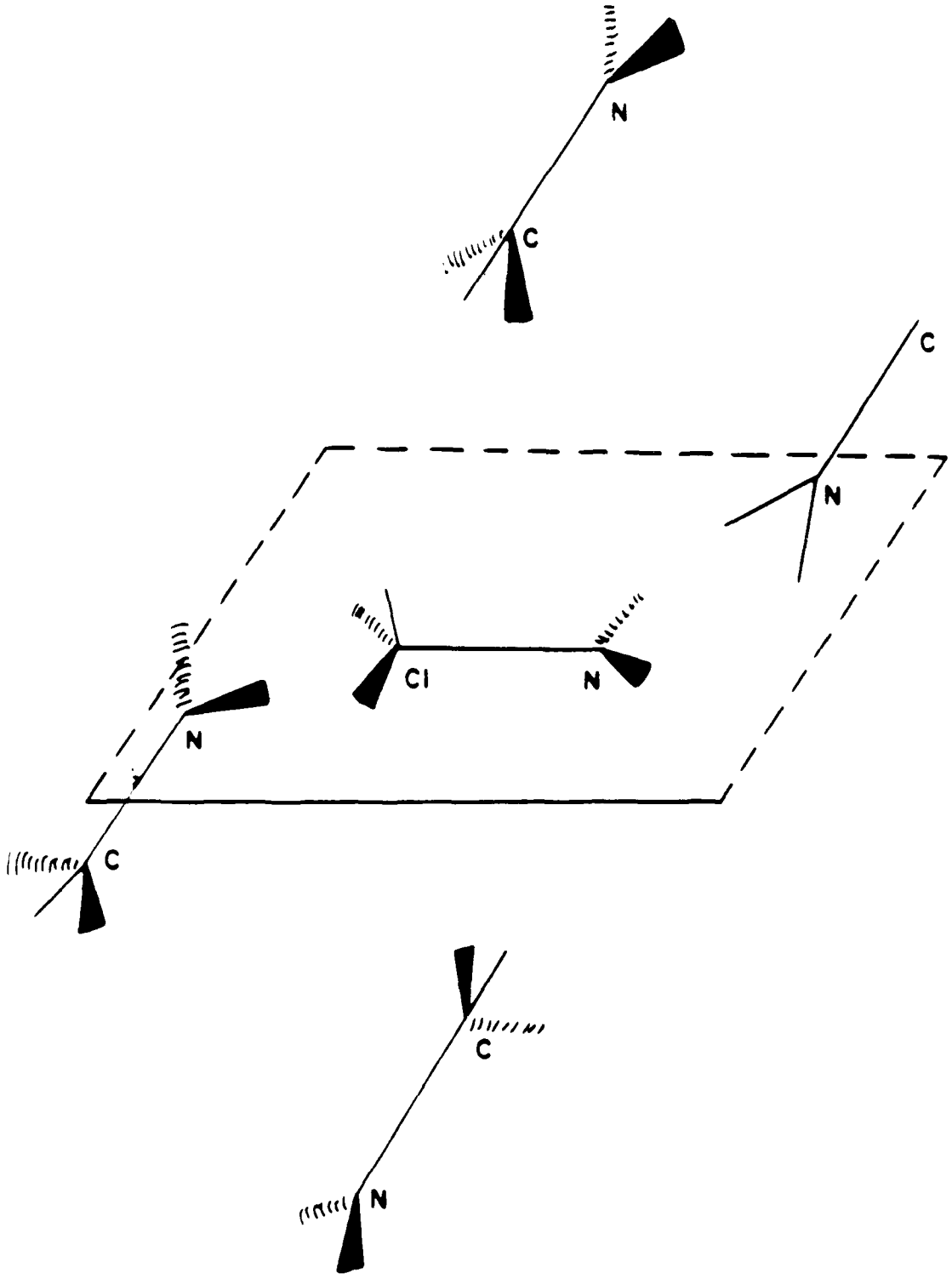

Figure III-3

TABLE III-1

Energies For Equilibrium Geometry (R_{CN} = 3.0 bohrs), Bond Dissociation Energy and Relative Error For Two Geometries For The Cluster of 3 Nitromethane Molecules (see Fig III-1) (energy in [a.u.])

CLUSTER	E_{SCF}	$E_{CI,EX}$	C-N bond dissociation energy, ΔE	relative error [%]
3 NITROMETHANES ε_1	-144.136254	-144.388879		
C - A - C' E_R [1)]	-48.051505	-48.304130	.0077714	
1 NITROMETHANE + 2 MULTIP in position C	-48.052639	-48.304109	.077683	0.027%
3 NITROMETHANES ε_1	-144.146063	-144.396239		
B - A - B' E_R [2)]	-48.061789	-48.311965	.085549	
1 NITROMETHANE + 2 MULTIP in position B	-48.062455	-48.312941	.086525	-1.14%

1) $E_R = \varepsilon_1 - E_{SCF}$ (C - C')
2) $E_R = \varepsilon_1 - E_{SCF}$ (B - B')

TABLE III-2

Total Energies, Reduced Energies, and Bond Dissociation Energies for Model Cluster of Nitromethane Molecules Within Different Approaches (energy in [a.u.])

Approach		E_{SCF}	$E_{CI,EX}$	C-N bond dissociation energy, ΔE
5 NITROMETHANES	ε_1	-240.238726	-240.489022	
	E_R [1]	-48.060579	-48.310875	-0.084458
3 NITROMETHANES + 2 MULTIP	ε_1	-144.154520	-144.404582	
	E_R [2]	-48.060636	-48.310698	-0.084282
3 NITROMETHANES	ε_1	-144.146063	-144.396239	
	E_R [3]	-48.0617891	-48.311965	-0.085549
NITROMETHANE + 4 MULTIP		-48.061205	-48.311927	-0.085511
NITROMETHANE + 2 MULTIP in position B		-48.062455	-48.312941	-0.086525
NITROMETHANE SINGLE FREE MOLECULE		-48.052639	-48.305044	-0.078628

1) $E_R = \varepsilon_1 - E_{SCF}$(4 NITROMETHANES, CBB'C')

2) $E_R = \varepsilon_1 - E_{SCF}$(2 NITROMETHANES, BB' + 2 MULTIP C,C')

3) $E_R = \varepsilon_1 - E_{SCF}$(2 NITROMETHANES, BB')

TABLE III-3

The Decomposition Pathway for C-N Bond in Nitromethane Crystal (Model Cluster) For Different Approaches (E_R Definition as in Table III-1) (Energies in (a.u.)

			R(bohrs)				
Approach			2.4	3.0	3.6	4.4	5.6
5 NITROMETHANES	SCF	ϵ_1	-240.136469	-240.238726	-240.213081	-240.148218	-240.093160
		E_R	-47.958322	-48.060579	-48.034934	-47.970071	-47.915013
	CI,EX	ϵ_1	-240.377082	-240.489022	-240.477147	-240.436309	-240.409352
		E_R	-48.198935	-48.310875	-48.29900	-48.258162	-48.231205
3 NITROMETHANES	SCF	ϵ_1	-144.052257	-144.154520	-144.128879	-144.064027	-144.008965
+ 2 MULTIP		E_R	-47.958374	-48.060637	-48.034966	-47.970144	-47.915082
	CI,EX	ϵ_1	-144.292831	-144.404582	-144.392823	-144.352081	-144.325114
		E_R	-48.198948	-48.310699	-48.298940	-48.258198	-48.231231
3 NITROMETHANES	SCF	ϵ_1	-144.043661	-144.146063	-144.055903	-144.001060	-144.120564
		E_R	-47.959387	-48.061789	-47.971629	-47.916786	-48.036296
	CI,EX	ϵ_1	-144.284262	-144.396239	-144.342200	-144.315709	-144.384172
		E_R	-48.199988	-48.311965	-48.257926	-48.231435	-48.299898
NITROMETHANE	SCF		-47.958700	-48.061205	-47.971256	-47.916364	-48.035808
+ 4 MULTIP	CI,EX		-48.200163	-48.311927	-48.261386	-48.234327	-48.300391
NITROMETHANE	SCF		-47.959796	-48.062455	-47.972867	-47.918212	-48.037213
+ 2 MULTIP	CI,EX		-48.200920	-48.312941	-48.261288	-48.233891	-48.301369
NITROMETHANE	SCF		-47.951319	-48.052639	-47.960508	-47.904654	-48.026188
SINGLE FREE MOLECULE	CI,EX		-48.193707	-48.305044	-48.261013	-48.237619	-48.291861

TABLE III-4

Total Energies, Reduced Energies, and Bond Dissociation Energies for Extended Cluster Of Nitromethane Molecules Within Different Approaches (energy in [a.u.], equilibrium distance R = 3.0 bohrs)

Approach		E_{SCF}	$E_{CI,EX}$	C-N bond dissociation energy, ΔE
5 NITROMETHANES + 8 MULTIP	ϵ_1	-240.254526	-240.502424	
	E_R [1)]	-48.069496	-48.317394	-0.090978
5 NITROMETHANES	ϵ_1	-240.231022	-240.480215	
	E_R [2)]	-48.063552	-48.912745	-0.086329
NITROMETHANES + 12 MULTIP		-48.070478	-48.319273	-0.092857
NITROMETHANE + 4 MULTIP		-48.066103	-48.315858	-0.089442
NITROMETHANE SINGLE FREE MOLECULE		-48.052639	-48.305044	-0.078628

1) $E_R = \epsilon_1 - E_{SCF}$(4 NITROMETHANES + 8 MULTIP)

2) $E_R = \epsilon_1 - E_{SCF}$(4 NITROMETHANES CLUSTER

TABLE III-4a

Total Energies, Reduced Energies, and Bond Dissociation Energies (corresponding to R_{CN} = 5.6 bohrs and $R_{CN} = \infty$) for Extended Cluster Within Different Approaches (energy in [a.u.])

Approach	$E_{SCF}(eq)$	$E_{CI,EX}(eq)$	$E_{CI,EX}(5.6)$	Bond Dissociation Energy $E_{CI,EX}(Eq) - E_{CI,EX}(Eq)$	Bond Dissociation Energy $E_{CI,EX}(Eq) - E_{CI,EX(\infty)}$
5 NITROMETHANES + 8 MULTIP	-240.254526	-240.502424	-240.395444	-.106980	-.090978
5 NITROMETHANES	-240.231022	-240.480215	-240.376844	-.103371	-.086329
NITROMETHANE + 12 MULTIP	-48.070478	-48.319273	-48.240434	-.078839	-.092857
NITROMETHANE + 4 MULTIP	-48.066103	-48.315858	-48.236404	-.079454	-.089442
NITROMETHANE SINGLE FREE MOLECULE	-48.052639	-48.305044	-48.237619	-.067425	-.078628

TABLE III-5

Total Energies, Reduced Energies, and Bond Dissociation Energies For Extended Cluster (Alternative Choice) Within Different Approaches (energy in [a.u.], equilibrium distance R = 3.0 bohrs)

Approach		E_{SCF}	$E_{CI,EX}$	C-N bond dissociation energy, ΔE
5 NITROMETHANES + 8 MULTIP	1)	ϵ_1 -240.262239	-240.510445	
		E_R -48.0684856	-48.316691	-.090275
5 NITROMETHANES	2)	ϵ_1 -240.232644	-240.484120	
		E_R -48.053121	-48.304597	-0.07818
NITROMETHANE + 12 MULTIP		-48.070478	-48.319273	-0.092857
NITROMETHANE + 12 MULTIP		-48.054486	-48.306896	-0.080480
NITROMETHANE SINGLE FREE MOLECULE		-48.052639	-48.305044	-0.07863

1) $E_R = \epsilon_1 - E_{SCF}$(4 NITROMETHANE + 8 MULTIP CLUSTER)

2) $E_R = \epsilon_1 - E_{SCF}$(4 NITROMETHANE CLUSTER)

TABLE III-5a

Total Energies, Reduced Energies, and Bond Dissociation Energies (corresponding to R_{CN}= 5.6 bohrs and R_{CN} = ∞) For Extended Cluster (Alternative Choice) Within Different Approaches (energy in [a.u.])

Approach	$E_{SCF}(eq)$	$E_{CI,EX}(eq)$	$E_{CI,EX}(5.6)$	Bond Dissociation Energy $E_{CI,EX}(Eq) - E_{CI,EX}(Eq)$	Bond Dissociation Energy $E_{CI,EX}(Eq) - E_{CI,EX(\infty)}$
5 NITROMETHANES + 8 MULTIP	-240.262239	-240.510445	-240.432304	-.078141	-.090275
5 NITROMETHANES	-240.232644	-240.484120	-240.416364	-.067756	-.078181
NITROMETHANE + 12 MULTIP	-48.070478	-48.319273	-48.240434	-.078839	-.092857
NITROMETHANE + 4 MULTIP	-48.054486	-48.306896	-48.241300	-.065596	-.080480
NITROMETHANE SINGLE FREE MOLECULE	-48.052639	-48.305044	-48.237619	-.067425	-.078628

TABLE III-6

The Decomposition Pathway for C-N bond in Nitromethane Crystal (extended cluster) for Different Approaches. (See definitions in Table I)

Type of Approach		R(bohrs)	2.4	3.0	3.6	4.4	5.6
5 NITROMETHANES + 8 MULTIP	SCF	ϵ_1	-240.152473	-240.254526	-240.228227	-240.161385	-240.102384
		E_R	-47.967443	-48.069496	-48.043197	-47.976355	-47.917354
	CI,EX	ϵ_1	-240.391721	-240.502424	-240.487931	-240.438240	-240.395444
		E_R	-48.206691	-48.317394	-48.302901	-48.253210	-48.210414
5 NITROMETHANES	SCF	ϵ_1	-240.128606	-240.231022	-240.205118	-240.138565	-240.078886
		E_R	-47.943576	-48.045992	-48.020088	-47.953535	-47.893856
	CI,EX	ϵ_1	-240.368461	-240.480215	-240.466442	-240.417775	-240.376844
		E_R	-48.183431	-48.295185	-48.281412	-48.232727	-48.191814
NITROMETHANE +12 MULTIP	SCF	ϵ_1	-47.967541	-48.070478	-48.045572	-47.982195	-47.930622
	CI,EX	ϵ_1	-48.207465	-48.319278	-48.307232	-48.264734	-48.240434
NITROMETHANE + 4 MULTIP	SCF	ϵ_1	-47.963298	-48.066103	-48.041008	-47.977022	-47.923381
	CI,EX	ϵ_1	-48.204001	-48.315858	-48.304253	-48.262308	-48.236404

TABLE III-7

The Decomposition Pathway for C-N bond in Nitromethane Crystal (Extended Cluster, Alternative Choice) For Different Approaches.

Type of Approach		R(bohrs)	2.4	3.0	3.6	4.4	5.6
5 NITROMETHANES + 8 MULTIP	SCF	ε_1	-240.159613	-240.262239	-240.237344	-240.174215	-240.122976
		E_R	-47.965859	-48.068485	-48.04359	-47.980461	-47.929222
	CI,EX	ε_1	-240.399064	-240.510445	-240.498235	-240.456217	-240.432304
		E_R	-48.205310	-48.316691	-48.304481	-48.262463	-48.23855
5 NITROMETHANES	SCF	ε_1	-240.131808	-240.232044	-240.205932	-240.140107	-240.084219
		E_R	-47.952285	-48.053121	-48.026409	-47.960584	-47.904696
	CI,EX	ε_1	-240.373485	-240.484120	-240.470746	-240.440670	-240.416364
		E_R	-48.193962	-48.304597	-48.291223	-48.261147	-48.236841
NITROMETHANE + 8 MULTIP	SCF	ε_1	Same as in extended cluster				
	CI,EX	ε_1	Same as in extended cluster				
NITROMETHANE + 4 MULTIP	SCF	ε_1	-47.953401	-48.054486	-48.027757	-47.961689	-47.905447
	CI,EX	ε_1	-48.196419	-48.306896	-48.293038	-48.263016	-48.241300

TABLE III-8

Nitrometnane - Crystal Orbital Calculations for Model Cluster

Crystal Orbital Calculations for 4 Molecules 3 Cell Calculations in z Axis Direction (Fig. III-1)

Total Energy for 4 molecules

3 $\vec{k}$ points E_4 = -192.195942921 a.u.

5 $\vec{k}$ points E_4 = -192.195942922 a.u.

Total Energy for 3 molecules

3 $\vec{k}$ points E_4 = -144.13503504 a.u.

5 $\vec{k}$ points E_4 = -144.13503504 a.u.

$E_R = E_4 - E_3$ = -48.0609079 a.u.

E_R energy from cluster calculations

E_R = -48.060579

IV. POLY-CRYST

POLY-CRYST is the program we previously derived and wrote for ab-initio calculations on crystals and polymers using the translational symmetry in a crystal and the translational-rotational symmetry in a polymer. Commensurate with the ONR priorities expressed to us by our ONR Contract Monitor, we devoted only minimal but still scientifically significant effort to further development and testing of the POLY-CRYST program. As options we had already included POLY-CRYST our own ab-initio MODPOT (ab-initio effective core model potentials) and VRDDO (a charge conserving integral prescreening procedure) options. It is these features particularly VRDDO which enables POLY-CRYST to handle molecular crystals of large molecules and with large numbers of large molecules per unit cell. This year we derived and incorporated into POLY-CRYST including the multipole effects of farther out molecules to take into account long range effects also. We then meshed this multipole procedure back into the MRD-CI programs to enable us to include multipole effects when breaking a chemical bond in a crystal. We also ran some tests on POLY-CRYST on integral thresholds and numbers of unit cells necessary for convergence. These preliminary tests identified necessary criteria.

Toward this convergence criteria goal, we also derived and implemented a procedure for calculating the charge imbalance caused by various integral thresholds to give a precise measure of the effect on the crystal orbital calculation of dropping integrals of various sizes. The POLY-CRYST program has promise for yielding important fundamental results on crystalline energetic materials.

As mentioned in Section III we also used this XTLORB program to calculate a 3 cell case of nitromethane to verify the validity and accuracy of the procedure we use for the effect of multipoles from farther out molecules on SCF calculations for molecular clusters from crystals the SCF calculation is carried out explicitly for all the molecules in a unit reference cell (or larger piece of the crystal). Our SCF results for the nitromethane molecular cluster from the nitromethane crystal field of yet further out molecules were very close to those full XTLORB results for nitromethane. The SCF orbitals are then localized and the MRD-CI calculations are carried out for breaking a chemical bond in a molecule in a crystal including explicitly in the MRD-CI calculation the localized orbitals in the region of interest.

V. Lectures Presented and Publications on This ONR Research

Presentations given and/or scheduled and papers published and/or submitted during the fiscal year.

A. Presentations Given Dr. Joyce J. Kaufman

1. Already Presented (* denotes invited lecture)

a. At National and International Meetings

* (1). "Ab-Initio MRD-CI Calculations for the Propagation Step in the Cationic Polymerization of Oxetanes Based on Localized Orbitals," an invited paper presented at the International Symposium on Atomic, Molecular and Solid State Theory, Marineland, Florida, March 1987.

* (2). "Comparison of Ab-Initio MODPOT and Ab-Initio Energy Partitioned Potential Functions for Nitromethane Dimer Against Large Basis Set Calculation," an invited paper presented at the Sanibel International Symposium on Atomic Molecular and Solid State Theory, Marineland, Florida, March 1987.

* (3). "Ab-Initio MRD-CI Calculations on Protonated Cyclic Ethers. I. Protonation Pathways Involve Multipotential Surfaces (Protonation of Oxetane) II. Differences from SCF in Dominant Configurations Upon Opening Non-Protonated Oxirane Rings (Epoxides)," an invited paper presented at the Sanibel International Symposium on Atomic Molecular and Solid State Theory, Marineland, Florida, March 1987.

* (4). "Ab-Initio Calculations on Large Molecules and Solids Using Desirable Computational Strategies," VIIIth International Conference on Computers in Chemical Research and Education, Beijing, China, June 1987.

(5). "Ab-Initio Quantum Chemical Calculations on Large Molecular Systems and Crystals," American Conference on Theoretical Chemistry, Gull Lake, Minnesota, July 1987.

* (6). "Ab-Initio MRD-CI Calculations Based on Localized Orbitals For Molecular Decomposition and Reactions of Large Systems," 1987 World Congress of World Association of Theoretical Organic Chemistry, Budapest, Hungary, August 1987.

(7). "Ab-Initio MRD-CI Calculations For Cationic Polymerization of Oxetanes Based on Localized Orbitals," Division of Physical Chemistry, 194th National Meeting, American Chemical Society, New Orleans, Louisiana, August 1987.

(8). "Comparison of Ab-Initio MODPOT and Ab-Initio Energy Partitioned Potential Functions for Nitromethane Dimer Against Large Basis Set Calculation," Division of Physical Chemistry, 194th National Meeting, American Chemical Society, New Orleans, Louisiana, August 1987.

b. Other Research Institutions

* (1). "Ab-Initio Quantum Chemical Calculations on Large Molecular Systems and Crystals," Maryland Section American Chemical Society, Baltimore, Maryland, February 1987.

c. At DOD Meetings and Workshops

* (1). "Quantum Chemical Characterization of Explosive Sensitivity," Working Group Meeting on Sensitivity of Explosives, Socorro, New Mexico, March 1987. (Presented by Dr. Walter S. Koski)

* (2). "Ab-Initio Quantum Chemical Studies on Energetic Nitrocompounds," Sixth Annual Working Group Meeting on Synthesis of High Energy Density Materials, Concord Hotel, Kiamesha Lake, New York, May 1987.

* (3). "Ab-Initio MRD-CI Calculations for Breaking a Chemical Bond in a Molecule in a Crystal," ONR Workshop on Dynamic Deformation, Fracture and Transient Combustion of Energetic Compounds, Great Oak, Maryland, May 1987.

* (4). "Desired Properties of Energetic Compounds That Can Be Calculated Reliably and Accurately From High Quality Ab-Initio Quantum Chemical Calculations," ONR Workshop on Crystalline and Polymeric Energetic Materials, Great Oak, Maryland August 1987.

2. To be presented

* a. "Ab-Initio MRD-CI Calculations for Breaking a Chemical Bond in a Molecule in a Crystal or Other Solid Environment," Sanibel International Symposium on Atomic, Molecular and Solid State Physics, Marineland, Florida, March 1988.

* b. "Ab-Initio MRD-CI Calculations for Breaking a Chemical Bond in a Molecule in a Crystal or Other Solid Environment", Symposium on the Physics and Chemistry of Brittle Fracture, American Physical Society National Meeting, New Orleans, March 1988.

c. "Ab-Initio MRD-CI Calculations for Breaking a Chemical Bond in a Molecule in a Crystal or Other Solid Environment," 3rd Chemical Congress of North America (joint with American Chemical Society), Toronto, Canada, June 1988.

B. Publications

1. Already Published

a. "Ab-Initio MRD-CI Calculations on the >C - NO_2 Decomposition Pathway of Nitrobenzene," Joyce J. Kaufman, P. C. Hariharan, S. Roszak and M. van Hemert. An invited plenary lecture presented at the Symposium on Computational and Mathematical Chemistry, Can. Inst. Chem. National Meeting, Saskatoon, Canada, June 1986. J. Comp. Chem. 8, 736-743 (1987).

b. "Ab-Initio Electrostatic Molecular Potential Contour Maps for Initiation Step and Ab-Initio MRD-CI Calculations for Propagation Step of Cationic Polymerization of Oxetanes", Joyce J. Kaufman, P. C. Hariharan, S. Roszak and P. B. Keegstra. An invited lecture presented at the IUPAC 5th International Symposium on Ring-Opening Polymerization, Blois, France, June 1986. Makromol. Chem., Macromol. Symposium. 6, 315-330 (1986)

c. "Symposium Note: More New Desirable Computational Strategies for Ab-Initio Calculations on Large Molecules, Clusters, Solids, and Crystals", Joyce J. Kaufman, Int. J. Quantum. Chem. 29, 179-184 (1987)

d. "Nonempirical Atom-Atom Potentials for Main Components of Intermolecular Interaction Energy," W. A. Sokalski, A. H. Lowrey, S. Roszak, V. Lewchenko, J. M. Blaisdell, P. C. Hariharan and Joyce J. Kaufman, J. Comp. Chem. 7, 693-700 (1986).

2. Accepted for Publication and in Press

a. "Ab-Initio Potential Functions For Crystals and Ab-Initio Crystal Orbitals," Joyce J. Kaufman. An invited lecture presented at the International Symposium on Molecules in Physics, Chemistry and Biology. Dedicated to Professor R. Daudel, Paris, France, June 1986. In press, Symposium Proceedings.

b. "Ab-Initio MRD-CI Calculations for the Propagation Step in the Cationic Polymerization of Oxetanes Based on Localized Orbitals," Joyce J. Kaufman, P. C. Hariharan and P. B. Keegstra. An invited paper presented at the International Sanibel Symposium on Atomic, Molecular and Solid State Theory, Marineland, Florida, March 1987. In press, Int. J. Quantum Chemistry, Symposium Issue.

c. "Comparison of Ab-Iitio MODPOT and Ab-Initio Energy Partitioned Potential Functions for Nitromethane Dimer Against Large Basis Set Calculations," An invited paper presented at the International Sanibel Symposium on Atomic, Molecular and Solid State Theory, Marineland, Florida, March 1987. W. A. Sokalski, P. C. Hariharan and Joyce J. Kaufman. In press, Int. J. Quantum Chemistry, Symposium Issue.

d. "Ab-Initio MRD-CI Calculations on Protonated Cyclic Ethers. I. Protonation Pathways Involve Multipotential Surfaces (Protonation of Oxetane) II. Differences from SCF in Dominant Configurations Upon Opening Non-Protonated Oxirane Rings (epoxides)," An

invited lecture presented at the International Sanibel Symposium on Atomic, Molecular and Solid State Theory, Marineland, Florida, March 1987. Joyce J. Kaufman, P. C. Hariharan, S. Roszak and P. B. Keegstra, In press, Int. J. Quantum Chemistry, Symposium Issue.

VI Project Personnel

Joyce J. Kaufman, Ph.D.

Principal Investigator

P. C. Hariharan, Ph.D.

Research Scientist

Overall responsibility for implementing new program developments and conversion to Cray computers. Quantum chemical calculations on energetic polymers, MRD-CI, GAMESS and POLY-CRYST calculations

Philip B. Keegstra, Ph.D.

Postdoctoral (October 1986 - August 1987)

MRD-CI calculations on cationic polymerization of oxetanes, implementation of inclusion of multipoles into POLY-CRYST, assistance on implementing multipoles into MRD-CI and with breaking chemical bond calculations, test calculations on POLY-CRYST

S. Roszak, Ph.D.

Visiting Scientist (February 1987 - November 1987)

Implementation of multipoles into MRD-CI and carrying out such calculations for breaking a chemical bond in a molecule in a crystal, MRD-CI calculations on propagation step of cationic polymerization of oxetanes.

W. A. Sokalski, Ph.D.

Visiting Scientist (July - August 1987)

Inclusion of correlation in calculation of multipoles and use in intermolecular calculations.

Ser 432/84/211 SYN
Revised January 1985

(SYN)

DISTRIBUTION LIST

Dr. R.S. Miller
Office of Naval Research
Code 432P
Arlington, VA 22217
(10 copies)

Dr. A.L. Slafkosky
Scientific Advisor
Commandant of the Marine Corps
Code RD-1
Washington, DC 20380

JHU Applied Physics Laboratory
ATTN: CPIA (Mr. T.W. Christian)
Johns Hopkins Rd.
Laurel, MD 20707

Dr. Kenneth D. Hartman
Hercules Aerospace Division
Hercules Incorporated
Alleghany Ballistic Lab
P.O. Box 210
Washington, DC 21502

Mr. Otto K. Heiney
AFATL-DLJG
Elgin AFB, FL 32542

Dr. Merrill K. King
Atlantic Research Corp.
5390 Cherokee Avenue
Alexandria, VA 22312

Dr. R.L. Lou
Aerojet Strategic Propulsion Co.
Bldg. 05025 - Dept 5400 - MS 167
P.O. Box 15699C
Sacramento, CA 95813

Dr. R. Olsen
Aerojet Strategic Propulsion Co.
Bldg. 05025 - Dept 5400 - MS 167
P.O. Box 15699C
Sacramento, CA 95813

Dr. J. Pastine
Naval Sea Systems Command
Code 06R
Washington, DC 20362

Dr. Henry P. Marshall
Dept. 93-50, Bldg 204
Lockheed Missile & Space Co.
3251 Hanover St.
Palo Alto, CA 94304

Dr. Ingo W. May
Army Ballistic Research Lab.
ARRADCOM
Code DRXBR - 18D
Aberdeen Proving Ground, MD 21

Dr. R. McGuire
Lawrence Livermore Laboratory
University of California
Code L-324
Livermore, CA 94550

P.A. Miller
736 Leavenworth Street, #6
San Francisco, CA 94109

Dr. W. Moniz
Naval Research Lab.
Code 6120
Washington, DC 20375

Dr. K.F. Mueller
Naval Surface Weapons Center
Code R11
White Oak
Silver Spring, MD 20910

Prof. M. Nicol
Dept. of Chemistry & Biochem.
University of California
Los Angeles, CA 90024

(SYN)

DISTRIBUTION LIST

Dr. Randy Peters
Aerojet Strategic Propulsion Co.
Bldg. 05025 - Dept 5400 - MS 167
P.O. Box 15699C
Sacramento, CA 95813

Dr. D. Mann
U.S. Army Research Office
Engineering Division
Box 12211
Research Triangle Park, NC 27709-2211

Mr. R. Geisler
ATTN: DY/MS-24
AFRPL
Edwards AFB, CA 93523

Naval Air Systems Command
ATTN: Mr. Bertram P. Sobers
NAVAIR-320G
Jefferson Plaza 1, RM 472
Washington, DC 20361

R.B. Steele
Aerojet Strategic Propulsion Co.
P.O. Box 15699C
Sacramento, CA 95813

Mr. M. Stosz
Naval Surface Weapons Center
Code R10B
White Oak
Silver Spring, MD 20910

Mr. E.S. Sutton
Thiokol Corporation
Elkton Division
P.O. Box 241
Elkton, MD 21921

Dr. Grant Thompson
Morton Thiokol, Inc.
Wasatch Division
MS 240 P.O. Box 524
Brigham City, UT 84302

Mr. L. Roslund
Naval Surface Weapons Center
Code R10C
White Oak, Silver Spring, MD [illegible]

Dr. David C. Sayles
Ballistic Missile Defense
Advanced Technology Center
P.O. Box 1500
Huntsville, AL 35807

Director
US Army Ballistic Research Lab.
ATTN: DRXBR-IBD
Aberdeen Proving Ground, MD 21005

Commander
US Army Missile Command
ATTN: DRSMI-RKL
Walter W. Wharton
Redstone Arsenal, AL 35898

T. Yee
Naval Weapons Center
Code 3265
China Lake, CA 93555

Dr. E. Zimet
Office of Naval Technology
Code 071
Arlington, VA 22217

Dr. Ronald L. Derr
Naval Weapons Center
Code 389
China Lake, CA 93555

T. Boggs
Naval Weapons Center
Code 389
China Lake, CA 93555

Lee C. Estabrook, P.E.
Morton Thiokol, Inc.
P.O. Box 30058
Shreveport, LA 71130

(SYN)

DISTRIBUTION LIST

Dr. R.F. Walker
Chief, Energetic Materials Division
DRSMC-LCE (D), B-3022
USA ARDC
Dover, NJ 07801

Dr. Janet Wall
Code 012
Director, Research Administration
Naval Postgraduate School
Monterey, CA 93943

R.E. Shenton
Atlantic Research Corp.
7511 Wellington Road
Gainesville, VA 22065

Mike Barnes
Atlantic Research Corp.
7511 Wellington Road
Gainesville, VA 22065

Dr. Lionel Dickinson
Naval Explosive Ordinance
Disposal Tech. Center
Code D
Indian Head, MD 20340

Prof. J.T. Dickinson
Washington State University
Dept. of Physics 4
Pullman, WA 99164-2814

M.H. Miles
Dept. of Physics
Washington State University
Pullman, WA 99164-2814

Dr. T.F. Davidson
Vice President, Technical
Morton Thiokol, Inc.
Aerospace Group
110 North Wacker Drive
Chicago, IL 60606

Dr. D.D. Dillehay
Morton Thiokol, Inc.
Longhorn Division
Marshall, TX 75670

G.T. Bowman
Atlantic Research Corp.
7511 Wellington Road
Gainesville, VA 22065

Brian Wheatley
Atlantic Research Corp.
7511 Wellington Road
Gainesville, VA 22065

Mr. G. Edwards
Naval Sea Systems Command
Code 62R32
Washington, DC 20362

C. Dickinson
Naval Surface Weapons Center
White Oak, Code R-13
Silver Spring, MD 20910

Prof. John Deutch
MIT
Department of Chemistry
Cambridge, MA 02139

Dr. E.H. deButts
Hercules Aerospace Co.
P.O. Box 27408
Salt Lake City, UT 84127

David A. Flanigan
Director, Advanced Technology
Morton Thiokol, Inc.
Aerospace Group
110 North Wacker Drive
Chicago, IL 60606

(SYN)

DISTRIBUTION LIST

Mr. J. Consaga
Naval Surface Weapons Center
Code R-16
Indian Head, MD 20640

Naval Sea Systems Command
ATTN: Mr. Charles M. Christensen
NAVSEA62R2
Crystal Plaza, Bldg. 6, Rm 806
Washington, DC 20362

Mr. R. Beauregard
Naval Sea Systems Command
SEA 64E
Washington, DC 20362

Dr. Anthony J. Matuszko
Air Force Office of Scientific Research
Directorate of Chemical & Atmospheric Sciences
Bolling Air Force Base
Washington, DC 20332

Dr. Michael Chaykovsky
Naval Surface Weapons Center
Code R11
White Oak
Silver Spring, MD 20910

J.J. Rocchio
USA Ballistic Research Lab.
Aberdeen Proving Ground, MD 21005-5066

G.A. Zimmerman
Aerojet Tactical Systems
P.O. Box 13400
Sacramento, CA 95813

B. Swanson
INC-4 MS C-346
Los Alamos National Laboratory
Los Alamos, NM 87545

Dr. L.H. Caveny
Air Force Office of Scientific Research
Directorate of Aerospace Sciences
Bolling Air Force Base
Washington, DC 20332

W.G. Roger
Code 5253
Naval Ordance Station
Indian Head, MD 20640

Dr. Donald L. Bell
Air Force Office of Scientific Research
Directorate of Chemical & Atmospheric Sciences
Bolling Air Force Base
Washington, DC 20332

Dr. H.G. Adolph
Naval Surface Weapons Center
Code R11
White Oak
Silver Spring, MD 20910

U.S. Army Research Office
Chemical & Biological Sciences Division
P.O. Box 12211
Research Triangle Park, NC [illegible]

G. Butcher
Hercules, Inc.
MS X2H
P.O. Box 98
Magna, Utah 84044

W. Waesche
Atlantic Research Corp.
7511 Wellington Road
Gainesville, VA 22065

Ser 32B4/211 SYN
Revised January 1985

(SYN)

DISTRIBUTION LIST

Dr. James T. Bryant
Naval Weapons Center
Code 3205B
China Lake, CA 93555

Dr. L. Rothstein
Assistant Director
Naval Explosives Dev. Engineering Dept.
Naval Weapons Station
Yorktown, VA 23691

Dr. M.J. Kamlet
Naval Surface Weapons Center
Code R11
White Oak, Silver Spring, MD 20910

Dr. Henry Webster, III
Manager, Chemical Sciences Branch
ATTN: Code 5063
Crane, IN 47522

Dr. R.S. Valentini
United Technologies Chemical Systems
P.O. Box 50015
San Jose, CA 95150-0015

Administrative Contracting
Officer (see contract for
address)
(1 copy)

Defense Technical Information Center
Bldg. 5, Cameron Station
Alexandria, VA 22314
(12 copies)

Arpad Junasz
Code DRDAR-IBD
Ballistic Research Lab
Aberdeen, MD 21005

Mr. C. Gotzmer
Naval Surface Weapons Center
Code R-11
White Oak
Silver Spring, MD 20910

Dr. John S. Wilkes, Jr.
FJSRL/NC
USAF Academy, CO 80840

Dr. H. Rosenwasser
Naval Air Systems Command
AIR-320R
Washington, DC 20361

Dr. A. Nielsen
Naval Weapons Center
Code 385
China Lake, CA 93555

Dr. Joyce J. Kaufman
The Johns Hopkins University
Department of Chemistry
Baltimore, MD 21218

Dr. J.R. West
Morton Thiokol, Inc.
P.O. Box 30058
Shreveport, LA 71130

Director
Naval Research Laboratory
Attn: Code 2627
Washington, DC 20375
(6 copies)

Dr. Robert J. Schmitt
SRI International
333 Ravenswood Avenue
Menlo Park, CA 94025

Dr. Michael D. Coburn
Los Alamos National Lab
M-1, Explosives Technology
Mail Stop, C920
Los Alamos, NM 87545

(SYN)

DISTRIBUTION LIST

Dr. G. Neece
Office of Naval Research
Code 413
Arlington, VA 22217

Mr. C.M. Havlik
0/83-10, B/157-3W
Lockheed Missiles & Space Co., Inc.
P.O. Box 504
Sunnvale, CA 94086

Dr. Philip Howe
Ballistic Research Labatory
Code DRXBR-TBD
Aberdeen Proving Ground, MD 21005

Prof. C. Sue Kim
Department of Chemistry
California State University, Sacramento
Sacramento, California 95819

Mr. J. Moniz
Naval Ordnance Station
Code 5253L
Indian Head, MD 20640

Dr. R. Reed Jr.
Naval Weapons Center
Code 38904
China Lake, CA 93555

L.H. Sperling
Materials Research Center #32
Lehigh University
Bethlehem, PA 18015

Dr. Kurt Baum
Fluorochem, Inc.
680 South Ayon Ave.
Azusa, CA 91702

Dr. Andrew C. Victor
Naval Weapons Center
Code 3208
China Lake, CA 93555

Dr. J.C. Hinshaw
Morton Thiokol Inc.
P.O. Box 524
Mail Stop 240
Brigham City, Utah 84302

Dr. V.J. Keenan
Anal-Syn Lab. Inc.
P.O. Box 547
Paoli, PA 19301

G.E Manser
Aerojet Strategic Propulsion Co.
Bldg. 05025, Dept. 2131
P.O. 15699C
Sacramento, CA 95852

P. Politzer
Chemistry Department
University of New Orleans
New Orleans, Louisiana 70148

Mr. David Siegel
Office of Naval Research
Code 253
Arlington, VA 22217

Dr. Rodney L. Willer
Morton Thiokol, Inc.
P.O. Box 241
Elkton, MD 21921

Dr. R. Atkins
Naval Weapons Center
Code 3852
China Lake, CA 93555

(SVV)

DISTRIBUTION LIST

Prof. J.H. Boyer
Chemistry Department
University of New Orleans
New Orleans, Louisianna 70148

Prof. J.C. Chien
University of Massachusetts
Department of Chemistry
Amherst, MA 03003

Dr. B. David Halpern
Polysciences, Inc.
Paul Valley Industrial Park
Warrington, PA 18976

Dr. M.S. Frankel
Rockwell International
Rocketdyne Division
6633 Canoga Avenue
Canoga Park, CA 91304

Dr. R.A. Earl
Hercules, Inc.
Magna, Utah 84109

Dr. C. Bedford
SRI International
333 Ravenswood Avenue
Menlo Park, CA 94025

Dr. Robert R. Ryan
INC-4, MS C346
Los Alamos National Laboratory
Los Alamos, New Mexico 87545

Dr. Robert D. Champman
AFRPL/LKLR
Edwards AFB, CA 93525

Dr. L. Erwin
MIT
Room 35-008
Cambridge, MA 02139

Dr. M. Farber
Space Sciences, Inc.
135 W. Maple Avenue
Monrovia, CA 91016

Dr. W.H. Graham
Morton Thiokol, Inc.
Hunstville Division
Hunstville, AL 35807-7501

Dr. C. Coon
Lawrence Livermore Lab.
University of California
P.O. Box 808
Livermore, CA 94550

Dr. R. Gilardi
Naval Research Laboratory
Code 6030
Washington, DC 20375

Dr. Alan Marchand
Dept. of Chemistry
North Texas State University
NTSU Station, Box 5068
Denton, Texas 76203

T.B. Brill
Department of Chemistry
University of Delaware
Newark, Delaware 19716

Dr. A.A. Defusco
Code 3858
Naval Weapons Center
China Lake, CA 93555

Dr. Richard A. Hollins
Naval Weapons Center
Code 3853
China Lake, CA 93555

Dr. R. Armstrong
MIT
Room 66-505
Cambridge, MA 02139

Professor Phillip E. Eaton
Department of Chemistry
University of Chicago
5735 South Ellis Avenue
Chicago, IL 60637

END
DATED
FILM
8-88
DTIC